Impact of Cold Atmospheric Plasma on the Structure and Functionality of Pea Protein

A THESIS
SUBMITTED TO THE FACULTY OF THE
UNIVERSITY OF MINNESOTA
BY

Fan Bu

IN PARTIAL FULFILLMENT OF THE REQUIREMENTS
FOR THE DEGREE OF
MASTER OF SCIENCE

Baraem P. Ismail, PhD
George Annor, PhD

April 2021

Acknowledgements

I would first like to acknowledgement my advisor, Dr. B. Pam Ismail, for the countless support, encouragement, and guidance throughout my Master journey. I have learned a lot from numerous presenting, networking, collaborating, and training opportunities you provided me. Your knowledge, intelligence, hardwork, persistence and perfectness have inspired me every day of my graduate school to better myself. I am also incredibly grateful for your continuous help and tireless guidance on my thesis writing, at the time you were fighting cancer. Thanks for my co-advisor, Dr. George Annor for providing me knowledge in carbohydrate chemistry and supporting my graduate study. I would also like to recognize Dr. Peter Bruggeman for generously providing cold atmospheric plasma technology and knowledge and being extremely helpful and approachable throughout my study. Thank you to Dr. Chi Chen for providing valuable insights into my project and help with LC-MS analysis. Many thanks to Dr. Gaurav Nayak for helping on cold plasma experiments and always patiently answering my naïve questions on cold plasma. Thank you Dr. V.S. Santosh K. Kondeti for helping with the plasma jet setup and Qingqing Mao for helping with LC-MS analysis. Thank you to the Plant Protein Innovation Center (PPIC), for funding this project!

I would like to recognize Ismail lab mates for being helpful and nice to me. Thank you to Chelsey Hinnenkamp, Lucy Hansen, Rachel Mitacek, and Maneka Malalgoda for training me on many of the analytical methods and instruments used in this study. I also want to thank Allie Schneider, Laura Eckhardt, Amy Mathiowetz and Holly Husband, for being supportive friends and comforting me when I feel stressed. I am extremely fortunate to make friends with all of you. I will never forget how much fun we had when watching *The Bachelor* in the evening, snowshoeing during the weekends, and eating dumplings while hiking.

A big thank you to my mom and dad for believing, supporting, and caring for me all the time. Without your support, I could not have studied abroad and experienced a different culture in the United States. To my best friends, Jiawei Li and Ziwei Yu, thank you for sharing fun stories, eating hotpots, and travelling with me. To Dr. Ye, thank you for encouraging and helping me when I encountered difficulties. Last but not least, to my cute cat, Tiger Bu, thank you for coming into my life and accompanying me.

Dedication

This thesis is dedicated to the memory of my grandmother, Gaiying Tang, for believing in the power of woman, and my grandfather, Lingyun Xu, for emphasizing the importance of education.

Abstract

Increased consumer demand for alternative plant protein sources other than soy, which is a GMO crop and "Big Eight" allergen, is driving the growth of the pea protein ingredient market. Yellow field peas (*Pisum sativum L.*), an easy to grow environment-friendly non-GMO crop, with currently low occurrence of allergenicity, have similar protein profile and nutritional quality compared to soy. Therefore, pea protein has the potential to replace soy protein in the global plant protein ingredient market. The functional properties of pea protein, however, are inferior to that of soy protein counterparts, hindering its expanded use. Current breeding efforts, extraction and processing advances, and traditional modification strategies are limited in improving the functional properties of pea protein while maintaining nutritional quality as well as feasible production cost.

Cold atmospheric plasma (CAP), a physical nonthermal processing technology that has been explored in electronics, material science, medicine, and agriculture, is being explored as a novel protein modification approach. Several studies reported unfolding and polymerization of proteins and corresponding improvements in functional properties after CAP treatment. However, the link between different plasma reactive species and observed structural changes, and consequent functional enhancement, has not been demonstrated. Additionally, only plasma sources that produce long-lived species (O_3, H_2O_2, NO_2^-, and NO_3^-) have been investigated in protein modification studies. Other plasma sources that can generate various short-lived species (such as OH radicals) are worth investigating to optimize CAP conditions for a directed enhancement in pea protein functionality. Therefore, the objectives of this study were: (1) investigate the impact of plasma reactive species, as well as pH conditions and salt content, on pea protein structure and

functionality; (2) investigate the impact of different plasma configurations, gas mixtures, and treatment time on pea protein structure and functionality.

For objective 1, the impact of RNS and ROS (O_3, N_xO_y, H_2O_2 and OH) at two pH conditions (pH 2 and pH 7), on the color, structure, and functionality of pea protein isolate (PPI) was evaluated. Structural characteristics of modified pea protein isolates (mPPIs) and PPI were compared by determining the protein profile using SDS-PAGE and SE-HPLC, protein denaturation by DSC, surface charge by measuring zeta potential, surface hydrophobicity as measured by a spectrophotometric method, and protein secondary structure by FTIR. Protein solubility, gelation, and emulsification properties were evaluated. For the second objectives three different CAP treatments, atmospheric pressure plasma jet (APPJ) coupled with Ar/O_2 mixture, two-dimension dielectric barrier discharge (2D-DBD) coupled with Ar/O_2 mixture, and nanosecond pulsed discharge (ns-pulsed) coupled with air, on the color, structure, functionality, and amino acid composition of PPI was evaluated. The effect of treatment time (5, 15, 30, and 45 min) was also determined. Structural characteristics and functional properties of PPI samples were determined following the same stated methods. The amino acid profile and non-protein components of the isolates were characterized using UPLC-MS.

Pronounced structural and functional changes were observed upon treatment with reactive species at pH 2. All reactive species induced the formation of disulfide-linked soluble aggregates. Protein denaturation was observed after treatment with all reactive species. A significant increase in β-sheet content and surface hydrophobicity was only induced by treatment with O_3 and OH, which resulted in the greatest enhancement in gelation and emulsification. While H_2O_2 enhanced PPI color by increasing whiteness, it

had the least impact on protein structure and functionality. Results indicated that the plasma sources that can generate OH and O_3 could be used for pea protein functionalization.

Accordingly, different plasmas sources that can generate O_3 and OH were further investigated in objective 2. All plasma treatments resulted in reduced yellow color of PPI, denaturation of the proteins, formation of disulfide-linked soluble aggregates, and increased surface hydrophobicity. The plasma-induced structural changes resulted in improvement of gel strength and emulsification capacity. The amino acid composition of PPI was not significantly impacted by 2D-DBD treatment, whereas a slight decrease in tyrosine content was observed after APPJ and ns-pulsed treatment. Results indicated that the 30-minute 2D-DBD (Ar + O_2) treatment was the most desirable treatment because of moderate changes in protein structure coupled with significant improvement in the gelation and emulsification properties of PPI, with minimal impact on the amino acid composition.

Overall, the study successfully demonstrated the link in structural changes induced by plasma reactive species (N_xO_y/O_3, O_3, H_2O_2, and OH) to improvement in functional properties. Results can be used to explain previously reported observations related to the impact of different CAP systems on the functional properties of proteins. Additionally, this work provided a detailed understanding of the potential of different CAP sources and associated reactive species in enhancing pea protein functionality.

Table of content

List of Tables

List of Figures

Chapter 1: Literature Review

1.1 Introduction

Protein is an essential macronutrient that is involved in a variety of physiological processes such as muscle growth and maintenance, satiety regulation, as well as weight management (Anderson & Moore, 2004; Henchion et al., 2017; Murphy et al., 2016). Global demand for protein is steeply increasing due to population growth, urbanization, increase in aging population, rising income, and recognition of the health benefits of protein (Delgado, 2003; Henchion et al., 2017; Popkin et al., 2012). Plant protein, perceived as a healthy diet component, augmented the demand for plant protein ingredients. Market Research Future (MRFR) reported that the global plant protein ingredient market is projected to accumulate $15.65 billion in revenue by 2024. In the past, the consumption of plant protein-based food products was limited to a small group of vegans and vegetarians. Recently, consumers across the dietary spectrum have started to include plant proteins in their diet and reduce their meat intake (Formanski & Analyst, 2019). This shift is largely attributed to the awareness of environmental sustainability, acknowledgment of the health benefits of plant proteins, religious and ethical beliefs, as well as the increased population of vegans, vegetarians, and flexitarians (Formanski & Analyst, 2019; Henchion et al., 2017).

With worldwide cultivation, high nutritional quality, and good functionality, soy protein has been the dominant protein in the plant protein market for the past few decades. However, as one of the “Big Eight” allergens recognized by the Food and Drug Administration, 6% of consumers are avoiding soy-based products (Formanski & Analyst, 2019). Additionally, 94% of soybeans in the US is genetically modified. Consumers who are looking for non-GMO products are likely to avoid soy- based products (Shahbandeh,

2020). With an increased demand for plant proteins and reduced interest in soy protein consumption, novel proteins obtained from other plant sources are needed to fill this gap.

As an easy to grow, environment-friendly, non-GMO crop, with currently low occurrence of allergenicity, yellow field peas (*Pisum sativum L.*) are gaining more traction as an alternative protein source (Barac et al., 2010). Pea protein ingredients have acceptable nutritional quality, thus are incorporated in many food applications as alternative to soy protein ingredients. Besides nutritional benefits, pea protein ingredients must demonstrate useful functional properties, such as solubility, gelling, foaming and emulsifying, in order to be widely incorporated into various food systems (Hettiarachchy & Ziegler, 1994). However, the overall functionality of pea protein ingredients is inferior to that of soy protein counterparts, hindering its expanded use. The inferior functionality of pea protein is largely attributed to the intrinsic protein profile and the under-researched isolation and functionalization processes in comparison to soy protein (Söderberg, 2013). Thus, to fill the market demand gap, the functionality of pea protein has to be enhanced.

Optimization of isolation processes and modification of protein structure are two common ways to improve protein functionality. Protein structural modification is intended to enhance specific functional properties for targeted applications. Enzymatic hydrolysis, Maillard-induced glycation, and physical modification approaches have been explored to alter the structure of pea protein and improve its functional properties. For example, the solubility of pea protein ingredients was enhanced upon specific enzymatical hydrolysis and Maillard-induced glycation (Barać et al., 2011; Barac et al., 2012; Kutzli et al., 2020). Traditional physical modifications, such as dry heating, steaming, and pressurization have been shown to improve the solubility, water binding capacity, and foaming of pea protein.

(Barać et al., 2004; Kester & Richardson, 1984). However, Millard-induced glycation and traditional physical modifications are usually associated with nutritional loss, whereas enzymatic hydrolysis may result in bitter taste that is unacceptable to consumers (Björck & Asp, 1983; Lin et al., 2020). Accordingly, alternative modification methods are needed to improve protein functionality and preserve the nutritional values and acceptability of pea protein.

Cold atmospheric plasma (CAP), a physical nonthermal processing technology, has been widely explored in electronics, material science, medicine, and agriculture, and recently for food applications (Misra, Schlüter, et al., 2016). CAP has been investigated for microbial inactivation (Moldgy et al., 2020), pesticide dissipation (Sarangapani et al., 2016), and enzyme inactivation (Pankaj et al., 2013). Additionally, CAP has been studied as a protein modification method (Bußler et al., 2015; Ji et al., 2018; Segat et al., 2015). Protein structural changes, such as oxidation, unfolding, polymerization, and hydrolysis can be induced by highly reactive oxygen species (ROS) (O, O_3, OH, H_2O_2) and reactive nitrogen species (RNS) (NO, NO_2, NO_3) produced during CAP treatment (Gorbanev et al., 2018; Mirmoghtadaie et al., 2016; Misra et al., 2016). Such structural changes will impact protein functionality. Changes in protein structure and improvement in protein functionality have been reported. Segat et al. (2015), Ji et al. (2018), and Sharifian et al. (2019) reported unfolding of the protein and a consequent improvement of emulsifying and foaming properties of whey, peanut, and myofibrillar proteins, respectively, after CAP treatments. Another study reported an increase in pea protein solubility after CAP treatment (Bußler et al., 2015). These findings indicate that CAP maybe a promising protein modification approach to improve functionality. However, the literature lacks systematic

structure and functionality characterization of the protein modified by CAP and provides little information on the optimal CAP conditions and resultant reactive species for a directed enhanced in functionality. To this end, it is important to study the impact of individual plasma species and different plasma sources on pea protein structure and functionality.

1.2 Hypothesis and objectives

We hypothesize that plasma reactive species under acidic versus neutral conditions will have a larger impact on the pea protein structure and functionality. Four distinctive isolated plasma reactive species will have various impacts on the pea protein denaturation state, bond cleavage, and polymerization. Specific structural changes will result in enhanced gelation and emulsification properties. Additionally, plasma generated by different apparatus and gas mixtures will result in various profile of reactive species that will uniquely impact the structure and functionality of pea protein. Testing different conditions will allow the selection of the treatment that result in the most enhanced functional properties of pea protein.

Therefore, the overall objective of this project was to investigate the use of CAP under different conditions to produce a functionally- enhanced pea protein ingredient. The specific objectives were:

1) Determine the impact of isolated plasma reactive speices, as well as pH conditions and salt content on pea protein structure and functionality.

2) Determine the impact of different plasma generating apparatus, gas mixtures, and treatment time on pea protein structure and functionality.

1.3 Plant protein ingredients demand and market

The annual protein demand is over 202 million tons for the 7.3 billion world population (Henchion et al., 2017). The global population is predicted to reach 9.5 billion (Henchion et al., 2017) in 2025, and the global protein consumption is expected to double (Porritt et al., 2016). Other than the population growth, rising income, expanded urbanization, increased aging, and awareness of the health benefits of protein in the diet, contribute further to the increased demand for protein (Delgado, 2003; Henchion et al., 2017; Popkin et al., 2012). The global protein market was valued at $41.28 billion in 2020 and is projected to reach $76.47 billion by 2027 (Grand View Research, 2020). With the growth of overall protein demand, both plant and animal protein ingredients markets are growing rapidly (Ismail et al., 2020).

Although the current animal protein ingredients market size is larger than that of plant protein, the compound annual growth rate (CAGR) of animal ingredients market (4.88%) is lower than that of plant protein ingredient market (7.2%) during the 2020 - 2026 forecast period (MarketsandMarkets Research, 2021; Knowledge Sourcing Intelligence, 2020). The global plant protein ingredient market is projected to accumulate $15.65 billion in revenue by 2024 (Market Research Future, 2021). This marked growth is largely attributed to environmental concerns, realization of the health benefits of plant proteins, and animal welfare concerns. All these factors combined resulted in an increase in vegans, vegetarians, and flexitarians (Formanski & Analyst, 2019; Henchion et al., 2017).

Soy protein has dominated the plant protein market for decades due to worldwide cultivation, high nutritional quality, and good functionality. Soy protein ingredients are extensively used in baked products and cereals and are used as protein supplements in

foods targeting children and elders (Grand View Research, 2020). However, as one of the "Big Eight" allergens recognized by the Food and Drug Administration and a GMO ingredient, consumers who are allergic to soy protein and avoiding GMO products, are looking for alternative plant proteins.

Yellow field peas (*Pisum sativum L.*), a non-GMO crop with currently low occurrence of allergenicity, is gaining more attention as a good source of protein (Barac et al., 2010). The global pea protein market was valued at $214. 3 million and is expected to expand at a CAGR of 15% during 2021- 2028 forecast period (Grand View Research, 2021). Pea protein ingredients have acceptable nutritional quality, thus are incorporated in many food applications as alternatives to soy protein ingredients. However, the overall functionality of pea protein ingredients is lagging behind that of soy protein counterparts, hindering its expanded use (Söderberg, 2013).

Although the pea protein ingredients market size is increasing significantly, soy protein ingredients market is still the biggest plant protein ingredients market, valued at 9.98 billion dollars in 2019 (Reports and Data, 2020). To expand pea protein ingredients market and eventually replace soy protein ingredients, it is crucial to enhance their functionality. The following section will outline available ingredients, protein structure and functionality of soy protein followed by pea protein, to illustrate differences, limitations, and potential ways to enhance pea protein functionality.

1.4 Soy protein ingredients

Throughout East Asia, people have consumed traditional soy foods for more than two thousand years (Fukushima, 2011). Whole soybeans have been traditionally used to

make many soy-based products. Traditional soy products can be classified as non-fermented and fermented. Soymilk, tofu, soy nuts, and soy pulps are considered as non-fermented soy foods; fermented soy foods include soy sauce and natto (Liu, 2008). Starting in the 1960s, the United States developed processes to produce soy protein ingredients, including soy flour, soy protein concentrate (SPC), soy protein isolate (SPI), and soy protein hydrolysate (SPH), and added them into formulated foods as functional ingredients (Fukushima, 2011).

1.4.1 Soy flour

The two types of soy flour produced from soybeans are full-fat soy flour (FFSF) and defatted soy flour (SF), with approximately 40% and 56 - 59% protein content, respectively **(Table 1, Figure 1)**. Depending on the final particle size, products can be classified as flours or grits. In order to be labelled as soy flour, at least 97% of materials should pass through No. 100 sieve, while for soy grits, materials should pass through sieves in the broad range of No. 8 to No. 80 (Deak et al., 2008). FFSF is often used directly into bakery products and ground meat whereas SF, which has a higher protein content, is not only used in bakery products and ground meat applications, but also is the starting material for the further production of soy protein concentrate (SPC) and soy protein isolate (SPI) (Riaz, 2011).

Table 1. Composition (%) (on dry basis) and utilization of defatted soy flour, soy protein concentrate, and soy protein isolate.

Composition	Defatted flour and grits[1]	Soy protein concentrate[1]	Soy protein isolate[1]
Protein	56-59	65-72	90-92
Fat	0.5-1.1	0.5-1.0	0.5-1.0
Ash	5.4-6.5	4.0-6.5	4.0-5.0
Carbohydrates	32-34	20-22	3.0-4.0
Utilization	ground meat and bakery products	meat and bakery products; textured vegetable protein	infant formulas and nutritional supplementation; meat and bakery products; meat analogs

[1]Data sources: (Deak et al., 2008; Endres, 2001)

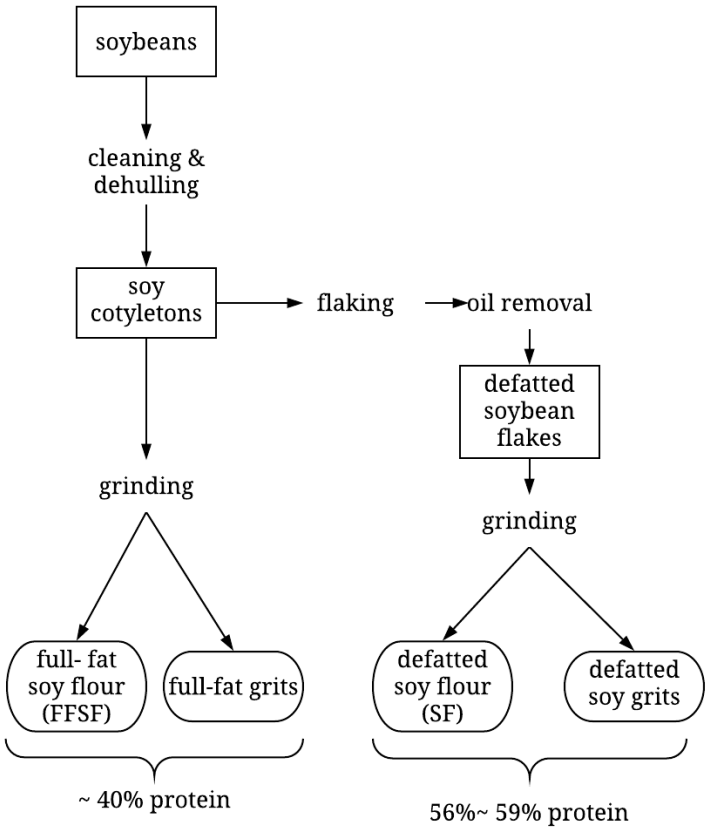

Figure 1. A schematic diagram of the production of full-fat and defatted soy flours and flakes from soybeans as described by Deak et al. (2008) and Riaz (2011).

1.4.2 Soy protein concentrate

Soy protein concentrate (SPC) is produced by removing small sugars and some flavor compounds from defatted soy flour and contains approximately 65 - 72% protein on dry basis (Riaz, 2011). Three different processing methods are used in industry to produce soy protein concentrates (Ma, 2015). One process involves the use of aqueous alcohol to extract alcohol soluble components, including sugars and flavor compounds, from the defatted flour. Another process involves the use of acid to precipitate proteins out and separate the protein from soluble sugars and soluble fiber. Lastly, is the process that utilizes aqueous thermal treatment to denature and precipitate proteins out. Insoluble components resulting from the three processes are SPCs **(Figure 2)**. Often, pH is adjusted to neutral followed by pasteurization and spray drying to obtain commercial SPC ingredients. SPC can be directly added into meat and bakery products or can be texturized to resemble meat products **(Table 1)**.

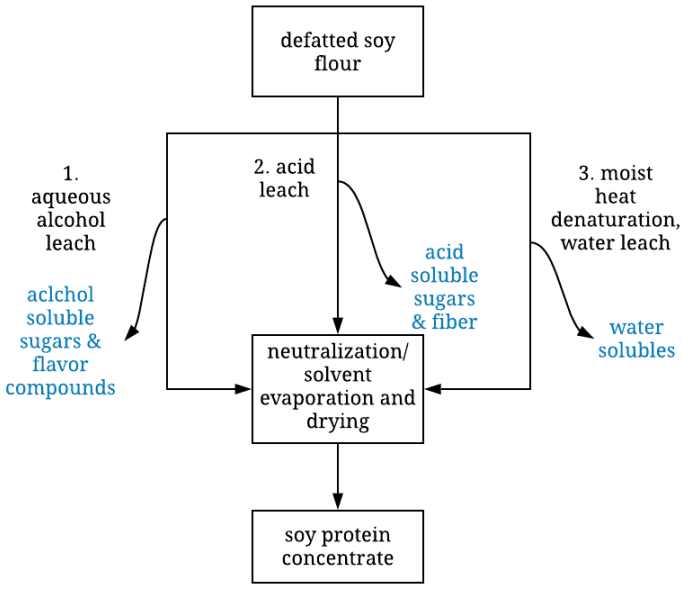

Figure 2. A schematic diagram of the production of soy protein concentrates from defatted soy flour as described by (Ma, 2015) and Riaz (2011).

1.4.3 Soy protein isolate

Soy protein isolate (SPI) is produced by removing not only soluble sugars and soluble fibers, but also insoluble fibers and other saccharides from soy flour, and contains at least 90% protein on dry basis (Deak et al., 2008). Alkaline extraction followed by isoelectric precipitation is the most common way of producing SPI in industry (Middelbos & Fahey, 2008). By solubilizing defatted soy flour under alkaline conditions (pH 7.5-9.5), insoluble fibers are removed, while soluble sugars and fibers, and proteins remain in solution. At the isoelectric point, proteins precipitate out of solution, and thus the proteins are further separated from the solubles. The precipitated protein is reconstituted in water followed by neutralization, pasteurization, and spray drying to obtain SPI. Salt extraction followed by salting out, reverse osmosis processing (UF-RO), and aqueous extraction are also used to produce SPI (Deak et al., 2008). However, these methods are not industrially common due to high associated cost of production and waste streams. SPI usually have good functional properties and is used in various food applications **(Table 1)**.

Both SPI and SPC contain low amounts of lipid, as the starting material is defatted soy flour **(Table 1)**. The major differences among SPI, SPC, and SF are the protein and the carbohydrate content, resulting in different functionalities suitable for various food applications.

1.4.4 Soy protein hydrolysate

Enzymatic hydrolysis is the main type of protein modification that has been industrially applied in the United States. SPI is used as the starting material to produce soy protein hydrolysates (SPH). Limited enzymatic hydrolysis is often carried out to enhance

functionality and bio-accessibility (Ashaolu, 2020; Tsumura et al., 2005). For instance, Zakaria and RF (1978) reported that SPH exhibited an improved emulsification capacity compared to SPI, while Were et al. (1997) reported an increase in foaming capacity and stability, and solubility after enzymatic hydrolysis.

Variations in functionality among commercially available SPH are caused by differences in the starting material, enzymes used (i.e., digestive, plant-origin, and microbial enzymes), pH, temperature, inactivation methods, and the resulting degree of the hydrolysis (DH). An improvement in solubility at pH 4.5 after enzymatic hydrolysis regardless of enzyme types was observed by Kim et al. (1990). However, alcalase hydrolyzed soy protein had a significantly higher solubility than liquozyme hydrolyzed soy protein (Kim et al., 1990). Tsumura et al. (2005) found that papain hydrolyzed soy protein had a significantly higher gel strength than pepsin hydrolyzed soy protein. Authors attributed differences in functionality to differences in resulting protein/peptide profile upon hydrolysis by different enzymes under different conditions.

SPH usually exhibit good nutritional quality, since the digestibility of soy protein is enhanced (Barać et al., 2004; Koopman et al., 2009). Additionally, SPH may have physiological benefits attributed to the presence of bioactive peptides (Barać et al., 2004). SPH can thus be promoted for physiological benefits such as prevention of obesity, cancer, and cardiovascular diseases (Ashaolu, 2019; Ashaolu, 2020). However, it is important to control hydrolysis and avoid excessive DH. A high DH usually causes loss of functionality as well as an increase of bitterness intensity. To better understand how the functionality or nutritional quality differs among soy protein ingredients, it is essential to understand the characteristics of soy protein.

1.5 Soy protein characteristics

1.5.1 Nutritional quality and health benefits

Dietary protein plays an essential role in the growth, maintenance, and repairment of the body. Essential amino acids, namely histidine, isoleucine, leucine, lysine, methionine, phenylalanine, threonine, tryptophan, and valine, cannot be synthesized in the body, therefore, it is crucial to include them in the diet (Smith, 2017). Thus, to formulate healthy and nutritious food products, protein quantity and quality must be considered. Protein quality is the combination of protein digestibility and amino acid composition (Smith, 2017). Protein quality can be determined by various assays, including protein efficiency ratio (PER), protein digestibility corrected amino acid score (PDCAAS), and digestible indispensable amino acid score (DIAAS) (Smith, 2017). Protein efficiency ratio is used to estimate the protein quality of infant food, while PDCAAS is used to determine the nutritional value of other foods as required by the Food and Drug Administration (FDA) (Smith, 2017; WHO, 1991).

PDCAAS is calculated by multiplying protein digestibility percentage and amino acid score, which is the amount of the first-limiting amino acid in a protein compared to that of a reference protein. The PDCAAS value for a specific ingredient/ product can range from 0 to1, where higher values represent better protein quality. The PDCAAS for soy protein ingredients ranges between 0.91 and 1.0, which is comparable to that of dairy and egg proteins (Joint et al., 2007; Van Vliet et al., 2015). Different soy protein ingredients have slightly different PDCAAS due to differences in isolation and processing conditions (Fukushima, 2011). Nevertheless, soy protein has the highest PDCAAS among all plant proteins.

With the well- balanced essential amino acids profile, soy protein is considered a complete protein (Hoffman & Falvo, 2004). In addition to excellent nutritional quality, soy protein also provides important physiological benefits. Numerous studies reported that consumption of soy protein can reduce the risk of heart diseases by lowering blood lipids levels, such as triglycerides, total cholesterols, and low-density lipoprotein (LDL)-cholesterol levels (Endres, 2001; Fukushima, 2011; Wong et al., 1998). Accordingly, in 1991 FDA released a statement confirming that the consumption of 25g of soy protein per day may reduce the risk of heart disease (Anderson et al., 1995). Soy protein has also been linked to muscle synthesis (Yang et al., 2012) and weight management (Koopman et al., 2009). In addition to nutritional and physiological benefits, soy protein also exhibits good functionality, which is mainly attributed to its unique protein components.

1.5.2 Soy protein components

Soy protein accounts for 38-44% of soybean seed mass, on dry basis. Soy protein fractions can be classified into two categories based on their physiological roles in the soy: storage proteins and bioactive proteins (Fukushima, 2011; Murphy, 2008). Storage protein does not have any biological activity in soy other than being reservoirs of nitrogen, sulfur and carbon. On the other hand, bioactive proteins such as enzymes and enzyme inhibitors (i.e., lipoxygenases and trypsin inhibitor) facilitates specific biochemical reactions in the soy (Fukushima, 2011). The storage proteins are the most abundant proteins in soy and accounts for around 80% of total seed proteins (Fukushima, 2011; Murphy, 2008).

Based on the sequential extraction of protein by different solvents, all seed proteins are classified into four categories: globulins (salt-soluble), albumins (water-soluble),

prolamins (alcohol-soluble), and glutelins (soluble in dilute acids or alkali) (Osborne, 1924). Globulins and albumins are the major proteins present in legume seeds. Storage protein fractions present in soy are globulin proteins.

Soy protein components are also classified based on their sedimentation coefficient (in Svedberg units, S), which is a factor of the molecular weight of the protein. A high sedimentation coefficient represents a large protein. The four main soy protein fractions are 2S, 7S, 11S, and 15S (Singh et al., 2015). 2S proteins are mostly enzymes and enzyme inhibitors, while 15S proteins are mainly different protein subunits associated together (Murphy, 2008; Singh et al., 2015). 11S glycinin and 7S β-conglycinin are the major storage proteins present in soy, which account for approximately 40% and 30% of the total seed protein, respectively (Maruyama et al., 2001). Since glycinin and β-conglycinin together account for around 70% of soy proteins and are the main contributors to the functionality of soy protein, it is important to understand their structure and assembly mechanism.

1.5.3 Glycinin and β-conglycinin structure and assembly mechanism

In mature seeds, 11S glycinin with the molecular weight of 300~380 kDa, is assembled as a hexameric protein, while in developing seeds, preproglycinin, a single polypeptide precursor is synthesized by gene expression **(Figure 3 & Figure 4)** (Prak et al., 2005). In the endoplasmic reticulum (ER), the signal sequence of preproglycinin is removed during the translation process, and the resultant proglycinin assembles into 8S trimers (Dickinson et al., 1989). The proglycinin trimers are transported to protein storage vacuoles (PSV) and is followed by a post-translational cleavage of the peptide bond between asparagine and glycine. The resultant mature monomer consists of an acidic (~ 40

kDa) and a basic (~ 20 kDa) subunit, α and β, respectively, associated by a disulfide linkage **(Figure 5)** (O'Kane et al., 2004). Finally, six monomers are assembled to form one hexameric 11S glycinin and stored in the dormant seed (Adachi et al., 2001).

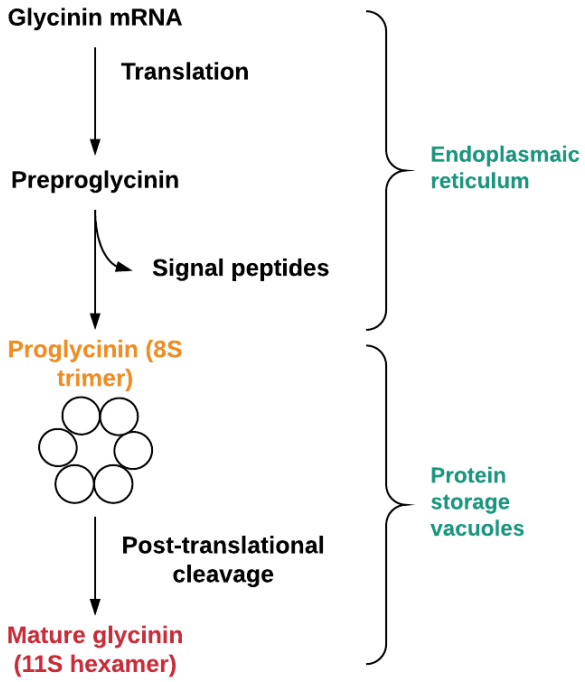

Figure 3. A schematic diagram of synthesis 11S hexametric glycinin sythesis as described by Prak et al. (2005), Dickinson et al. (1989), and Adachi et al. (2001).

The five major glycinin monomers are A1aB1b (53.6 kDa), A1bB2 (52.2 kDa), A2B1a (52.4 kDa), A3B4 (55.4 kDa) and A5A4B3 (61.2 kDa), which differ in their primary structure (Fukushima, 2011). According to the homology in their sequences, the five monomers are classified into Group I (A1aB1b, A1bB2 and A2B1a) and Group II (A3B4 and A5A4B3), with similarity of more than 84% in a group and 45- 49% between groups (Prak et al., 2005).

The structure and assembly mechanism of glycinin A3B4 homo-hexamer have been determined (Adachi et al., 2003) **(Figure 4)**. Three monomers are assembled into a trimer through strong hydrophobic interactions. Electrostatic interactions and hydrogen bonding **(Figure 6)** play an important role in linking the two trimers to form a stable hexamer (Adachi et al., 2003).

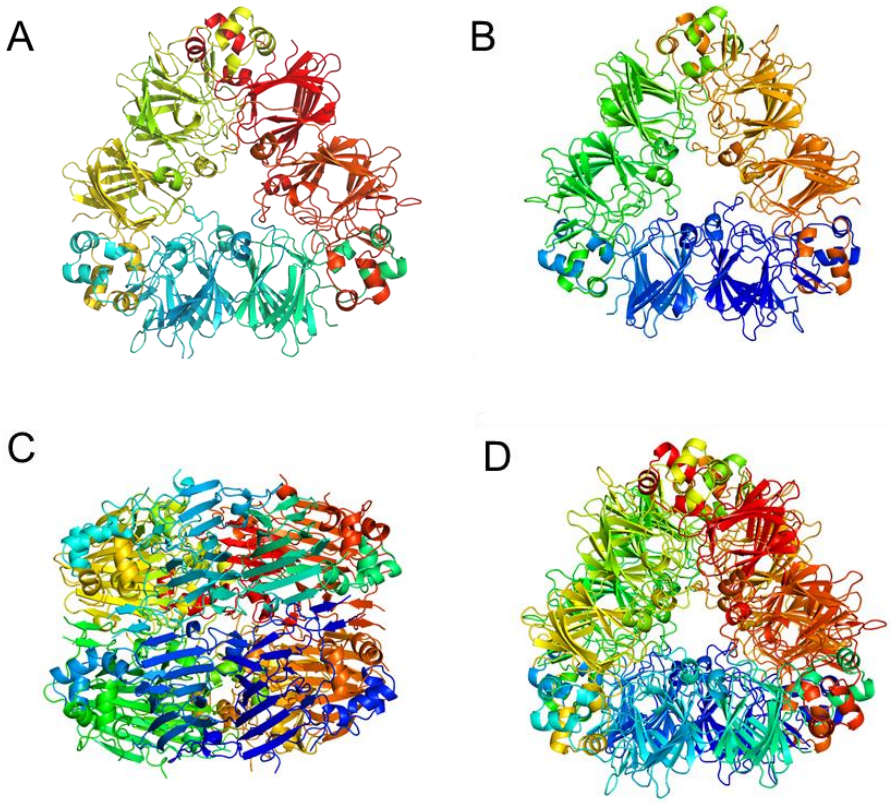

Figure 4. The crystal structure of the glycinin A3B4 homo-hexamer (PDB: 1OD5). (A) the glycinin homotrimers at the top of the glycinin hexamer. (B) the glycinin homotrimers at the bottom of the glycinin hexamer. (C) the side view of glycinin hexamer. (D) the top view of glycinin hexamer.

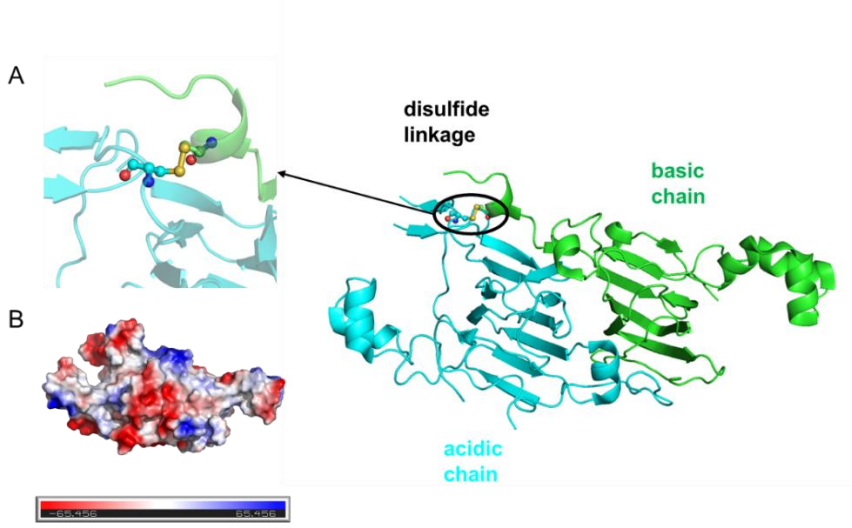

Figure 5. Disulfide linkage between the acidic chain and basic chain in the A3B4 monomer (PDB: 1OD5). (A) the -S-S- linkage. (B) the electrostatic potential surface of the A3B4 monomer.

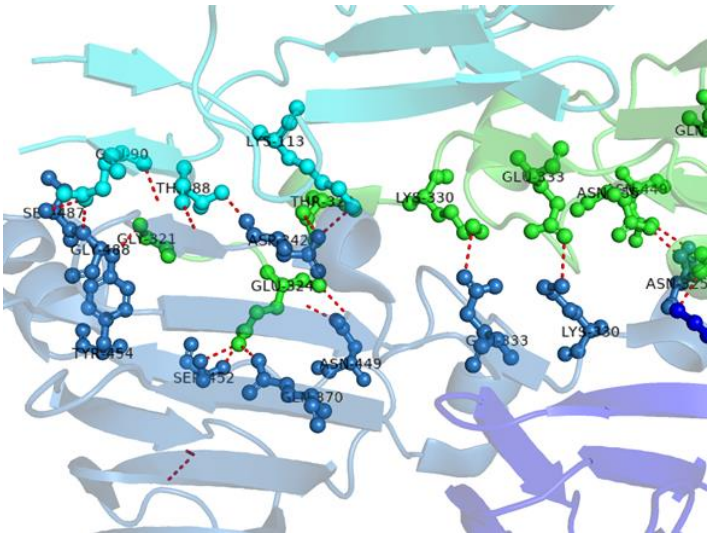

Figure 6. Hydrogen bonds and ionic bridges between two trimers of the glycinin A3B4 homo-hexamer (PDB: 1OD5).

β-conglycinin, with a molecular weight of 150~200 kDa, is assembled as a trimer (Fukushima, 2011). The three major subunits of β-conglycinin are α, α', and β subunits with molecular weights of 68, 72, and 52 kDa, respectively (Vu Huu & Kazuo, 1977). In

soybean seeds, many molecular species of β-conglycinin trimers are present, and seven of them are identified as α′β2, αβ2, αα′β, α2β, α2α′, α3 and β3 (Fukushima, 2011; Thanh & Shibasaki, 1978; Yamauchi et al., 1981).

There are two major differences between β-conglycinin and glycinin. First, glycinin subunits contain cysteine residues and disulfide bonds, whereas β-conglycinin subunits are devoid of disulfide bonds (Tandang-Silvas et al., 2010). Second, β-conglycinin is a glycosylated protein, while glycinin is not. The α, α' and β subunits are all glycosylated via asparagine residues, with one site in β (Asn 328) and two sites in α (Asn 199 and Asn 455) and α' (Asn 215 and Ash 471) (Murphy, 2008).

The structure of the native (glycosylated-) and recombinant (nonglycosylated-) β-conglycinin β homotrimers have been determined (Maruyama et al., 2001; Maruyama et al., 2003). Each subunit of the native β homotrimer has one glycosylated site at the Asn 328 position **(Figure 7)**. Interactions among the monomers are mostly hydrophobic. Hydrogen bonds and one ionic bridge were also found to contribute to the trimerization (Maruyama et al., 2001).

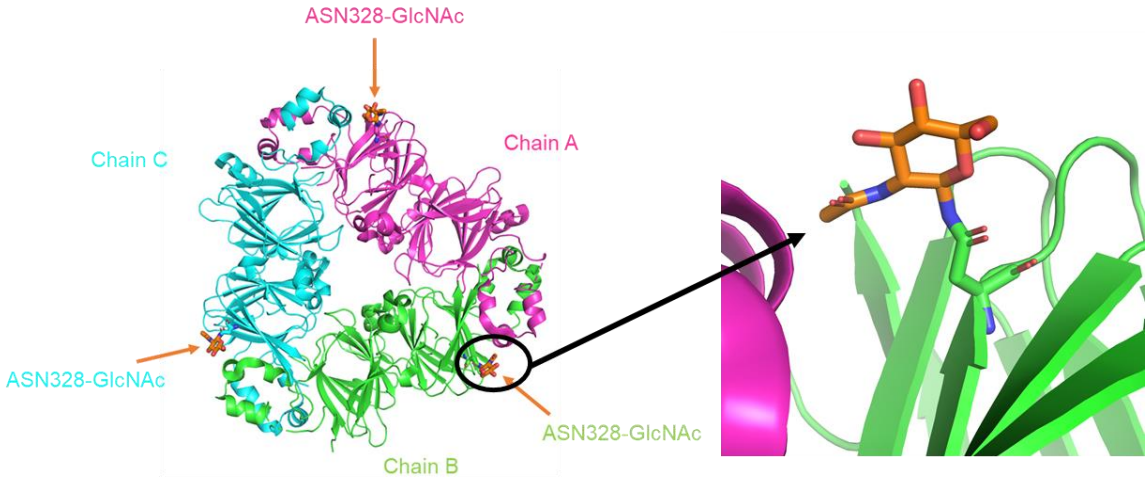

Figure 7. The crystal structure of native β-conglycinin β homotrimer and the asparagine 328 glycosylated sites (PDB: 1IPJ).

The core region of α, α' and β are highly homologous, while α and α' subunits have additional 125 and 141 amino-acid residues, respectively, present in N- terminal region. Because of the presence of the extended N- terminal region and higher amount of carbohydrates, scientists found that it is difficult to crystallize the entire sequence of α and α' homotrimers (Maruyama et al., 2004). Therefore, only the structure of the core region in α' homotrimers (α'_c) have been determined. The structure of α'_c and β homotrimers are highly similar because of the high sequence homology. However, there are still some differences in their structure. First, α'_c homotrimers are higher in surface hydrophobic residues and lower in surface charged residues, compared to β homotrimers. Second, although hydrophobic interactions are still the major intermolecular interactions, β homotrimers are also linked by ionic interactions. Third, α'_c homotrimers have larger total cavity volume. Overall, α'_c has lower thermal stability and higher structural flexibility (Maruyama et al., 2004). Therefore, the overall protein structure is largely attributed by the amino acid sequence of the protein (i.e., primary structure). Since the functionality of a protein is dictated by its structure, β-conglycinin and glycinin exhibit different functionality.

In fact, compared to glycinin, a smaller size β-conglycinin, associated mostly through non-covalent interactions, exhibits superior emulsification properties because of the easiness of moving to the oil/water interface and unfolding (Fukushima, 2011; Kinsella, 1979; Rickert et al., 2004). On the other hand, due to the presence of disulfide linkages and cysteine residues, as well as higher molecular weight, surface hydrophobicity and thermal stability, glycinin forms a stronger gel compared to β-conglycinin (Utsumi et al., 1997;

Yada, 2017). Glycinin is always recognized as a key contributor to the gelling properties of soy protein ingredients.

β-conglycinin is more soluble than glycinin due to several reasons. β-conglycinin is a glycosylated protein making it more hydrophilic. The high percentage of hydrophobic amino acids and the large molecular size contribute to poor solubility of the glycinin (Mo et al., 2006). On the other hand, β-conglycinin is more thermally labile (denatured at72 °C) (Renkema et al., 2001) than glycinin which denatures at 90°C (Hou & Chang, 2004). Both proteins are more soluble at alkaline pH compared to acidic pH and have an isoelectric point (pI) around pH 4-5.

Due to the structural differences, monomers within β-conglycinin exhibit different functionality. The lower thermal stability of α' and α subunits of β-conglycinin compared to β subunits as result of lack in intermolecular electrostatic interactions, resulting in better emulsification properties (Maruyama et al., 2004; Utsumi et al., 1997). In addition, due to the presence of the extended N- terminal region with a high amount of carbohydrates, α and α' subunits of β-conglycinin have higher solubility than β subunits (Maruyama et al., 2004).

Therefore, the functionality of soy protein ingredients is largely impacted by the type of glycinin and β-conglycinin monomers and the ratio of glycinin and β-conglycinin present in the ingredient. (Fukushima, 2011; Tzitzikas et al., 2006). The functional properties and potential applications of soy protein ingredients vary because of the differences in protein profile and structure.

1.6 Soy protein functionality

Proteins are used to in food formulation, not only for adding nutritional value but also for their functional properties. Proteins functional properties include solubility, water holding, viscosity, viscoelasticity, gelation, and emulsification. Proteins also contribute to flavor and color development (Hettiarachchy & Ziegler, 1994). Traditionally, animal-based protein ingredients have been widely used in various food applications. With a better understanding in structure and functionality, soy protein has been incorporated in food applications as alternatives to meat and dairy proteins, providing comparable nutritional value and functional properties (Thrane et al., 2017). With the advantages of the nutritional quality, functional properties, and affordability, soy protein ingredients have been used in beverages, meat products, bakery products, and frozen desserts (Hettiarachchy & Ziegler, 1994; Thrane et al., 2017). Due to the differences in protein content, the ratio of glycinin and β-conglycinin, as well as the protein structure as a result of different processing conditions, SF, SPC, SPI, and SPH are used in different applications **(Table 2)**.

The functional properties of defatted soy flour and grits are mainly hydration and color control (Endres, 2001). Defatted soy flour experiences minimal processing and thus the proteins remain relatively intact compared to other further processed ingredients (Endres, 2001). Native proteins in defatted soy flours and grits are less prone to aggregate and precipitate out and consequently exhibit good solubility for beverage application, and good hydration properties for meat applications. Due to mild processing conditions, defatted flour has high lipoxygenase activity. Therefore, soy flour is usually added into wheat dough systems to bleach carotenoids, resulting in the production of bread with white

color (Dubois & Hoover, 1981; Endres, 2001). With the presence of starch and fibers, soy flour and grits are added to soups and graves to increase the viscosity.

Table 2. Functional properties of soy protein ingredients in food system[1,2].

General property	Function	Mechanism	Food system	Soy protein ingredients
Hydration	Solubility	Hydrophilicity	Beverages	F, C, I, H
	Water absorption and binding	Hydrogen bonding, entrapment water	Meat, sausages, breads, cakes	F, C
	Viscosity	Hydrodynamic, water binding	Soup, gravies	F, C, I
Structural, textural and rheological	Gelation	Water entrapment and immobilization	Meat, curds, cheeses	C, I
	Cohesion- adhesion	Hydrophobic, ionic, and hydrogen bonding	Meat, sausages, baked goods, pasta products	F, C, I
	Elasticity	Hydrophobic, disulfide linkages	Meats, bakery items	I
Surface activity	Emulsification	Adsorption at interfaces, film formation	Sausages, bologna, soups, cakes	F, C, I
	Foaming	Interfacial adsorption, film formation	Whipped toppings, chiffon desserts, angel cakes	I, H
	Fat adsorption	Hydrophobic interactions	Meats, sausages, doughnuts	F, C, I
Organoleptic	Flavor- binding	Adsorption, entrapment	Simulated meats, bakery items	C, I, H
	Color control	Bleaching (lipoxygenase)	Breads	F

[1]Data sources: Endres (2001) and Hettiarachchy and Ziegler (1994)

[2]Abbreviation: F: soy flour, C: soy protein concentrate, I: soy protein isolate, and H: soy protein hydrolysate

In general, SPC exhibits good water holding and oil binding capacity, and has improved flavor compared to soy flour (Endres, 2001; Hettiarachchy & Ziegler, 1994). Flavor molecules are partially removed during the additional isolation steps of SPC production (Altschul & Wilcke, 2013). Slightly denatured protein due to the processing is able to interact with both water and oil, resulting in good emulsification properties. SPC

produced by different processing methods as described earlier (Figure 2) exhibit different functionalities. For instance, SPC produced by aqueous thermal treatment and alcohol extraction have denatured proteins and consequently have lower solubility, compared to SPC produced by acid precipitation. Therefore, SPC produced by acid precipitation is suitable for beverages, soups, and gravies (Altschul & Wilcke, 2013; Endres, 2001).

SPI exhibits good solubility, gelling properties, viscosity, and emulsification capacity, and thus can be used in various food products (Altschul & Wilcke, 2013). However, the functionality of SPI is largely impacted by the extraction protocols. For instance, Deak and Johnson (2007) reported that the solubility of SPI decreased when the temperature of alkaline extraction increased. The decrease in functionality is attributed to the higher degree of denaturation and surface hydrophobicity caused by elevated temperature. Usually, mild extraction conditions (low alkalinity and temperature) lead to better functionality due to the preservation of the native protein structure. The functionality of SPI is also influenced by the ratio of glycinin to β-conglycinin. SPI produced from a cultivar that has higher glycinin:β-conglycinin ratio exhibited better gelling properties due to higher cysteine residues (Morr, 1990).

SPH tends to be more soluble over a wider range of pH compared to SPI due to the presence of smaller molecular weight peptides, making it be suitable for acidic beverages (Lee, 2011). Foaming capacity and stability are also enhanced upon enzymatic hydrolysis, making SPH a good foaming agent (Endres, 2001; Kinsella et al., 1985). While SPH and all other soy protein ingredients are very functional and can be incorporated in many food applications, there are still some limitations for their continued use.

1.7 Limitation of soy protein

Even though soy protein is a complete protein and has physiological benefits, there are still two factors that limit the nutritional value of soy protein. Soy protein has relatively low amount of methionine that can easily be oxidized and degraded during processing and storage. The presence of enzyme inhibitors, such as trypsin and α-amylase inhibitors, decrease the digestibility of soy-based products and thus jeopardize its nutritional quality. Thermal processing can be used to inactivate such inhibitors and make products more desirable (Friedman & Brandon, 2001). Extensive thermal processing of soy protein, however, can be detrimental to the nutritional properties including less of essential amino acids and reduced digestibility.

Currently, one major concern related to soy protein products is allergenicity. Soy is one of the eight major food allergens that account for approximately 90% of reported allergenicity to food (Labeling & Act, 2004). Mandatory labelling of allergens is requested by FDA. Major allergens found in soybeans are glycoproteins (GlymBd 30k and GlymBd 28k), glycinin, as well as α and β subunits of β- conglycinin (Ma et al., 2010; Ogawa et al., 1991). Many studies investigated methods to reduce the allergenicity of soy proteins, including extrusion (Ohishi et al., 1994), thermal treatment (Son et al., 2000), enzymatic modification (Govindaraju & Srinivas, 2007) and glycation (Walter et al., 2016). While those methods are able to reduce allergenicity, none were effective in making soy protein hypoallergenic while maintaining its functionality.

Another major concern related to the use of soy protein ingredients is genetic modification. 94% of soybean in the US is genetically modified (GMO). Consumers who are looking for non-GMO products are likely to avoid soy- based products (Shahbandeh,

2020). In addition, consumers who prefer organic products are less likely to purchase products containing soy protein ingredients, since GMO ingredients are not allowed in products labeled as organic (Singh et al., 2008). Therefore, to address the growing global demand plant proteins, other alternative plant protein sources must be developed and promoted. Peas are of the most interest for various reasons as will be discussed in the following sections.

1.8 Pea protein market growth

Pea protein is gaining traction in the plant protein market, replacing soy protein in many applications. In 2020, the global pea protein market was valued at $214.3 billion and is projected to reach $641.1 billion in 2028 (Grand View Research, 2021). The growth of the pea protein ingredients market is driven by several factors. Peas are environmentally sustainable non-GMO crops, and have the low occurrence of allergenicity (Barac et al., 2010; Gwiazda et al., 1979). Additionally, pea protein has acceptable nutritional quality and modest functional properties. Accordingly, efforts toward manufacturing of functional pea proteins intensified over the past couple of decades. While utilization of pea protein in different food applications has rapidly increased, pea protein market is still lagging behind that of soy protein. To further expand the pea protein market, it is important to explore new manufacturing and processing technologies to enhance pea protein ingredient functionality.

1.9 Pea protein ingredients

There are several species of peas that are cultivated for protein ingredient production and for direct food uses. Fresh peas (snap and garden pea) are commonly sold

as canned or frozen, whereas yellow field peas (*Pisum sativum* L. subsp. *arvense*), also known as split peas and dry peas, are typically used for the production of pea protein ingredients (Elzebroek, 2008; Tulbek et al., 2017). There are four major pea protein ingredients available in the market: whole and dehulled pea flour, air classified pea protein concentrate, pea protein isolate, and pea protein hydrolysate (Arntfield & Maskus, 2011).

1.9.1 Pea flour and pea protein concentrate

The production of pea flour and pea protein concentrate (PPC) is illustrated in **Figure 8**. The starting materials are fresh yellow field peas that have a protein content of approximately 20% on dry basis. Cleaning to remove impurities is followed by seed dehulling which reduces fiber (~70% cellulose) and antinutrients (Tosh & Yada, 2010), and seed splitting. Unlike soy, peas are naturally deficient in fat and consequently do not need a defatting step (Gwiazda et al., 1979). Thus, the split peas are directly dry milled into either coarse or fine flours that have a protein content of 25-27% (Tulbek et al., 2017) **(Table 3)**. Pea flour can be directly used as an ingredient in baked products, cereal snacks and meat analogue (Maninder et al., 2007). Pea flour is rich in lipoxygenase, thereby is added into breads, cookies, and donuts to control the color (Tulbek et al., 2017). Pea flour, on the other hand, is added into cereal snacks as a nutritional supplement, due to the high lysine content, which is the limiting essential amino acid of cereals (Tulbek et al., 2017). Additionally, pea flour exhibits similar functional properties like soy flour does, such as water binding, oil binding, and emulsification. Therefore, pea flour is often added into meat analogues as a texture improver (Tulbek et al., 2017). In addition being added directly into

food products, fine flour can be further processed to produce PPC by air classification (Tyler et al., 1981).

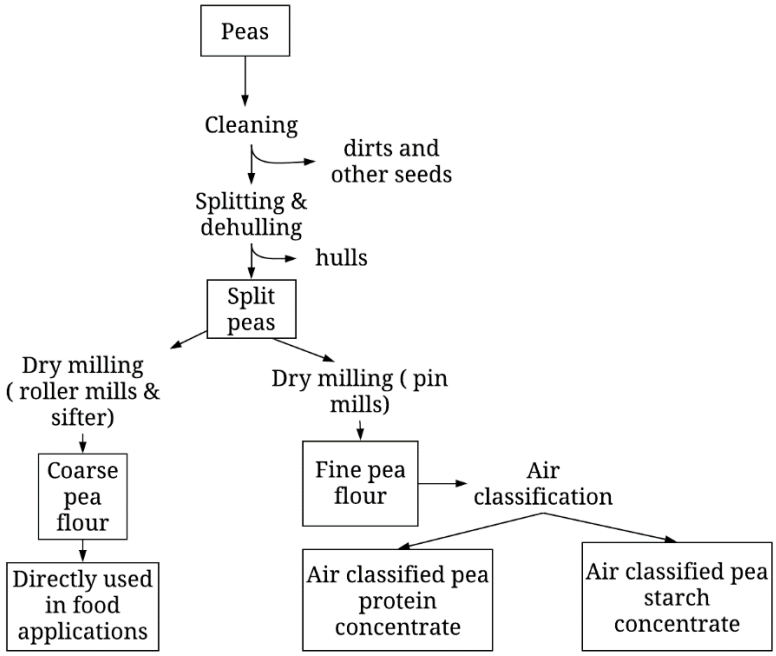

Figure 8. A schematic diagram of the production of pea flour and pea protein concentrate as described by Tulbek et al. (2017), Tosh and Yada (2010), and Reichert (1982).

Table 3. Proximate analysis of whole pea, dehulled split pea, pea protein concentrates, pea protein isolates on dry basis.

	Protein (%)	Starch (%)	Fat (%)	Ash (%)
Whole pea	21-24[1]	42-46	1.5-2.0	1.9-2.2
Pea flour	25-27	46-52	1.5-2.0	2.3-2.5
Pea protein concentrate	48-55	5-10	2.5-3.0	2.7-3.1
Pea protein isolate	~ 90	~6	~1	~3

[1]Data sources: (Arntfield & Maskus, 2011; Barac et al., 2010; Feyzi et al., 2018; Tulbek et al., 2017)

During air classification, a clean label fractionation technology, heavy particle fractions (starch rich fraction) is separated from light particles fraction (protein rich fraction) by air stream (Reichert, 1982; Tulbek et al., 2017). The protein content of the

resultant two fractions, PPC and pea starch concentrate is 46-63% and 5-10%, respectively **(Table 3)**. Water-binding, oil-binding, foaming and emulsifying properties are major functional properties of PPC; thus, it is incorporated into food applications such as meat and bakery products, similar to SPC.

1.9.2 Pea protein isolate

Since air classification is limited in concentrating the protein component to no more than 65%, wet processing is used to obtain products with a higher protein content (85~92%) (Arntfield & Maskus, 2011) **(Table 3)**. Alkaline extraction, salt extraction, and micellar precipitation can be used to produce pea protein isolates (PPI) (Stone et al., 2015; Tanger et al., 2020). Acidic extraction and ultrasonic assisted alkaline extraction methods have also been reported (Feyzi et al., 2018; Wang et al., 2020). However, alkaline extraction is most commonly utilized industrially.

Alkaline extraction starts with the dispersion of pea flour at a pH between 7 and 10 to solubilize the protein and separate it from starch and insoluble fiber. The solubilized protein is then precipitated at its isoelectric point (4~5) to separate it from soluble sugars, color, and soluble fibers. The precipitate is resuspended in water at pH 7, pasteurized and spray dried to obtain final PPI (Feyzi et al., 2018). Higher extraction pH is often used to increase protein yield, but it is detrimental to the functional properties.

PPI, as a functional ingredient, has been added into various foods, such as beef patties (Baugreet et al., 2016), and salad dressing (Ma et al., 2016). In addition, PPI is added into gluten-free products as a replacement of cereal proteins (Han et al., 2010).

1.9.3 Pea protein hydrolysate

Pea protein hydrolysate (PPH) are produced by hydrolyzing PPI with a variety of enzymes under different conditions. Accordingly, several PPHs that vary in functional properties are available in the market. Differences in functionality are attributed to the enzymes and conditions used to produce PPH. Considerable research has been conducted to determine the functionality of the PPH produced by different enzymes (Barać et al., 2011; Humiski & Aluko, 2007). Tamm et al. (2016) reported that trypsin PPH formed smaller oil droplets and stabilized interfacial tension better than alcalse PPH because of the increased surface charge and less aggregation. Klost and Drusch (2019) also reported the improvement in emulsion stability upon trypsin hydrolysis. Barać et al. (2011), on the other hand, reported that chymosin hydrolysis resulted in improved solubility, emulsification and foaming of PPI. The functional properties of PPH and other pea protein ingredients are not only impacted by isolation and processing conditions, but also are impacted by the inherent protein characteristics.

1.10 Pea protein characteristics

1.10.1 Nutritional quality and health benefits

Peas have a lower protein nutritional quality compared to soy. The protein PDCAAS of pea protein ranges between 0.597~0.889, which is lower than that of soy protein (0.9~1.00) (Arntfield & Maskus, 2011). There are several reasons why pea has a lower PDCAAS value. Compared to soy, peas contain a higher amount of antinutrients such as tannins, raffinose, and verbascose, which limit protein digestibility (Tulbek et al., 2017). Additionally, the overall essential amino acid content is less in peas than in soybeans

(Stone et al., 2015; Tulbek et al., 2017). Specifically, peas are deficient in essential sulfur-containing amino acids, methionine and cysteine. However, pea protein has better nutritional quality than other protein sources such as grains. The nutritional quality of pea protein is impacted by cultivar, environment, and processing. The protein content of peas is highly variable, with the lowest being 13.7% and highest 27.5% protein (Nosworthy & House, 2017). Pea protein isolates and concentrates have enhanced digestibility compared to pea flour because of reduced level of antinutrients and increased level of protein (Boye & Ma, 2015; Rutherfurd et al., 2015).

Even though the nutritional quality of pea protein is inferior to that of soy protein, pea protein exhibits physiological benefits similar to that of soy protein. Sirtori et al. (2012) reported that the intake of pea protein along with soluble fibers reduced plasma total and LDL-cholesterol level. Other physiological benefits include improved gut microbiota (Świątecka et al., 2012; Tong et al.) and athletic performance (Babault et al., 2015).

In addition to nutritional and physiological benefits, pea protein must exhibit good functionality to be successfully incorporated into food products. Functional properties are affected by protein profile and structural properties.

1.10.2 Pea protein components

Similar to soy, the most abundant proteins in peas are globulins, representing 50~82% of total seed proteins depending on genetic variations and environmental factors (Tzitzikas et al., 2006). 11S legumin and 7S vicilin are the two major globulins in peas, accounting for 6~25% and 25~52% of total seed proteins, respectively. 8S convicilin is a third type of globulin only present in peas, and its content ranges from 4~9% (Tzitzikas et

al., 2006). Albumins (2S) are the second most abundant proteins in peas, contributing 18~25% of total seed proteins (Lu et al., 2019). Prolamins and glutelins are present only in a small amount, ranging from 4% - 5% and 3% - 4%, respectively. The globulins, legumin, vicilin and convicilin, are the main proteins contributing to the functional properties of pea protein ingredients. Their structural characteristics dictates their functionality. The following section will summarize differences in the structural characteristics of the main globulins in peas.

1.10.3 Structural characterization of legumin, vicilin and convicilin

Similar to glycinin in soy, legumin in peas consists of six monomers, each consisting of an (α) acidic chain (~40 kDa) and a (β) basic chain (~ 20 kDa) linked by one interchain disulfide linkage (Barac et al., 2010). Based on the homology of the peptide sequence, monomers can be classified into three families: LegA family (LegA, A2, B, C, and E), LegJ family (LegJ, K, L, and M), and LegS family (LegS is the only monomer in this family). The molecular weight of monomers in LegA and Leg J families is 60-65 kDa, while the molecular weight of LegS monomer is around 80 kDa (Altschul et al., 1966; Tzitzikas et al., 2006). The synthesis pathway and assembly mechanism of legumin are identical to that of glycinin in soy. Three monomers are assembled into a trimer mainly through strong hydrophobic interactions. Through electrostatic interactions and hydrogen bonds, two trimers are assembled to a hexameric form.

Vicilin, similar to β-conglycinin in soy, consists of three subunits that associate through hydrophobic interactions to form a trimer. Unlike legumin monomers, none of the vicilin monomers contains inter- or intra-chain disulfide linkages. Trimeric vicilin is a

heterogeneous protein that has a molecular weight of 150 kDa to 170 kDa (Gatehouse et al., 1982). The molecular weight of each subunit is around 47 kDa to 50 kDa. Some subunits have "nicks" caused by post-translational cleavages and are broken down into small fractions in mature seeds (Gatehouse et al., 1983). The resultant vicilin fractions are α, β, γ, βγ, and αβ with the molecular weight of 19 kDa, 13.5 kDa, 12.5 kDa, 30 kDa, and 33 kDa, respectively. These fractions are associated through noncovalent interaction within the monomer (Tzitzikas et al., 2006). Vicilin is a glycosylated protein with the glycosylated site close to the C terminus of each subunit (Badenoch-Jones et al., 1981).

Convicilin is a trimer with a molecular weight of ~210 kDa. Each subunit is around 70 kDa (Tzitzikas et al., 2006). The amino acid sequences of the convicilin subunits are homologous to that of vicilin subunits but has a highly charged extended N- terminus (Bown et al., 1988).

While the structure of 11S legumin and 7S vicilin in pea is similar to that of 11S glycinin and 7S β-conglycinin in soy, the ratio of 7S to 11S (1.2~8) in peas is higher than that in soy (0.47~0.79) (Tzitzikas et al., 2006). Significantly lower amount of 11S legumin present in pea compared to soy, contributes to differences in their functionality.

1.11 Pea protein functionality and limitations

While there is the structural similarity in the storge proteins present in soy and pea, their functional properties of are not similar. However, the inferior pea protein functionality compared to that of soy is largely attributed to differences in protein profiles. The amount of 11S legumins present in pea, which is 6~25% of the total seed protein, is less than that of 11S glycinin in soy, which accounts to about 40% of the total seed proteins (Maruyama

et al., 2001; Tzitzikas et al., 2006). The presence of 11S globulins is crucial for the gelation properties since it is the only globulin that contains cysteine residues and disulfide linkages, which are important for the formation of strong gels (Tzitzikas et al., 2006). Thus, with less amount of 11S legumin proteins, pea protein exhibits inferior gelling properties in comparison to soy protein. Bildstein et al. (2008) reported that the gel strength of PPI was lower than that of SPI. Instead of forming rigid and transparent gels, PPI formed unstructured and opaque gels like pastes (Shand et al., 2007; Söderberg, 2013). The importance of 11S globulin in gel formation is proved by Bora et al. (1994), who observed that the hardness of pea protein gels increased with the increase in legumin concentration. Additionally, the amount of albumin present in pea (8~25%) is higher than that in soy (<10%) (Lu et al., 2019). 2S albumins are low molecular weight non-functional proteins (González-Pérez & Arellano, 2009). However, 2S albumins are high in cysteine, and thus have the potential to associate into high molecular functional proteins through disulfide linkages induced by processing conditions or targeted modifications (González-Pérez & Arellano, 2009).

Pea protein, on the other hand, exhibits comparable foaming properties as soy protein (Arntfield & Maskus, 2011). This is largely attributed to pea protein being rich in vicilin, which is a soluble and flexible protein. Vicilin can unfold easier than legumin due to its lack of disulfide linkages, and thus can quickly migrate to the interface of water and air and exhibit good foaming properties (Barac et al., 2012; Tulbek et al., 2017).

The solubility of pea protein is largely impacted by processing conditions and extraction techniques. Harsh extraction and processing conditions, such as high extraction pH, high solubilization temperature, and spray-drying, usually result in denaturation of the

protein and formation of high molecular aggregates, thereby lowering the solubility of pea protein ingredients (Stone et al., 2015). Gao et al. (2020) reported that the solubility of PPI decreased with increasing extraction pH. PPI extracted at pH 9 contained the highest content of aggregates and exhibited the lowest solubility. Stone et al. (2015) reported that salt extracted PPI exhibited higher solubility than pH extracted PPI because the salt extracted PPI was less denatured than pH extracted PPI.

The protein profile of pea protein is also impacted by different cultivars and consequently result in different functional properties. O'Kane et al. (2005) found that the gel strength of pea protein isolates is associated with differences between cultivars that differ in the amount of the sulfur-containing amino acids. As aforementioned, cysteine residues can form disulfide linkages which is crucial for the formation of 3D gel matrix. Therefore, cultivars containing less cysteine resulted in a weaker gel.

Therefore, breeding efforts in cultivating peas high in legumin and low in albumin, and optimization of extraction and processing conditions could obtain pea protein ingredients with better functionality. However, to further improve the functional properties of pea protein ingredients and compete with soy protein ingredients, protein modification is needed to alter the structure of the protein.

1.13 Protein modification

Protein modification refers to the alteration of the protein structure to improve protein functionality, reduce allergenicity, or increase nutritional value (Schwenke, 1997). Traditional modification techniques include chemical modification, enzymatic hydrolysis, Maillard-induced glycation, and physical processes.

Studies have shown that chemical modification methods such as acylation and phosphorylation significantly improve the solubility and emulsifying and foaming properties of pea protein (Johnson & Brekke, 1983; Liu et al., 2020). Due to nutritional loss, the formation of toxic compounds, and the non-eco-friendly processes, chemical modification methods of food proteins are mostly presented in patent and literature and are not allowed in the US food industry (Feeney, 1977; Ge et al., 2020).

Enzymatic hydrolysis, on the other hand, is widely used in industry to produce PPH with improved functionality and nutritional value (Ge et al., 2020). However, the improvement in functionality is not sufficient enough for PPH to replace soy protein ingredients. Additionally, hydrolysates have bitter tastes due to the release of hydrophobic peptides, compromising their sensory value (Arteaga et al., 2020).

Maillard-induced glycation is the covalent reaction between the carbonyl groups of reducing sugars and reactive amino groups of proteins (Liu et al., 2012). Lysine, because of the presence of ε-amino group, is a highly reactive amino acid in Maillard- induced glycation. Pea protein is rich in lysine, which makes it suitable for this modification. Maillard-induced glycation has been shown to improve the solubility of pea protein (Kutzli et al., 2020). Enhanced solubility is contributed to increased net surface charge and steric hindrance. However, Maillard reaction is very complex and hard to control. Research in this area is only emerging, thus further investigations are required to make the process industrially feasible with limited adverse effects, such as undesirable browning, the production of advanced glycation products (Lin et al., 2020).

Traditional physical modifications of food proteins such as dry heating, steaming, and pressurization have been studied for decades (Mirmoghtadaie et al., 2016). Heat is a

key component of traditional physical modification methods, which can induce partial denaturation of proteins and the formation of high molecular weight polymers (Mirmoghtadaie et al., 2016). The resultant denatured proteins have a more flexible structure compared to native proteins and thus can easily migrate to oil: water or air: water interfaces, thereby exhibiting higher emulsifying and foaming properties (Chao & Aluko, 2018; Chao et al., 2018; Pietrysiak et al., 2018). Gelation, on the other hand, is improved by the presence of high molecular weight proteins upon heating. Soluble proteins with large molecular weight are prone to form a strong continuous 3D gel networking, whereas small molecular weight proteins and insoluble aggregates are unable to form a good protein network to hold water (Mirmoghtadaie et al., 2016). The biggest concern of high temperature processing is the reduction of nutritional quality attributed to a significant loss of lysine due to the Maillard reaction, and a decrease in digestibility due to excessive polymerization (Björck & Asp, 1983; Mirmoghtadaie et al., 2016). Additionally, traditional physical modifications require high energy input, which makes them costly. Also, insoluble aggregates formed during traditional physical modifications may hinder the extent of the improvement in functionality (Mirmoghtadaie et al., 2016). Accordingly, alternative energy-efficient and low-temperature modification method must be explored.

1.14 Cold atmospheric plasma (CAP)

Plasma, the fourth state of matter, is produced by subjecting gases, such as air, oxygen, and argon, to high electrical energy. Depending on the temperature, plasma can be classified into thermal plasma (~ 15,000 K) and nonthermal plasma (mostly below 5,000 K) (Lu et al., 2016; Misra, Schlüter, et al., 2016). Cold plasma for biomedical applications

operates typically below 100 °C. Based on the generation condition, cold plasma can be classified into low pressure cold plasma and cold atmospheric pressure plasma (CAP). Different configurations are needed to generate atmospheric pressure plasma and low-pressure plasma. CAP is cheaper to operate than low pressure plasma because there is no need for vacuum system.

CAP, a novel physical modification method, operates at low temperature, and demonstrates high energy efficiency. CAP is produced by subjecting gases, such as air, oxygen, and argon, to high electrical energy between two electrodes. The resultant ionized gas is a cocktail of highly reactive oxygen species (ROS) (O, O_3, OH, H_2O_2) and reactive nitrogen species (RNS) (NO, NO_2, NO_3) (Gorbanev et al., 2018; Graves, 2012).

The reactive species in CAP (gas phase) can be directly applied to dry samples, or to samples in solution. CAP interacts with water to form additional reactive species, such as hydroxyl radicals, hydrogen peroxide, nitrous and nitric acids (Samukawa et al., 2012). Gas phase plasma only have surface effects and the penetration of reactive species (O, O_3, and NO) into dry food materials depends on the food composition, moisture content, as well as the porosity. Thus, gas phase plasma is usually applied to decontaminate food with limited penetration depth, whereas in liquid phase, plasma species can interact with all surrounding components (Gorbanev et al., 2018; Surowsky et al., 2016). Based on the plasma-liquid interactions, plasma-liquid systems can be classified into direct discharges in liquid and discharges in the gas phase over a liquid (Bruggeman et al., 2016). During direct plasma treatment, not only long-lived reactive species are persistently present during the treatment, but short-lived radicals, atomic and molecular species, and electrons are also transferred into the liquid (Gorbanev et al., 2018).

1.15. Cold atmospheric plasma sources

Dielectric barrier discharge, corona discharge, glow discharge and plasma jet are prominent CAP sources that have been used in food science related research (Lu et al., 2016; Muhammad et al., 2018; Tolouie et al., 2018). The generation principles of those configurations are described below.

1.15.1 Dielectric barrier discharge

Dielectric barrier discharge (DBD) is defined by its configuration, where the current and charge transfer are limited by the dielectric barrier layer covering the electrode (Lu et al., 2016). Since the insulating materials (glass, ceramics, silicon, quartz and polymers) can avoid plasma transfer into a spark or an arc discharge, DBD is a safe configuration to generate CAP (Bruggeman et al., 2017; Lu et al., 2016). Also, DBD is one of the most effective plasma configurations that can produce O_3 (Bahrami et al., 2016). DBDs can be generated by using alternate current (AC) (1-100kV, 50HZ – 1MHZ) or pulsed voltage. Power source, the energy input, is associated with the intensity of plasma species, whereas gas type is related to the type of plasma species (Lu et al., 2016).

There are various DBD electrode arrangements that can be used to produce CAP (Bruggeman et al., 2017; Lu et al., 2016; Tolouie et al., 2018), which are depicted in **Figure 9**. For example, volume DBD is comprised of two electrodes separated with a gap, and the insulating materials can be placed on one electrode or two electrodes **(Figure 9 a, b, c)**. Atmospheric DBD plasma jet is another popular configuration **(Figure 9 d)**. In order to call a plasma jet as a DBD plasma jet, the frequency of the voltage should match with that of typical DBD (Bruggeman et al., 2017; Lu et al., 2016).

Among various plasma sources, DBD is one of the most cost-effective CAP sources (Subedi et al., 2017). In addition, DBD effectively generates highly reactive plasma species, and has been widely used in many applications, including material science, biomedical science, and food and agriculture science (Subedi et al., 2017).

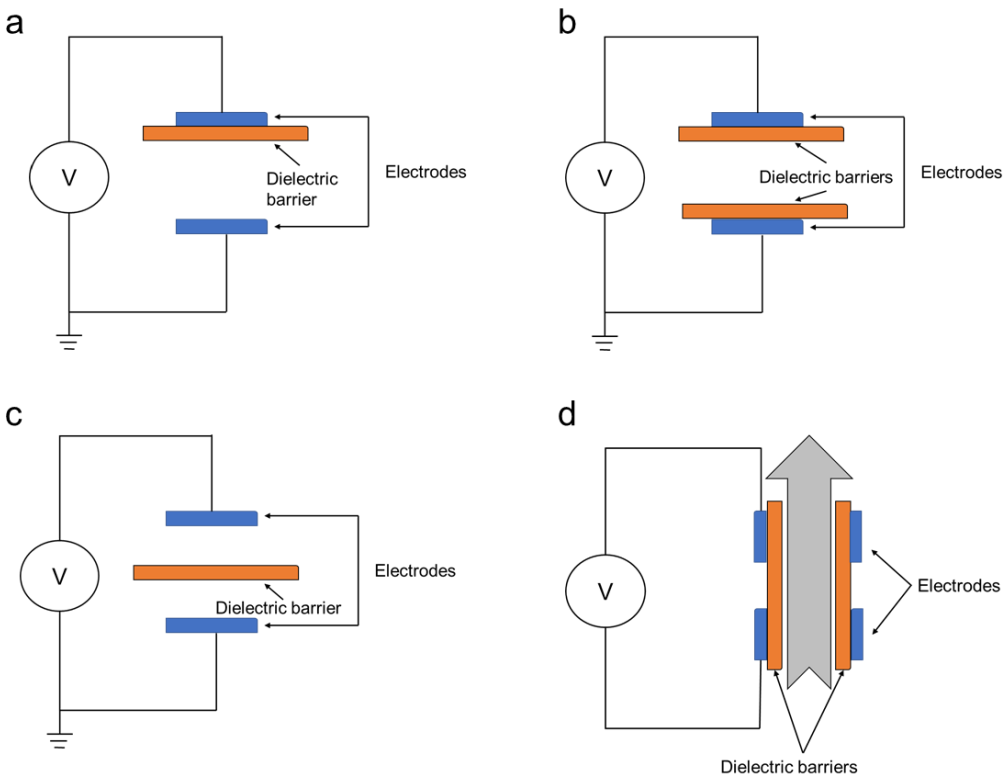

Figure 9. Typical configurations of dielectric barrier discharge as adapted from Tolouie et al. (2018), Bruggeman et al. (2017) and P. Lu et al. (2016).

1.15.2 Corona discharge

The generation of corona discharge requires high electric field at atmospheric pressure. Usually, near a sharp point or a thin wire, electric field is high enough to initiate the ionization process of the gas used and develop an illuminated region, called “corona” **(Figure 10)**. Active anode and cathode electrodes are referred to as positive and negative corona discharge, respectively (Lu et al., 2016; Muhammad et al., 2018; Tolouie et al.,

2018). The application of corona discharge is limited because of the restricted area of the discharge (Subedi et al., 2017). Corona discharge is not commonly used in agriculture or food science area, but is commonly used in electrophotography because the small dimension of charge can be incorporated into a printer (Chang et al., 1991).

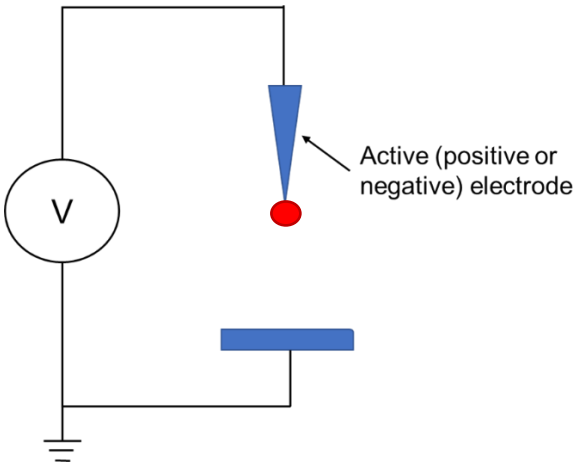

Figure 10. The typical configuration of corona discharge as adapted from Tolouie et al. (2018), Bruggeman et al. (2017) and P. Lu et al. (2016).

1.15.3 Glow discharge

Glow discharge is a well-studied and self-sustained plasma discharge widely used in analytical spectroscopy (Marcus & Broekaert, 2003), textile industry (Samanta et al., 2006), and seed germination (Braşoveanu et al., 2015). Unlike corona discharge, glow discharge is a homogenous and stable plasma source. With the high electron densities and the large size of the glow, glow discharge can efficiently infuse nitrogen species in aqueous solution, and the resultant plasma activated water (PAW) in large volume is suitable for treating large quantities of grains for germination (Lindsay et al., 2014).

Generally, glow discharge is easy to be produced and operated under low pressure. With elevated pressure, glow discharge is prone to be unstable and transfer into a spark

(Lu et al., 2016). Thus, special configurations are needed to obtain stable and uniform glow discharge at atmospheric pressure. For instance, the frequency of power supply should be higher than 1 kHz, dielectric barriers are needed, and the operating gas is best be helium (Lu et al., 2016; Okazaki et al., 1993).

1.15.4 Atmospheric pressure plasma jets

Atmospheric pressure plasma jet (APPJ) is a broad concept, which includes any plasma source with an open electrode and projection of plasma species into an open area (Winter et al., 2015). The unique characteristic of plasma jet configuration is that it can project stable plasma effluent out of a nozzle into another environment. For example, thermal arc jet is a conventional plasma jet that is widely used in the material industry for applications such as etching and cutting (Jeong et al., 1998). APPJs are also popular in biomedical sciences such as wound healing and dental treatment because they can be made in different sizes, as well as operated with various power supplies (AC, DC, RF, pulsed and microwave) and gases (Lu et al., 2016). In recent years, APPJ has been used in food safety and quality applications, such as inactivation of microorganisms (Liao et al., 2017) and enzymes (Misra et al., 2016). However, due to its small dimension, APPJ is commonly used for treating samples in small quantity (Jiang et al., 2020).

1.16 Potential use of CAP for pea protein modification

Since CAP is comprised of a cocktail of ROS (O, O_3, OH, H_2O_2) and RNS (NO, NO_2, NO_3), many chemical reactions can happen in a food system (Gorbanev et al., 2018; Mirmoghtadaie et al., 2016; Misra, Schlüter, et al., 2016). While considerable research

focused on microbial inactivation, enzyme inactivation, pesticide dissipation, and starch modification, there is limited research regarding the use of plasma for protein modification (Misra, Schlüter, et al., 2016). The basic mechanism of protein modification using CAP is through changing the protein structure by oxidation, bond cleavage, unfolding, and polymerization. Such changes will consequently impact protein functionality.

Several studies reported changes in protein structure (primary, secondary and quaternary structure) and functionality (solubility, foaming, and emulsification) after CAP treatment. Nyaisaba et al. (2019) reported the reduction in free sulfhydryl groups and the formation of high molecular weight protein aggregates after DBD treatment of squid mantle protein, along with an increase in water holding capacity and enhancement in gelling properties. The improvement in functionality was largely attributed to the formation of high molecular weight polymers through disulfide linkages induced by oxidation (Meinlschmidt et al., 2016). Furthermore, Ji et al. (2018) reported an increase in β-sheet content and a decrease in enthalpy, along with improved emulsification and water holding capacity, after DBD treatment of peanut protein. The observed structural changes in the study revealed that DBD resulted in protein unfolding. Unfolded protein is more flexible than globular proteins and thus easily migrates to the oil/water interface, exhibiting good emulsification properties. Segat et al. (2015), Ekezie et al. (2019), and Sharifian et al. (2019) also observed protein unfolding and improvement in foaming and emulsification properties after DBD and APPJ treatment of whey and myofibrillar proteins.

Protein unfolding and polymerization through disulfide linkages were the two major reported structural changes induced by CAP, according to those studies. With the insufficient amount of legumin but high amount of albumin rich in cysteine residues, CAP

becomes a promising technology to improve the poor gelling properties of PPI through polymerization of sulfur-containing amino acids. Unfolding caused by CAP has the potential to improve the emulsification of pea protein as well.

While the reported findings are promising, it remains unclear how plasma-induced structural changes impacted functionality of pea protein. The link between different plasma species and the observed structural changes, and consequent functional enhancement, is not demonstrated in studies on the impact of CAP on protein functionality. Additionally, only remote dielectric barrier discharge (DBD) and atmospheric pressure plasma jet (APPJ) that generate long-lived reactive species, have been investigated in protein modification studies. Other plasma sources that can generate short-lived reactive species (NO, OH, singlet oxygen, and electrons) are worth investigating further to obtain optimal conditions for pea protein functionalization.

1.17 Summary and conclusions

Although the pea protein ingredients market size is increasing significantly, soy protein ingredients market remains the biggest plant protein ingredients market. 11S and 7S globulins are the major functional storage proteins present in both soy and pea, however, in different proportion resulting in different functional properties. Unlike soy, pea contains less 11S proteins, resulting in inferior functionality. Protein structure and profile can be altered, and consequently functionality can be enhanced by modifications.

CAP is a favorable physical modification method that can induce unfolding and polymerization. With the insufficient amounts of legumins but high amounts of albumins rich in cysteine residues, CAP-induced polymerization could result in enhanced pea protein

functionality, namely gelation and emulsification. However, the link between different plasma species and structural changes, and consequent functional enhancement, is unclear. In addition, only remote dielectric barrier discharge (DBD) and atmospheric pressure plasma jet (APPJ) have been investigated in protein modification studies. None of the other plasma sources that can generate various long-lived (O_3, NO_3^- and NO_2^-) and short-lived reactive species (NO, OH, singlet oxygen, and electrons) has been investigated. Lastly, DBD and APPJ operating with different parameters was used in different studies, whereas none of them indicated the optimal CAP treatment (plasma configuration and feed gas) to produce functionally enhanced pea protein ingredients. Therefore, a thorough study of the impact of plasma species and configurations on the structural changes of pea protein isolate and consequent functionality allow will for the determination of optimal CAP conditions for producing modified pea protein ingredients with enhanced functionality.

Chapter 2: Impact of Plasma Reactive Species on the Structure and Functionality of Pea Protein Isolate

2.1 Overview

The impact of plasma-produced reactive oxygen and nitrogen species and in particular O_3, N_xO_y, H_2O_2 and OH on the structure and functionality of pea protein isolate (PPI) was evaluated. The species were produced through a combination of control measurements and plasma treatments. Pronounced structural and functional effects were observed upon treatment with reactive species at pH 2. All reactive species induced the formation of disulfide-linked soluble aggregates. Protein denaturation was observed after treatment with all reactive species. A significant increase in β-sheet content and surface hydrophobicity was only induced by treatment with O_3 and OH, which resulted in the greatest enhancement in gelation and emulsification. While H_2O_2 enhanced PPI color by increasing whiteness, it had the least impact on protein structure and functionality. Results of this work can be used to optimize cold atmospheric plasma treatment of PPI to induce specific structural changes and a directed enhancement in functionality.

2.2 Introduction

The global plant protein ingredient market is projected to accumulate $15.65 billion in revenue by 2024 (Market Research Future, 2021). The steep increase in the plant protein market is largely attributed to environment and animal welfare concerns, as well as awareness of the health benefits of plant proteins (Ismail et al., 2020). Soy protein, a nutritious and functional protein, remains the dominant protein in the plant protein market. However, soy is one of the "Big Eight" allergens and is mostly a genetically modified

(GMO) crop. Therefore, consumers are seeking alternatives to soy protein, and the food industry accordingly is searching for effective replacement, one being pea protein.

Pea protein is rapidly replacing soy protein in the market due to readily available non-GMO sources (yellow field peas), low cost of production, nutritional benefits, and low occurrence of allergenicity (Barac et al., 2010). However, the functional properties of pea protein ingredients (e.g., solubility, gelation, and emulsification) are inferior to those of soy protein counterparts. Inferior functionality is largely attributed to the intrinsic protein profile and structure. Additionally, pea protein lags behind soy protein in the development of isolation and processing technologies. To better compete with soy protein, the functional properties, such as gelation and emulsification, of pea protein must be enhanced.

To enhance the functionality of pea protein ingredients, research has focused on modifying the inherent protein structure. Protein modification included enzymatic hydrolysis, Maillard-induced glycation, and physical modifications. Protein enzymatic hydrolysis is widely used in industry to produce hydrolysates with enhanced functionality and nutritional value (Ge et al., 2020). Pea protein hydrolysates demonstrated better solubility, and enhanced emulsifying and foaming properties compared to pea protein isolates (Barać et al., 2011; Barac et al., 2012). However, the degree of hydrolysis (DH) is strongly correlated to bitterness, compromising the sensory quality of the ingredient (Arteaga et al., 2020). Mallard-induced glycation has also been shown to improve the solubility of pea protein (Kutzli et al., 2020). However, research in this area is only emerging and further investigations are required to make the process industrially feasible with limited adverse effects, such as the production of advanced glycation products (Lin et al., 2020). Traditional physical modifications of pea protein, such as heating (Chao &

Aluko, 2018), steaming (Pietrysiak et al., 2018) and extrusion (Osen et al., 2014), have been explored as well. Heat is a key component of traditional physical modification methods that can induce partial denaturation of proteins and the formation of high molecular weight soluble aggregates (Mirmoghtadaie et al., 2016). Traditional, heat-based physical modifications contribute to modestly enhanced solubility, oil holding capacity, emulsification, foaming, and texturization properties of pea protein (Chao & Aluko, 2018; Chao et al., 2018; Osen et al., 2014; Pietrysiak et al., 2018). The biggest concern of high temperature processing is the reduction of nutritional quality attributed to a significant loss of lysine due to the Maillard reaction, and a decrease in digestibility due to excessive polymerization (Björck & Asp, 1983). Additionally, traditional physical modifications require high energy input, making them cost-intensive.

Cold atmospheric plasma (CAP), an ionized gas near room temperature, enables the production of reactive oxygen and nitrogen species at ambient temperatures and is being explored as a novel physical protein modification method. Key advantages of the approach include its operation at room temperature and potential for high energy efficiency. Considerable research explored the utilization of CAP for waste management (Harris et al., 2018), water disinfection (Prakash et al., 2017), microbial inactivation (Moldgy et al., 2020), wound healing (Boekema et al., 2015), enzyme inactivation (Pankaj et al., 2013), and surface modification (Cheng et al., 2006). Cold plasma is produced by subjecting gases, such as air, oxygen, and argon, to a high voltage, typically applied across two metal electrodes. The resulting electric field enables ionization and acceleration of energetic electrons that lead to dissociation of molecules resulting in a cocktail of highly reactive oxygen species (ROS) (O, O_3, OH, H_2O_2) and reactive nitrogen species (RNS),

NO_2 and N_2O_5 (Gorbanev et al., 2018). Different gases and plasma generating approaches result in various profiles of reactive species, which may induce different chemical reactions, such as oxidation, polymerization, and bond cleavages (Tolouie et al., 2018). For example, dielectric barrier discharge (DBD), i.e., a plasma generated between two metal electrodes covered by a dielectric material, is one of the most effective plasma configurations enabling the production of O_3 using air or O_2 (Bahrami et al., 2016). Hydroxyl radicals (OH) and hydrogen peroxide (H_2O_2), on the other hand, are produced when water vapor is present in the feed gas (Bruggeman & Schram, 2010).

The utilization of CAP as a physical modification of food proteins has also garnered interest. Recently, several studies reported the impact of CAP on plant and animal proteins (Ji et al., 2018; Sharifian et al., 2019), with few reports on the impact of CAP on pea proteins (Bußler et al., 2015; Mahdavian Mehr & Koocheki, 2020). Bußler et al. (2015) reported an increase in solubility and water binding capacity of pea protein after DBD treatment. Improvement in emulsion properties and solubility of pea protein after a short-time DBD treatment was also reported by Mahdavian Mehr and Koocheki (2020). While the reported findings are promising, it remains unclear how plasma-induced structural changes impacted functionality. Additionally, the link between different plasma species and the observed structural changes, and consequent functional enhancement, is not demonstrated in similar studies on impact of CAP on protein functionality. Therefore, the objective of this study was to evaluate the impact of plasma reactive species (N_xO_y, O_3, H_2O_2, OH) on the structure and functionality of pea protein isolate. This study will demonstrate how plasma-produced reactive species induce protein structural changes and will provide basic information needed for identifying optimal CAP treatment (plasma

generation approach and feed gas) to produce functionally enhanced pea protein ingredients.

2.3 Materials and Methods

2.3.1 Materials

Yellow field pea flour was kindly provided by AGT Foods (Regina, SK, Canada). Defatted soy flour (7B, 53% protein) was kindly provided by Archer Daniels Midland (ADM) (Decatur, IL, USA). Commercial pea protein isolate (cPPI, 81.2% protein, 3.86% ash) PURIS™, was kindly provided by Puris Foods (Minneapolis, MN, USA). Samples were stored at -20°C before the usage. Criterion™ TGX™ 4-20% precast gels, Laemmli sample buffer, 10X Tris/Glycine/sodium dodecyl sulfate (SDS) running buffer, Imperial™ Protein Stain, and Precision Plus molecular weight marker were purchased from Bio-Rad Laboratories, Inc. (Hercules, CA, USA). Superdex™ 200 Increase 10/300 GL Prepacked Tricorn™ Column, gel filtration LMW calibration kit, and gel filtration HMW calibration kit were purchased from Cytiva (Marlborough, MA, USA). SnakeSkin™ dialysis tubing with 3.5 kDa molecular weight cut off (MWCO) and Sudan Red 7B were purchased from Thermo Fisher Scientific™ (Waltham, MA, USA). Aluminum crucibles (40 µL, with pin) for DSC were purchased from Mettler-Toledo (Columbus, OH, USA). Folded capillary cuvettes for zeta potential were purchased from Malvern (Malvern, UK). Costar® solid opaque black 96-well plates and 8-anilino-1-napthalenesulfonic acid ammonium salt (ANS) were purchased from Sigma-Aldrich (St. Louis, MO, USA). Pure corn oil (Mazola) was purchased from a grocery store. All other analytical grade reagents were purchased from Thermo Fisher Scientific or Sigma-Aldrich.

2.3.2. Preparation of pea protein isolate (PPI)

Pea protein isolate (PPI) was produced following a pH extraction method (alkaline solubilization with isoelectric precipitation extraction) optimized by Hansen (2020). Pea flour was fully dispersed in a tenfold volume of double distilled water (DDW) and adjusted to pH 7.5 with 2 N NaOH. Protein slurries were stirred for 1 hour at room temperature, then centrifuged at 5000 × g for 30 minutes to precipitate insoluble materials. The pellet was re-suspended in a tenfold volume of DDW and adjusted to pH 7.5 for another 1-hour solubilization, followed by 30-minutes centrifugation at 5000 × g. Supernatant from both solubilizations were combined and adjusted to the isoelectric point (pH 4.5), followed by 10-minutes centrifugation at 5000 × g to precipitate the protein. The protein pellet was then re-suspended in DDW (1:4 w/v), neutralized, dialyzed, and lyophilized. The protein content of PPI (89.8 %) was determined by the Dumas method (AOAC 990.03), using a LECO® FP828 nitrogen analyzer (LECO, St. Joseph, MI, USA), with a conversion factor of 6.25.

2.3.3 Plasma species treatment

2.3.3.1 Ozone (O_3) and reactive nitrogen species (RNS) treatment

The flow-through plasma reactor used in this work is shown in **Figure 11**. For a detailed description, the readers are referred to Nayak et al. (2018). Briefly, the reactor consisted of an electrode arrangement embedded in a homemade electrode holder made of polytetrafluoroethylene (PTFE). The holder allows for applying a gas flow through the

electrode where it is treated by the plasma. The electrode is a two-dimensional array of 105 integrated coaxial micro-holes (600 μm in diameter) punched through two internal and parallel ultra-thin metal (gold and nickel) plates covered and separated by alumina as the dielectric material. One of the metal plates was powered while the other was grounded. The discharge was ignited in these micro-holes by applying a high voltage sinusoidal signal at 20 kHz generated by an AC power source (PVM500, Information Unlimited), and is referred to as the two-dimensional dielectric barrier discharge or 2D-DBD. The power was measured using the Lissajous method as described in (Nayak, Du, et al., 2017) by measuring the high voltage across the electrode using a high-voltage probe (Tektronix P6015A), and the charge across a 20 nF capacitor on the grounded side using a passive voltage probe (Tektronix TPP0200).

The discharge was operated at atmospheric pressure in dry air (Laboratory Grade) as well as in argon (Ar) with 20% admixture of O_2 (Ultra-Pure-Carrier Grade 99.9993%) at a constant total gas flow rate of 5 standard liters per minute. The plasma power was kept constant at 14.5±0.1 W in air and at 10.3±1.1 W in Ar/O_2. The air plasma was used to generate reactive oxygen and nitrogen species (RONS), while the Ar/O_2 plasma dominantly produced O_3 as the long-lived species. The ozone densities in air and Ar/O_2 plasmas were $(1.6\pm0.1)\times10^{22}$ m^{-3} and $(1.4\pm0.2)\times10^{22}$ m^{-3}, respectively, as measured with the UV absorption spectroscopy at 253.4 nm(Nayak, Sousa, et al., 2017).

For protein treatment, the effluent of the 2D-DBD confined within a polycarbonate tube was sent through a 100 mL protein solution (5% w/v protein in DDW) in a bubbler (PYREX® 500 mL Gas Washing Bottle with Coarse Fritted Cylinder) for treatment time of 30 minutes. The gas residence time in the effluent of the plasma till it reaches the protein

solution is ~12 s. As such, for Ar/O_2 plasma, O_3 is the dominant reactive species reaching the protein solution. For air plasma, owing to such large timescales, O_3 could react with RNS to form NO_2 and N_2O_5. With a larger Henry's law solubility constant compared to NO and NO_2, N_2O_5 will more readily dissolve in the protein solution to produce subsequent secondary reactive chemistry in the liquid-phase (Kimura et al., 2018; Moldgy et al., 2020).

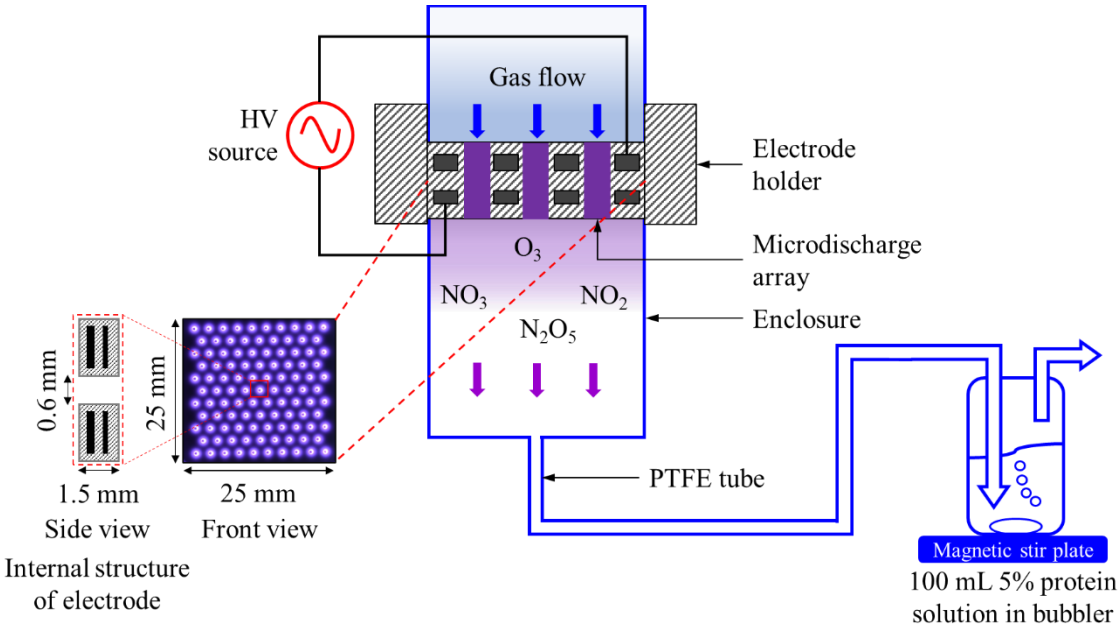

Figure 11. A schematic of the 2D-DBD apparatus used for generating N_xO_y/O_3 and O_3 plasma reactive species using air and Ar + 20% O_2, respectively, at a total gas flow rate of 5 slm.

2.3.3.2 H_2O_2 treatment

To investigate the effect of hydrogen peroxide (H_2O_2) on protein, 100 mL of 3 mM H_2O_2 was added to 100 mL of protein solution (5% w/v protein in DDW). The final concentration of H_2O_2 was1.5 mM.

2.3.3.3 OH radical treatment

To determine the effect of hydroxyl (OH) radical on the protein structure and functionality, Fenton's reaction (Pignatello et al., 2006) was used to generate OH radicals in the bulk of the protein solution. For this, 50 mL of 6 mM H_2O_2 was added to 100 mL of protein solution (5% w/v protein in DDW), followed by the addition of 50 mL of 6 mM ferrous sulfate ($Fe(II)SO_4$) solution. This results into a final concentration of equimolar concentrations of H_2O_2 and Fe(II) ions (1.5 mM) generating OH radicals in the bulk of the solution.

2.3.4 Handling of the protein solutions

PPI solutions (5% w/v protein in DDW) were prepared, in triplicate, at pH 2 or pH 7, for all four plasma species treatments, to evaluate the impact of plasma species on structural and functional changes. Since a decrease in pH, close to the isoelectric point (pI, pH 4.5) of pea protein after plasma treatment, was observed in our preliminary studies and other published work (Ekezie et al., 2019), protein solutions were adjusted to pH 2, where protein remained charged and soluble, to avoid protein precipitation during the treatment. The two pH treatments allowed for the observation of different chemical reactions and intensities induced by the different plasma species. Solutions of modified pea protein isolates (mPPIs) at both pHs were adjusted to pH 7 immediately after treatment. An additional dialysis step was applied to mPPIs at pH 2 to achieve the same protein and ash content as that of mPPIs treated at pH 7. After pH adjustment, mPPIs were lyophilized and stored at 4°C. In addition, non-dialyzed mPPIs treated at pH 2 were also collected to evaluate the effect of higher salt content (as a result of pH adjustments) on their structure

and functionality. Protein content of lyophilized mPPIs was determined following the Dumas method, and ash content was determined by the AOAC dry ashing method (AOAC 942.05).

2.3.5. Color measurement

The color of PPI, cPPI and plasma modified samples was assessed, in triplicate, using a Chroma Meter CR-221 (Minolta Camera Co., Osaka, Japan). Before analysis of the samples, the Chroma Meter was calibrated with a white CR-221 calibration plate (Minolta). The color of the samples was recorded using the CIE (International Commission on Illumination) 1976 L* a * b * color space system, where L* indicates lightness, ranging from 0 (black) to 100 (white); positive a* values represent red; negative a* values represent green; positive b* values represent yellow, while negative b* values represent blue. To assess the effect of plasma species treatment on color, total color difference (ΔE) between modified and non-modified PPI was calculated.

2.3.6 Protein profiling by gel electrophoresis

Protein profiling of PPI, cPPI and plasma modified samples (mPPIs) was performed using sodium dodecyl sulfate polyacrylamide gel electrophoresis (SDS-PAGE), as described by Boyle et al. (2018). Briefly, samples (5 µL; containing ~ 50 µg protein) and Precision Plus™ MW standard (10 µL) were loaded onto a Criterion™ TGX™ 4-20% precast Tris-HCl gradient gel. The gel was electrophoresed, stained/destained, and imaged as outlined by Boyle et al. (2018).

2.3.7. Molecular weight distribution by size-exclusion – high-performance liquid chromatography (SE-HPLC)

PPI, cPPI and mPPIs were subjected to size-exclusion HPLC (SE-HPLC) using a Shimadzu HPLC system (Shimadzu Scientific Instruments, Colombia, MD, USA) equipped with SIL-10AF auto injector, LC-20AT pump system, CTO-20A column oven, SPD-M20A photo diode array detector, and a CBM-20A communication module. A Superdex 200 Increase 10/300 GL Prepacked Tricorn™ Column was used to separate proteins based on molecular weight. The analysis was performed at room temperature following the method of Bruckner-Guhmann et al. (2018), with modifications. Samples (1% protein, w/v), in triplicate, were solubilized in pH 7 phosphate buffer (0.05 M sodium phosphate with 0.1 M sodium chloride) at room temperature for 2 hours, then passed through a 0.45 μm filter, automatically injected (100 μL) and separated isocratically using pH 7 phosphate buffer mobile phase at a flow rate of 0.5 mL per minute for a total run time of 80 minutes. Detection and analysis were performed at 280 nm. Molecular weights were calculated by running gel filtration calibration standards (HMW and LMW kits) **(Appendix A)**. Relative peak areas—the ratio of the area of a single peak to total peak area for a sample—were used to monitor differences in molecular weight distribution among the samples. Peak identities were assigned based on reported molecular weights (Barac et al., 2010; Gatehouse et al., 1982; Tzitzikas et al., 2006).

2.3.8. Differential scanning calorimetry (DSC)

Protein denaturation temperature and enthalpy of the different samples were determined using a DSC instrument (DSC 1 STARe System, Mettler Toledo, Columbus,

OH, USA), according to the method outlined by Boyle et al. (2018). Samples, in triplicate, were solubilized in DDW (20% protein, w/v) and stirred overnight at room temperature. An aliquot (20 µL, delivering approximately 4 µg protein) was transferred to an aluminum pan and hermetically sealed. An empty sealed pan was run simultaneously as reference. The pans were held at 25°C for 5 minutes, then heated from 25°C to 110°C at an increment rate of 5°C/min. Thermograms were manually integrated to obtain the peak denaturation temperature and enthalpy of denaturation for each protein using Mettler Toledo's STARe Software version 11.00.

2.3.9. Attenuated total reflectance fourier transform infrared spectroscopy (ATR-FTIR)

ATR-FTIR spectra of modified and non-modified protein isolates were recorded using Fourier transform infrared spectrometer (Thermofisher Nicolett iS50 FTIR). Protein lyophilized powders were placed on diamond ATR and scanned from 400–4000 cm^{-1} by DLaTGS detector. ATR spectra were converted to transmission spectra using OMNIC® software. Second derivative of Amide I band (1600cm^{-1} -1700 cm^{-1}) were obtained by PeakFit v. 4.12 to identify alpha-helix, beta-sheet, beta-turn, and random coil **(Appendix B)**.

2.3.10 Measurement of protein surface properties

Surface hydrophobicity was determined fluorometrically using an 8-anilino-1-napthalenesulfonic acid ammonium salt (ANS) probe, based on the method outlined by Boyle et al. (2018), with modifications in fluorescence gain (40) and the use of black 96-

well plate. A sample calculation for determining surface hydrophobicity index is shown in **Appendix C**. Zeta potential was measured using a dynamic light scattering instrument (Malvern Nano Z-S Zetasizer). Protein solutions (10 mL of 0.1% protein in DDW, w/v), in triplicate, were adjusted to pH 7, and stirred for 2 hours. An aliquot (1 mL) of each solution was dispensed into a folded capillary cell and inserted into the Zetasizer. After a 30 second equilibration period, electrophoretic mobility was measured by two sub-rep readings taken every 10 seconds for each replicate. Zeta potential was determined by Malvern's Zetasizer software (version 7.13) using the Smoluchowski model.

2.3.11 Protein solubility

Protein solubility at pH 7 was determined following the method described by (Wang & Ismail, 2012), with modifications in sample size (5 mL) and duration of solubilization (2 hours). Protein solutions (5 mL) were prepared, in triplicate, at 5% protein (w/v in DDW) and adjusted to pH 7 using 2 N NaOH and an Orion™ ROSS Ultra™ pH Electrode (Thermo Scientific). Samples were assessed at room temperature and post thermal treatment (80°C for 30 min). Solubility was expressed as the percentage of soluble protein (present in the supernatant post centrifugation) compared to the total protein content determined following the Dumas method **(Appendix D)**.

2.3.12. Gel strength

Strength of heat-induced gels was determined following the method described by Boyle et al. (2018), with modifications. Protein solutions (5 mL) were prepared, in triplicate, at 15% and 20% protein (w/v, in DDW), adjusted to pH 7, and stirred for 2 hours.

Aliquots (1 mL) were dispensed into lightly oiled microcentrifuge tubes using a positive displacement pipette. Samples were heated in a water bath at 95°C (± 2°C) for 20 min. After cooling to room temperature, gels were removed from the microcentrifuge tubes and gel strength was measured by a TA-TX Plus Texture Analyzer (Stable Micro Systems LTD, Surrey, UK) using a 100 mm diameter probe, 5 mm/s test speed, and a target distance of 0.5 mm from the plate. The maximum force measured in Newton was the rupture force of the gel.

2.3.13 Emulsification capacity

Emulsification capacity (EC) was determined following the methods outlined by Boyle et al. (2018) with modifications in the sample solubilization protocol and the oil titration speed. Protein samples, in triplicate, were solubilized in DDW (20 mL, at 2% protein concentration, w/v), adjusted to pH 7, and stirred for 2 hours. Corn oil dyed with Sudan Red 7B was titrated into an aliquot of each protein solution (5 mL) at a steady flow rate of 2 mL per min for the first 3 min and then increased to 6 mL per min for the remainder of the titration, while blending using a homogenizer (IKA® RW 20 Digital, IKA Works Inc., Wilmington, NC, US) with a 4 blade, 50 mm diameter shaft (IKA® R 1342) rotating at 860 - 870 rpm. Samples were homogenized while titrating with oil until a phase inversion was observed. Emulsification capacity was expressed as g of oil emulsified by one g of protein, as shown in **Appendix E**.

2.3.14 Statistical analysis

Analysis of variance (ANOVA) was determined using SigmaPlot software version 14.0 for windows (Systat Software, San Jose, CA). Tukey-Kramer multiple means comparison test was used to determine significant differences ($P \leq 0.05$) between the means ($n = 3$) of at least three different samples. ANOVA tables can be found in **Appendix F (Tables 11-66)**. A student's unpaired t-test was used to test for significant differences ($P \leq 0.05$) between the means ($n = 3$) of two different samples.

2.4 Results and Discussion

2.4.1 Protein and ash content of treated and untreated pea protein isolates

The protein and ash contents (total amount of minerals) of the control PPI and mPPIs treated at pH 7 were in the range of 89.6 - 91.2% and 3.8 - 4.5%, respectively. The protein and ash contents of the control PPI and mPPIs treated at pH 2 were in the range of 80.0 - 84.5% and 10.1 - 15.1%, respectively. The decrease in protein content and increase in ash content in the mPPIs treated at pH 2 were attributed to the formation of NaCl after several pH adjustments, as well as the formation of salts by dissolving long-lived plasma species into the protein solutions. An additional dialysis step was performed for the mPPIs treated at pH 2 to obtain similar protein (89.8 -92.2%) and ash (3.8-4.5%) contents as those of mPPIs treated at pH 7.

2.4.2 Effect of plasma species on the color of the isolates

An increase in the total color difference (ΔE) of PPI was observed after plasma species (N_xO_y/O_3, O_3, H_2O_2, and OH) treatment at pH 2 **(Appendix G: Table 156)**.

Similarly, Bußler et al. (2015) reported an increase in ΔE of pea protein powder after DBD (air) treatment, which was comprised of N_xO_y and O_3 species. A decrease in lightness (L*) and an increase in green color were observed after RNS/O_3 treatment. Also, O_3 treatment alone significantly decreased the lightness compared to PPI controls. However, H_2O_2 resulted in a significant increase in lightness compared to PPI controls. This observation is reasonable given the fact that food-grade H_2O_2 is usually used as a bleaching agent in food processing (Farr et al., 2000). mPPI treated with OH radicals at pH 2 (mPPI- OH pH2) demonstrated the largest total color difference compared to PPI controls, which was mostly attributed to the reduction in yellow color **(Appendix G: Table 156)**. Bußler et al. (2015) reported an increase in the yellow color of whey protein solution after DBD (air) treatment, which used a similar setup and gas as N_xO_y/O_3 treatment in this study. However, none of the reactive species in this study significantly increased the yellow color of PPI, unlike the observation of Segat et al. (2015), who attributed the increase in yellow color to O_3 species. Since protein samples were dissolved in phosphate buffer during the plasma treatment in Segat et al. (2015) study, it is possible that phosphorylation of protein happened during the DBD treatment, resulting in the increase in yellow color (Kaewruang et al., 2014). Overall, none of the plasma species in this study resulted in consequential change in color that may negatively impact the physical quality of the protein powders.

2.4.3 Effect of plasma species on protein profile and changes in molecular weight

Plasma treatments at both pH 7 and pH 2 resulted in protein polymerization compared to the control PPI, as indicated by the smearing in the upper molecular weight region of the gel (**Figure 12 a & b**). Under reducing conditions, the smearing was no longer

evident, indicating that the polymerization was via disulfide linkages. As oxidants, the plasma reactive species promoted disulfide interchange. Mahdavian Mehr and Koocheki (2020) and Nyaisaba et al. (2019) found protein polymerization after DBD (air) treatment of pea protein and squid protein, respectively. Again, plasma generated by remote DBD with air is a mixture of O_3 and N_xO_y, on timescales corresponding to protein treatment in this study (~12 s). O_3 in this study induced protein polymerization **(Figure 12a & b)**. Therefore, the protein polymerization reported by Mahdavian Mehr and Koocheki (2020) and Nyaisaba et al. (2019) could be attributed to O_3. Since N_xO_y/O_3 mixture induced similar protein polymerization as well **(Figure 12a, lane 3, Figure 2b, lane 16)**, a further study with RNS alone may elucidate its effect on protein polymerization.

Comparing the smearing intensity in lanes 15-19 **(Figure 12b)** to lanes 2-6 **(Figure 12a)**, it is apparent that plasma species treatment at pH 2 resulted in more polymerization in mPPI than treatment at pH 7. To a lesser degree, high molecular weight polymers were also observed in pH 2 PPI control, while none were evident for pH 7 PPI control. This observation, indicated that, independent of plasma species treatment, extreme acidic pH caused protein unfolding due to like charges and disruption of ionic bonding within the protein. Unfolded protein will have higher tendency to polymerize due to the exposure of hydrophobic groups as well as sulfhydryl groups. However, the degree of polymerization at pH 2, as evident by darker smearing, was intensified upon plasma species treatment **(Figure 12b, lanes 16-19)**. The formation of high molecular weight polymers that may remain soluble (i.e. soluble aggregates) may enhance functional properties, namely gelation and emulsification (Mahdavian Mehr & Koocheki, 2020; Utsumi et al., 1997).

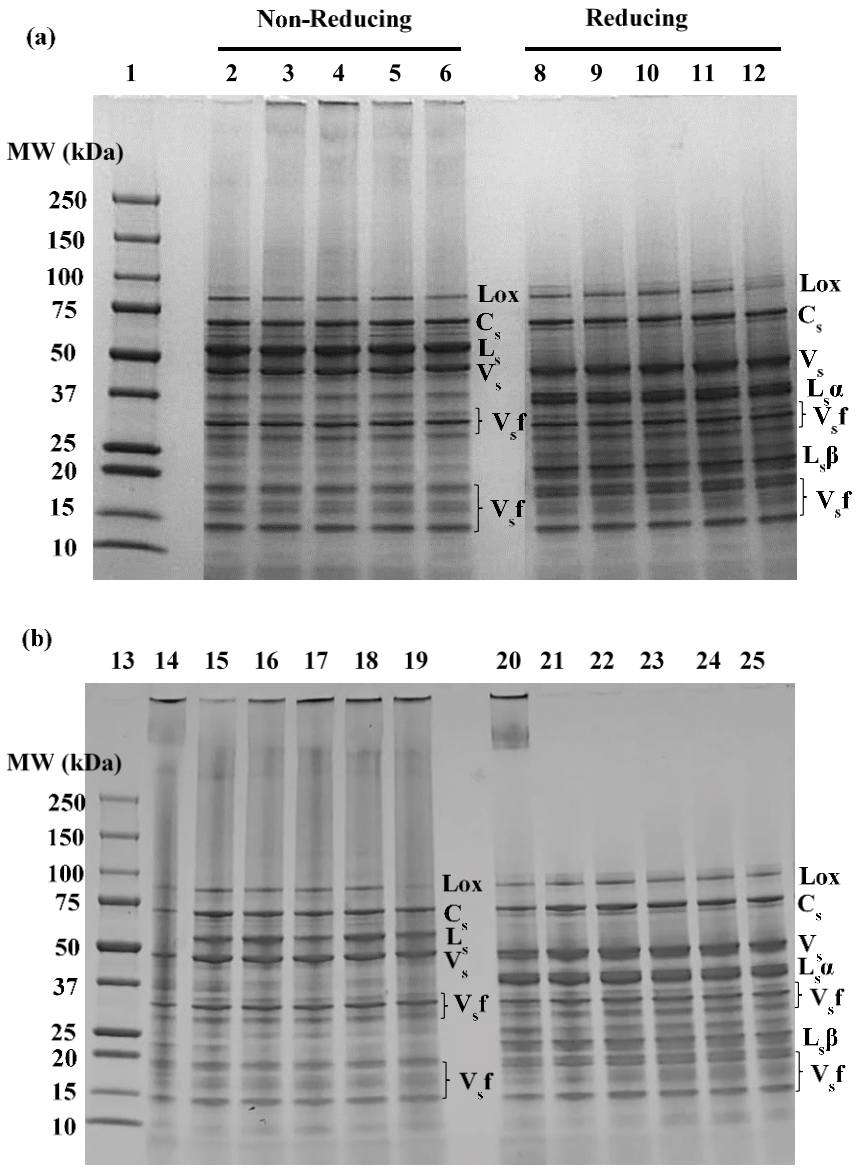

Figure 12. SDS-PAGE gel visualization of the protein profiles of the PPI samples treated at (a) pH 7 and (b) pH 2 and a reference sample (cPPI) under nonreducing (lane 2-6 and lane15-20) and reducing (lane 8-12 and lane 21-25) conditions. Lane 1,14: Molecular weight (MW) marker; Lane 2, 8: PPI Control-pH 7; Lane 14,20: cPPI reference; Lane 3, 9: mPPI- N_xO_y /O_3 pH7; Lane 4, 10: mPPI- O_3 pH7; Lane 5, 11: mPPI- H_2O_2 pH7; Lane 6, 12: mPPI- OH pH7; Lane 15, 21: cPPI; Lane 16, 22: PPI Control-pH2; Lane 17, 23: mPPI- N_xO_y /O_3 pH2; Lane 18, 24: mPPI- O_3 pH2; Lane 19, 25: mPPI- H_2O_2 pH2; Lane 20, 26: mPPI- OH pH2. Lox: lipoxygenase; C_s: subunits of convicilin; V_s: subunits of vicilin; $L_s\alpha$: acidic peptides cleaved from legumin subunits; $L_s\beta$: basic peptide cleavage from legumin subunit; V_sf: fractions of vicilin subunits result from post-translational cleavages.

Under non-reducing conditions, highly polymerized proteins were apparent in cPPI, analyzed as a reference protein **(Figure 12b, lane 14)**, as noted by the smearing and presence of dark bands at the top of the gel. Under reducing conditions, the smearing was less apparent, yet distinct high intensity bands remained in the upper part of the gel, indicating that some of the polymers in cPPI are formed by covalent linkages other than disulfide interactions **(Figure 12b, lane 20)**. Such high level of polymerization in this case may be detrimental to the functional properties.

The molecular weight distribution of soluble aggregates, legumin, vicilin, and convicilin proteins were further characterized using SE-HPLC. The relative abundance of soluble aggregates, functional proteins (legumin, vicilin and convicilin), and low molecular weight proteins is shown in **Figure 13** and **Table 4**. Neither non-covalent interactions nor disulfide linkages among the protein subunits were disrupted during the analysis due to the absence of SDS and a reducing agent. Therefore, additional information on protein profile and molecular distribution as influenced by plasma reactive species was obtained.

The molecular weight of soluble aggregates was about 1,200 kDa, while that of hexameric legumin, trimeric convicilin, and trimeric vicilin **(Table 4)** fell within the expected ranges (Barac et al., 2010; Gatehouse et al., 1982; Tzitzikas et al., 2006). Insoluble aggregates did not pass through the 0.45 μm filter and thus were not observed. In cPPI, the abundance of functional proteins was low (**Figure 13**), with only a small percentage of vicilin present (**Table 4**) relative to other smaller molecular weight polypeptides. The low relative abundance of functional proteins and soluble aggregates in cPPI confirmed that most of the functional proteins formed insoluble aggregates, thus were filtered out prior to the analysis.

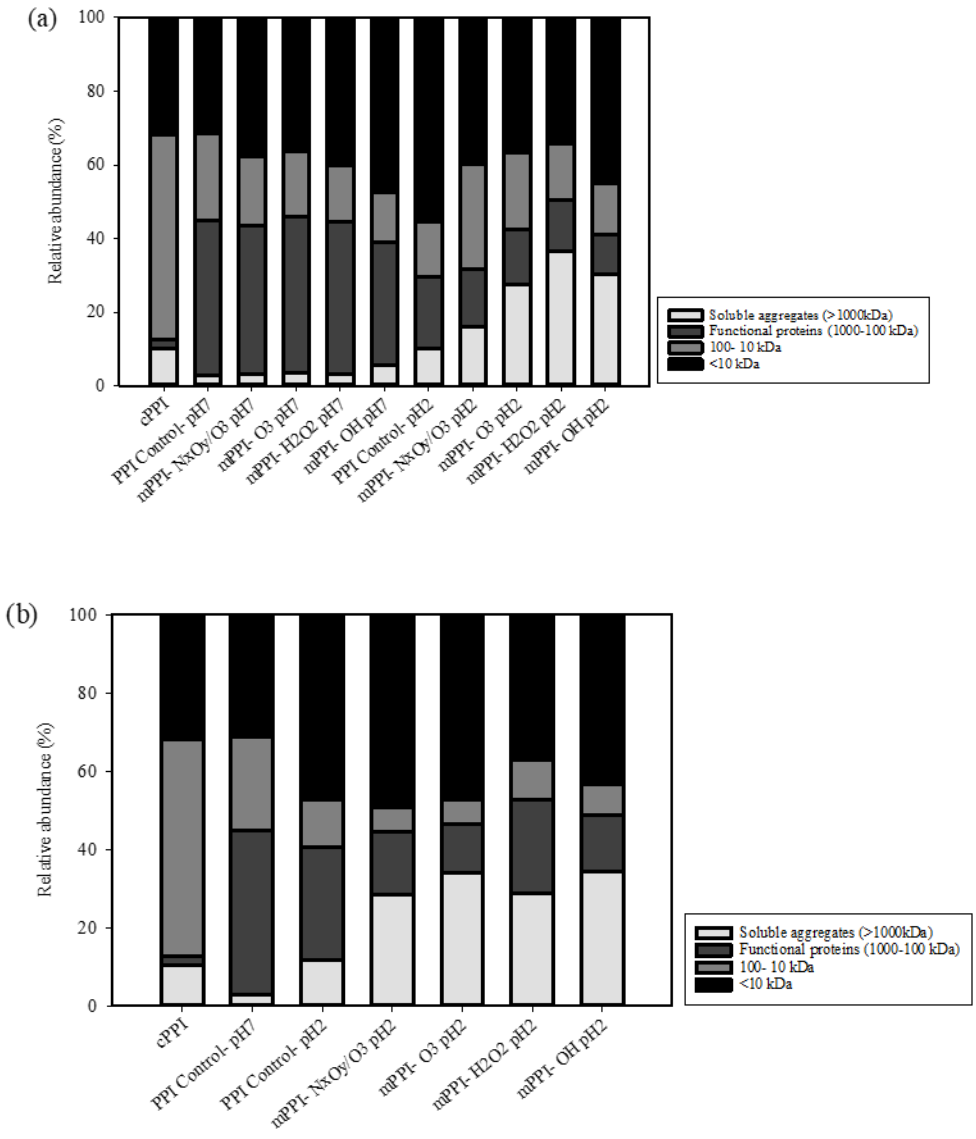

Figure 13. Percent relative abundance of different protein fractions in commercial pea protein reference, non-modified pea protein controls, modified pea protein isolates at pH7 and pH 2 without dialysis (a), and modified pea protein isolates at pH 2 with dialysis (b). Samples were dissolved in pH 7 phosphate buffer and analyzed by size-exclusion high-performance chromatography (SE-HPLC). Bars distribution represents means of n = 3.

Table 4. Molecular weight and relative abundance of soluble aggregates, legumin, convicilin, and vicilin present in commercial pea protein reference, non-modified pea protein controls, and plasma modified pea protein isolates at pH 2 (with dialysis), as analyzed by size-exclusion high-performance liquid chromatography (SE-HPLC).

Protein Fractions[1]	Molecular weight (kDa)	Relative Abundance (%)[2]						
		cPPI	PPI Control-pH7	PPI Control-pH2	mPPI- N_xO_y /O_3 pH2	mPPI- O_3 pH2	mPPI- H_2O_2 pH2	mPPI- OH pH2
Soluble aggregates (association of legumin, vicilin and other protein fractions)	~1200	10.27[4b]	2.82[b]	11.80[b]	28.57[a]	34.16[a]	28.83[a]	34.43[a]
Legumin	~450	*[3]	22.01[a]	10.11[b]	5.12[c]	4.43[c]	10.14[b]	4.86[c]
Convicilin	~ 250	*	8.52[ab]	8.97[a]	5.21[cd]	3.84[de]	6.94[bc]	4.70[d]
Vicilin	~160	2.36[e]	11.59[a]	9.64[b]	5.62[cd]	3.99[d]	6.94[c]	4.92[d]

[1]Samples were dissolved in pH 7 phosphate buffer and analyzed by high-performance size exclusion chromatography (SE-HPLC); [2]Relative abundance (%) is the area of a specific peak divided by the total peak area for that sample; [3]An asterisk (*) represents no peak was apparent in this molecular weight range; [4]Means (n=3) in each row with different lowercase letters indicate significant differences according to the Tukey-Kramer multiple means comparison test ($P < 0.05$).

In comparison to pH 7 control, mPPI treated with OH radicals at pH 7 (mPPI-OH pH7) had significantly lower relative abundance of legumin, convicilin and vicilin, accompanied by a significantly higher abundance of soluble aggregates **(Appendix H: Table 157)**. Treatment with O_3, N_xO_y/O_3 mixture, and H_2O_2 at pH 7 resulted in a significant decrease in the relative abundance of convicilin and vicilin, but not legumin, and a slight increase in soluble aggregates. The salt content in the non-dialyzed samples treated at pH 2, including the pH 2 control, contributed to a marked increase in soluble aggregates accompanied by a major decrease in legumin and vicilin **(Appendix H: Table 157).** The presence of salt is known to enhance protein association. The impact of plasma species treatment was masked by the presence of salt. Dialysis to remove excess salt was, therefore, necessary to observe the actual impact of plasma species at acidic pH on the protein molecular association and distribution.

After dialysis, results showed that all plasma species, N_xO_y/O_3 mixture, O_3, H_2O_2, and OH radicals at pH 2 resulted in a significant increase in soluble aggregates, coupled with a significant decrease in the relative abundance of legumin, convicilin, and vicilin, compared to controls, with the O_3 and OH treatments having the greatest effect **(Figure 13b, Table 4**). ROS, especially OH radicals as well as O_3, preferably attack sulfur-containing amino acids (Segat et al., 2014; Surowsky et al., 2016), resulting in the formation of inter- and intra- chain disulfide linkages. While the relative abundance of soluble aggregates in PPI Control- pH2 was higher than that of PPI Control- pH7, it was not as high as in the mPPI samples, indicating that the treatment with plasma species had more pronounced effect on the formation of soluble aggregates than that of treatment pH. Acidic pH compared to neutral pH, however, facilitated more interactions with plasma

species that resulted in the formation of a relatively higher abundance of soluble aggregates. Since extreme acidic pH will cause protein unfolding as mentioned previously, a higher surface area of the protein was exposed to plasma reactive species at pH 2 than at pH 7. Additionally, O_3 is more prone to degradation at high pH than at low pH solutions (Gardoni et al., 2012). Therefore, it is reasonable that plasma species had a bigger impact on the protein structure at pH 2 than at pH 7. Because of the higher impact of treatment at pH 2, further characterization was performed on mPPI samples that were treated at pH 2 and dialyzed to remove salt interference.

2.4.4 Effect of plasma species on the protein denaturation state

Interaction of plasma species with the protein can result in protein unfolding, i.e., denaturation. Several studies have reported protein denaturation/unfolding upon CAP treatment (Ekezie et al., 2019; Meinlschmidt et al., 2016; Sharifian et al., 2019). Therefore, in this study, DSC was performed to determine the impact of different plasma reactive species on the denaturation state of proteins in PPI. Two endothermic peaks corresponding to vicilin and legumin were observed in pH 7 control PPI **(Table 5)**. Convicilin did not show up as a separate endothermic peak on the thermogram. This observation can be primarily attributed to the structural similarity between convicilin and vicilin, and thus potentially showing up as one endothermic peak. As, expected, no endothermic peaks were observed for cPPI reference, indicating complete denaturation. cPPI might have been subjected to severe extraction and processing conditions that lead to denaturation and the subsequent polymerization discussed earlier **(Figure 12b)**.

Table 5. Denaturation temperatures and enthalpy, secondary structure, surface hydrophobicity and surface charge of commercial pea protein reference, non-modified pea protein controls, and plasma modified pea protein isolates at pH 2 (with dialysis).

Samples	Denaturation Temperature and Enthalpy				Surface Properties		Secondary Structure			
	Vicilin		Legumin		Surface Hydrophobicity	Surface Charge	α Helix	β Sheet	β Turn	Random Coil
	Denaturation Temperature (Td, °C)	Enthalpy of Denaturation (ΔH, J g-1)	Denaturation Temperature (Td, °C)	Enthalpy of Denaturation (ΔH, J g-1)	RFI	mV	Relative Percentage			
cPPI	*[1]	*	*	*	12719[a]	-27.2[a]	14.5[b]	46.3[bc]	24.8[a]	14.5[a]
PPI Control- pH7	84.5[2a]	6.39[a]	91.4	1.48	8545[d]	-37.6[b]	23.3[a]	44.9[c]	22.8[b]	9.02[a]
PPI Control- pH2	81.7[b]	2.45[b]	*	*	9148[cd]	-37.8[b]	22.7[a]	46.0[bc]	18.8[bc]	12.5[a]
mPPI- N_xO_y /O_3 pH2	80.2[c]	1.84[c]	*	*	10393[bcd]	-39.5[b]	23.0[a]	42.8[c]	20.6[bc]	13.5[a]
mPPI- O_3 pH2	80.7[bc]	1.28[d]	*	*	11964[ab]	-38.8[b]	20.2[a]	51.3[a]	19.4[bc]	9.15[a]
mPPI- H_2O_2 pH2	82.1[b]	1.98[c]	*	*	11095[abc]	-38.6[b]	21.0[a]	50.1[ab]	19.0[bc]	10.0[a]
mPPI- OH pH2	81.5[bc]	1.13[d]	*	*	12386[ab]	-38.5[b]	19.3[ab]	53.3[a]	13.3[c]	14.2[a]

[1]An asterisk (*) represents no peak of denaturation observed; [2]Means (n = 3) in each column with different lowercase letters indicate significant differences among samples, according to the Tukey-Kramer multiple means comparison test ($P < 0.05$).

On the other hand, pH 2 control had only one endothermic peak for vicilin, with significantly lower enthalpy compared to the pH 7 control. The extreme pH resulted in protein unfolding as noted by the complete disappearance of the legumin endothermic peak, and the marked reduction in the denaturation enthalpy of vicilin. It is worth noting that legumin abundance in pea protein is much lower than that of vicilin (vicilin: legumin up to 8:1) (Tzitzikas et al., 2006), hence its endothermic peak could be hard to detect or distinguish from the adjacent vicilin peak, especially when significant unfolding occurs. Reactive species treatment at pH 7 had hardly any impact on the protein denaturation state **(Appendix I: Table 158)**. A significantly higher denaturation temperature for vicilin, observed for non-dialyzed mPPIs treated at pH 2, was attributed to the presence of high amount of salt **(Appendix I: Table 158)**. In dialyzed samples, the denaturation temperature of vicilin in mPPIs treated at pH 2 was similar to that of the control sample. Compared to pH 2 control, treatment with plasma species resulted in further significant reduction in the denaturation enthalpy of vicilin, with O_3 and OH radicals having the most impact **(Table 5)**. As aforementioned, O_3 (Segat et al., 2014) and OH radicals (Surowsky et al., 2016) are impactful plasma reactive species that oxidize sulfide-containing amino acids. The unfolding process of protein could be triggered during the formation of inter-chain disulfide interchange. Moreover, the proximity of two proteins caused by newly formed disulfide linkages could lead to further unfolding of the proteins due to steric hindrance from adjacent side chains. This observation further explains the higher abundance of soluble aggregates in PPI samples treated with O_3 and OH radicals **(Figure 13, Table 4)**, since unfolded proteins have higher tendency to polymerize.

2.4.5 Effect of plasma species on the protein surface properties

The unfolding of the globular protein leads to the exposure of the hydrophobic core, thus increasing surface hydrophobicity. Increases in surface hydrophobicity impact protein interactions and thus functional properties such as solubility, gelation, and emulsification. Segat et al. (2015) reported a significant increase in surface hydrophobicity of whey protein, and improved emulsifying and foaming properties after DBD (air) treatment that was comprised of a mixture of N_xO_y and O_3. Similar observation in surface hydrophobicity was also reported by Ekezie et al. (2019). However, the impact of various reactive species on the unfolding process was not clear. Therefore, changes in surface hydrophobicity were monitored as impacted by plasma species treatment (**Table 5**) in comparison to the reference sample, cPPI, and the PPI controls. The reference cPPI exhibited the highest surface hydrophobicity among all samples, complementing denaturation data and degree of polymerization discussed earlier. Plasma species treatment at pH 7 had no significant impact on surface hydrophobicity **(Appendix I: Table 158)**. However, a significant increase in surface hydrophobicity was observed after treatment with O_3 and OH at pH 2 compared to pH 2 and pH 7 controls **(Table 5)**. These results complemented the observed impact of O_3 and OH reactive species at pH 2 on denaturation and unfolding. Increases in surface hydrophobicity were observed after treatment with N_xO_y /O_3 at pH 2 but were not statistically significant. Although a similar amount of O_3 was produced in both N_xO_y /O_3 and O_3 treatments, the presence of RNS appeared to reduce the O_3 effect on protein unfolding. Lukes et al. (2014) found that the presence of RNS such as nitrites were able to rapidly decompose O_3 in liquid and generate oxygen molecules instead. Therefore,

compared to O_3 treatment, RNS/O_3 treatment had less impact on the denaturation state of the proteins in PPI.

Another important protein surface property is the surface charge (zeta potential, ζ), which, together with surface hydrophobicity, has a direct bearing on the protein's solubility, gelation and emulsification properties. Protein denaturation and polymerization could also affect the surface charge due to changes in conformation and relative exposure of different groups. Accordingly, the surface charge as impacted by plasma species treatment was monitored.

The surface charge of the PPI control at pH 7 was -37.6 mV similar to previously reported values (Ladjal-Ettoumi et al., 2016). The net surface charge of cPPI was significantly lower than that of the PPI controls, an observation attributed to its high degree of denaturation and polymerization induced by extreme processing conditions, resulting in insoluble aggregates. In non-dialyzed pH 2 samples, the high salt content contributed to a significant decrease in surface charge **(Appendix I: Table 158)**. However, the surface charge was restored upon dialysis, revealing no significant impact of plasma species treatment **(Table 5)**. This could be attributed to the formation of high molecular weight soluble aggregates, which could be highly charged due to moderate unfolding and polymerization of proteins induced by plasma treatment. Maintenance of high surface charge will have a positive impact on functionality. Mahdavian Mehr and Koocheki (2020), on the other hand, reported a significant increase in the surface net charge of pea protein after DBD (air) treatment. They attributed this observation to the oxidation of certain amino acids that could have led to the formation of negatively charged amino acids. Reports on changes in zeta potential after CAP treatment are limited.

2.4.6 Effect of plasma species on the protein secondary structure

In addition to protein profile, protein denaturation state, and surface properties, protein secondary structure was also impacted by the reactive species. The relative abundance of α helix, β sheet, β turn and random coil in PPI Control- pH7 **(Table 5)** was similar to that reported by S. M. Beck et al. (2017). The reference cPPI had the least relative amount of α helix, and the lowest ratio of α helix to β sheet, indicating protein denaturation at the secondary structure level (Ekezie et al., 2019). As with other structural data presented thus far, treatment at pH 7 had no significant impact on the protein secondary structure **(Appendix I: Table 158)**. On the other hand, the relative abundance of the β-sheet in PPI samples treated with O_3 or OH radicals was significantly higher than that of PPI controls. Accordingly, the α-helix to β-sheet ratio in PPI was significantly reduced after O_3 and OH treatment, which also indicated denaturation at the secondary structure level. Protein polymerization and unfolding induced by O_3 and OH radicals could be responsible for the increases in β-sheet content. The formation of interchain β-sheet could be initiated by proximity of proteins and exposed amino acids residues, caused by polymerization and unfolding, respectively. Several studies also reported similar secondary structure changes after CAP treatment (Ekezie et al., 2019; Ji et al., 2018; Sharifian et al., 2019). Sharifian et al. (2019) observed a decrease in α helix content, while Ji et al. (2018) reported an increase in β sheet content and a decrease in α helix content, after air DBD treatment. The increase in β sheet content after CAP treatment could directly improve protein functionality. For example, amyloid fibrils produced from plant protein isolates, which were only comprised

of β sheet structure, exhibited significantly improved emulsification and gelling properties compared to original counterparts (Cao & Mezzenga, 2019).

2.4.7 Effect of plasma species on protein functionality

Protein solubility is an important functionality as it can influence several other functional properties, including gelation and emulsification. Adequate protein solubility is needed for utilization in food systems, especially in high protein beverage applications. Contradictory solubility results after CAP treatment were observed in different studies. Contradictory findings are attributed to differences in the conditions of the reported solubility tests, as well as differences in the intensity and profile of the plasma reactive species. Ekezie et al. (2019) reported a decrease in protein solubility after atmospheric pressure plasma jet (APPJ) treatment in air, whereas Bußler et al. (2015) reported an increase in protein solubility after air DBD treatment. Ekezie et al. (2019) observed a decrease in pH during APPJ treatment, but APPJ-treated samples were directly tested for solubility without adjusting the pH to resemble that of the control. The pH after the APPJ treatment was close to the isoelectric point of the protein, thus explaining the reduced solubility. Bußler et al. (2015), on the other hand, compared the solubility of DBD treated samples to that of the control at the same pH. Moreover, different plasma units and power sources were used in the two studies, thus contributing to differences in intensities and profiles of the generated plasma reactive species, which could further explain the contradictory solubility results. Accordingly, in this study, the pH of the treated protein solution was adjusted to 7 and lyophilized prior to testing solubility. Thus, any changes in protein solubility were attributed to the treatment with the different plasma species.

Given that treatment at pH 7 did not impart major changes in the protein profile and structure, changes in functional properties were minimal **(Appendix J: Table 159)**. On the other hand, significant enhancement in functionality was noted for PPI samples treated with different plasma species at pH 2 in comparison to the controls as well as the reference cPPI **(Table 6**).

The reference cPPI exhibited the lowest protein solubility under both heated and non-heated conditions (**Table 6**). This was largely attributed to the high degree of denaturation, high level of polymerization and insoluble aggregates, high surface hydrophobicity, and comparatively low surface charge. The PPI samples treated with O_3 and OH radicals had comparable solubility to that of pH 7 PPI control, and significantly higher solubility under non-heated condition than that of the pH 2 PPI control. The observed increase in solubility could be mostly attributed to the formation of soluble aggregates and the retained high surface charge, which could have offset the observed increase in surface hydrophobicity.

The reference cPPI and the PPI controls did not form a gel at 15% protein concentration (**Table 6**). This observation confirms their poor gelling ability. Even at 20% protein concentration, both the reference cPPI and the pH 7 control PPI had low gel strength. The low gelling properties of cPPI is attributed to its low solubility, high level of denaturation and aggregation, and imbalance of surface hydrophobicity to the surface charge. To form a well-structured gel, a good hydrophilic/lipophilic balance (HLB) on the protein surface is needed to facilitate protein-protein interactions and protein-water interactions.

Table 6. Solubility, gel strength and emulsification capacity of commercial pea protein reference, non-modified pea protein controls, and plasma modified pea protein isolates at pH 2 (with dialysis).

Samples	Solubility (5% protein)		Gel Strength (15% protein)	Gel Strength (20% protein)	Emulsification Capacity (2% protein)
	Non-Heated	Heated (80°C for 30 min)	Strength (N)	Strength (N)	mL oil/g protein
cPPI	23.9[2c]	41.9[b]	*[1]	2.73[d]	229.4[d]
PPI Control- pH7	82.4[a]	79.6[a]	*	5.69[cd]	341.0[c]
PPI Control- pH2	66.9[b]	76.0[a]	*	11.7[bc]	644.8[b]
mPPI- N_xO_y /O_3 pH2	78.1[a]	81.9[a]	2.21[a]	21.9[a]	685.1[b]
mPPI- O_3 pH2	81.6[a]	83.7[a]	3.34[a]	25.2[a]	809.1[a]
mPPI- H_2O_2 pH2	71.2[b]	75.5[a]	*	12.1[bc]	634.0[b]
mPPI- OH pH2	80.0[a]	84.3[a]	1.23[a]	18.5[ab]	823.1[a]

[1]An asterisk (*) represents no measurable gels formed at 15% protein concentration; [2]Means (n = 3) in each column with different lowercase letters indicate significant differences among samples, according to the Tukey-Kramer multiple means comparison test ($P < 0.05$).

The low gelling properties of the PPI controls could be attributed to higher proportion of low molecular weight proteins to that of soluble aggregates, which promote gel matrix formation. On the other hand, PPI samples treated with O_3, N_xO_y /O_3 mixture, and OH species formed a gel at 15% protein, and had the greatest gel strength at 20% protein concentration. This observation could be attributed to the enhanced protein solubility, increases in soluble aggregates, and the potentially good balance between surface hydrophobicity and surface charge. The gelling properties of pea protein as impacted by CAP treatment has not been reported previously. The results of this study demonstrate the potential of using CAP that enable the delivery of O_3 and OH species, to improve the gelling properties of pea protein isolates.

The reference cPPI exhibited the lowest emulsification capacity (EC), again mostly due to high level of denatured, aggregated, and insoluble proteins with low surface charge **(Table 6)**. The EC was significantly increased after treatment with all plasma species, compared to pH 7 control. The EC of pH 2 control PPI was significantly higher than that of the pH 7 control and was comparable to the samples treated with N_xO_y /O_3 and H_2O_2, indicating in this case that the enhancement was only attributed to the structural changes induced by the acidic environment. In contrast, treatments with O_3 and OH radicals resulted in further enhancement in EC, an observation attributed to the significantly different structural characteristics. Good HLB and flexible protein structures are required to interact with both oil and water phases. Accordingly, the enhanced EC after treatment with O_3 and OH is attributed to good solubility, favorable balance between surface charge and hydrophobicity, increased β-sheet content, partially unfolded and thus more flexible proteins, and the relatively high amounts of soluble aggregates that could form a strong

protein film at the interface. Segat et al. (2015), Ji et al. (2018), and Mahdavian Mehr and Koocheki (2020) reported an enhancement in emulsification properties of whey, peanut, and pea protein, respectively, after air DBD treatment. Since DBD treatment used in these studies was remote with negligible water content in the dry compressed air, the impact of any plasma generated OH radicals can be neglected, thus the enhanced emulsification properties were largely attributed to O_3. Since the presence of N_xO_y appeared to reduce the O_3 effect on the structure and functionality of PPI, O_2 instead of air seems to have advantages as feed gas to generate plasma that could significantly enhance functionality. Additionally, due to the significant effect of OH radicals, generated in this study from the Fenton's reaction, on the structure of the proteins, direct plasma application to the protein solution, allowing the production of OH radicals, might be beneficial to further enhance functional properties.

2.5 Conclusions

For the first time, the findings of this work successfully demonstrated the impact of different plasma-produced reactive species (N_xO_y /O_3, O_3, H_2O_2, and OH) on the secondary, tertiary, and quaternary structures of pea protein, and the consequent changes in functional properties. Results can be used to explain previously reported observations related to the impact of different CAP systems on the functional properties of proteins. These results can also be used to optimize CAP treatment, in terms of plasma species production, to induce specific structural changes and a directed enhancement in functionality. Results indicated that O_3 and OH radicals are the most impactful species on the pea protein structure among all four investigated species. In addition, results highlighted that plasma sources that could effectively generate O_3 and OH radicals

(oxidizing species) are preferable for pea protein functionalization. Further investigation on the role of N_xO_y on protein modification is needed to further optimize CAP treatments. Finally, characterization of the interaction of O_3 and OH radicals with specific amino acid residues could further explain the observed structural changes. Nevertheless, this work provides a more detailed understanding of the potential of CAP and associated reactive species in enhancing pea protein functionality.

Chapter 3: Impact of Different Cold Plasma Configurations on the Structure and Functionality of Pea Protein Isolate

3.1 Overview

The impact of three cold atmospheric pressure (CAP) sources, atmospheric pressure plasma jet (APPJ), two- dimension dielectric barrier discharge (2D-DBD), and nanosecond pulsed discharge (ns-pulsed), on the color, protein structure and functionality, as wells as amino acid composition of pea protein isolate (PPI) was evaluated. Different plasma sources and associated reactive species resulted in protein denaturation, increased surface hydrophobicity, formation of soluble aggregates mostly by disulfide linkages, and changes in the protein secondary structure. Enhancement in surface properties, presence of soluble aggregates, and increase in β-sheet resulted in significant enhancement in gelation and emulsification properties. Differences among CAP treated samples were attributed to composition and intensity of plasma species. Treatment with 2D-DBD ($Ar + O_2$) for 30 min could be a comparatively appreciable functionalization approach due its modest and desirable structural changes and insignificant effect on amino acid composition.

3.2 Introduction

Pea protein ingredients are gaining traction in the global plant protein market because of their low occurrence of allergenicity, good nutritional quality, and non-GMO characteristics (Barac et al., 2010). However, the functionality of pea protein is lagging behind that of soy protein, which is increasingly avoided by consumers, mainly because it is a “Big Eight” allergen and a GMO ingredient. In order for pea protein to successfully replace soy protein in various food application, its functionality needs to be improved by feasible means.

Several protein modification approaches, including enzymatic hydrolysis (Arteaga et al., 2020), Maillard-induced glycation (Liu et al., 2012), and physical modifications (Mirmoghtadaie et al., 2016), have been explored to enhance pea protein functionality. However, each of these modifications has limitations including negative impact on flavor, loss of nutritional value, limited industrial feasibility, and/or high energy input and production cost. Additionally, the inherently lower content of the functional, high molecular weight legumin in pea compared to soy, cannot be ameliorated by enzymatic hydrolysis or other traditional physical modifications. It is, therefore, worthwhile investigating other modification approaches such as cold atmospheric plasma (CAP).

CAP, a novel non-thermal processing technology, has been explored for various applications including pesticide dissipation (Sarangapani et al., 2016), enzyme inactivation (Misra, Pankaj, et al., 2016), water disinfection (Prakash et al., 2017), and microbial inactivation (Moldgy et al., 2020). Advantages, including low temperature, high energy efficiency, and absence of solvents, make CAP a desirable food processing strategy. Plasma, generated by subjecting gases to high voltage, comprises various highly reactive species, such as reactive oxygen species (ROS) (O, O_3, OH, and H_2O_2) and reactive nitrogen species (RNS) (NO_2, and N_2O_5) (Gorbanev et al., 2018; Moldgy et al., 2020). Different plasma sources produce various reactive species profiles that may induce different chemical reactions including oxidation, polymerization, and bond cleavage. Such reactions can alter the structures of pesticides, enzymes, microbes, and food components such as starch and protein (Surowsky et al., 2016).

CAP, as a protein modification approach to enhance functionality, has garnered interest in recent years (Tolouie et al., 2018). Several studies have reported changes in

protein structure and improvements in functionality after CAP treatment. Nyaisaba et al. (2019) have reported a reduction in sulfhydryl groups coupled with the formation of high molecular weight protein aggregates, along with an increase in water holding capacity and an enhancement in gelation properties of CAP-treated squid proteins. Ji et al. (2018) observed an increase in β-sheet content, along with an enhancement in emulsification properties and water holding capacity of CAP-treated peanut protein.

There are a few reports on the impact of CAP on pea protein functionality (Bußler et al., 2015; Mahdavian Mehr & Koocheki, 2020). Bußler et al. (2015) reported enhancement in solubility and water binding capacity of CAP-treated pea protein. Mahdavian Mehr and Koocheki (2020) also reported improvement in solubility and emulsion properties of CAP-treated pea protein. While the reported findings are promising, it remains unclear how plasma-induced structural changes impacted pea protein functionality.

Various reactive species can be generated by different plasma configurations and gases. However, only remote dielectric barrier discharge (DBD) and atmospheric pressure plasma jet (APPJ), combined with air, have been investigated in protein modification studies. Long-lived RNS and ROS (O_3, H_2O_2, NO_2^-, and NO_3^-) dominate in those treatments, in contrast to short-lived species (NO, OH, singlet oxygen, and electrons) (Gorbanev et al., 2018). However, short-lived species are the main contributors to structural changes of organic compounds (Attri et al., 2016). OH and O_3, compared to N_xO_y and H_2O_2, had the most significant effect on protein structure and functionality **(Chapter 2)**. Thus, plasma configurations and gases that can generate shot-lived species and O_3 need

to be investigated further, while elucidating structural changes as they relate to consequent enhancement in functionality.

In this study, pea protein isolate (PPI) was treated with direct APPJ coupled with Ar and O_2, remote DBD coupled with Ar and O_2, and nanosecond (ns)-pulsed discharge coupled with air. The overall goal was to investigate the effects of different plasma configurations and gas mixtures, as well as treatment times, on pea protein structural and functional changes. This comprehensive work will demonstrate the potential of CAP as a modification approach in inducing a directed enhancement in pea protein functionality.

3.3 Materials and Methods

3.3.1 Materials

Materials. Yellow field pea flour, defatted soy flour (7B, 53% protein), and commercial pea protein isolate (cPPI, 81.2% protein, 3.86% ash) PURIS™ were kindly provided by AGT Foods (Regina, SK, Canada), Archer Daniels Midland (ADM) (Decatur, IL, USA), and Puris Foods (Minneapolis, MN, USA), respectively. Criterion™ TGX™ 4-20% precast gels, Laemmli sample buffer, 10X Tris/Glycine/sodium dodecyl sulfate (SDS) running buffer, Imperial™ Protein Stain, and Precision Plus molecular weight marker were purchased from Bio-Rad Laboratories, Inc. (Hercules, CA, USA). Superdex™ 200 Increase 10/300 GL Prepacked Tricorn™ Column, gel filtration LMW calibration kit, and gel filtration HMW calibration kit were purchased from Cytiva (Marlborough, MA, USA). SnakeSkin™ dialysis tubing with 3.5 kDa molecular weight cut off and Sudan Red 7B were purchased from Thermo Fisher Scientific™ (Waltham, MA, USA). Aluminum crucibles (40 µL, with pin) for DSC were purchased from Mettler-Toledo (Columbus, OH,

USA). Folded capillary cuvettes for zeta potential were purchased from Malvern (Malvern, UK). Costar® solid opaque black 96-well plates, 8-anilino-1-napthalenesulfonic acid ammonium salt (ANS), dansyl chloride (DC), d5-tryptophan, sulfadimethoxine, and amino acid standards were purchased from Sigma-Aldrich (St. Louis, MO, USA). High performance liquid chromatograph grade water and acetonitrile (ACN) were purchased from Fisher Scientific (Houston, TX, USA). All other analytical grade reagents were purchased from Thermo Fisher Scientific or Sigma-Aldrich.

3.3.2 Preparation of pea protein isolate (PPI)

Pea protein isolate (PPI) was produced following a pH extraction method (alkaline solubilization with isoelectric precipitation extraction) optimized by Hansen (2020) and reported in **Section 2.3.2**. The protein content of PPI (89.8 %) was determined by the Dumas method (AOAC 990.03), using a LECO® FP828 nitrogen analyzer (LECO, St. Joseph, MI, USA), with a conversion factor of 6.25.

3.3.3 Different plasma treatments

3.3.3.1 Atmospheric pressure plasma jet (APPJ) treatment

A radio frequency (RF) driven modulated APPJ, as shown in **Figure 14**, and described by Kondeti et al. (2020) was used to treat PPI, with modifications. Briefly, a 2 mm (ID) × 3 mm (OD) cylindrical quartz tube surrounded a 1 mm (ϕ) tungsten needle electrode. A 20 kHz modulated RF signal (13.1MHz) with a duty cycle of 20% was generated by a function generator (Tektronix AFG 2021), amplified by an RF amplifier (Amplifier Research AF75A250A), and applied through a matching box to the tungsten

needle electrode. Argon, at a flow rate of 1.5 standard liters per minute (slm), flowed through the quartz tube and acted as a feed gas for generating the plasma. Oxygen, at a flow rate of 2 slm, flowed through a 12.7 mm (ID) x 19 mm (OD) shielding tube and acted as a shielding gas for preventing the formation of RNS. A 72 mm × 55 mm 100 mL glass beaker containing 50 mL of protein solution (5% w/v protein in DDW) was placed on a magnetic stir plate and at a distance of 10 mm below the APPJ nozzle. The dissipated power when the plasma was in contact with the surface of the protein solution was 6.69 ± 1.84 W. Protein solutions, in triplicates, were subjected to plasma treatment for 5, 15, 30, and 45 min, with constant stirring at 200 rpm.

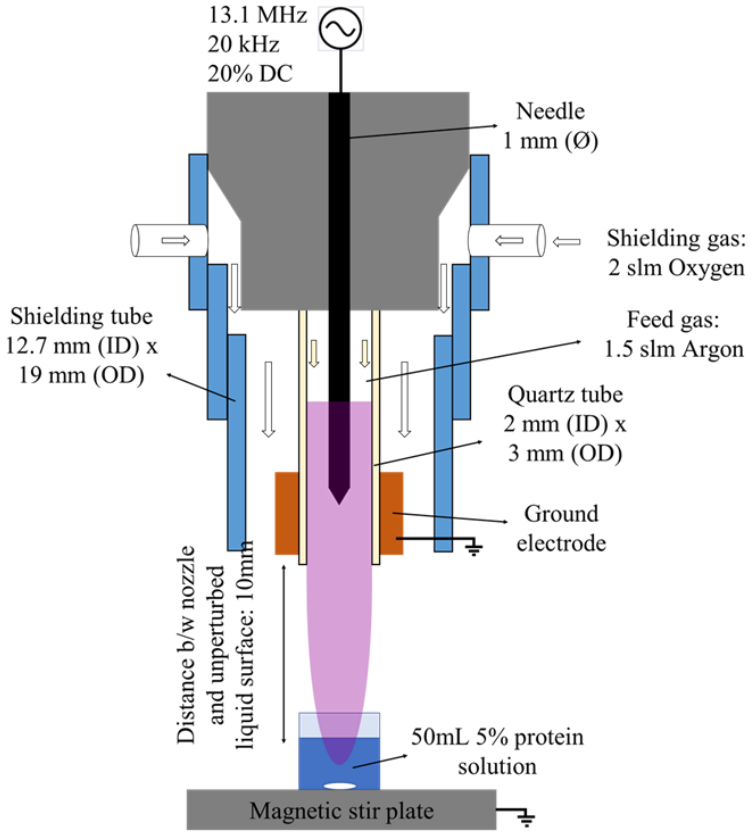

Figure 14. Schematic of radio frequency (RF) driven atmospheric pressure plasma jet (APPJ) using Ar/O2 plasma at a total gas flow rate of 3.5 slm.

3.3.3.2 Remote two-dimensional dielectric barrier discharge (2D-DBD) treatment.

The flow-through plasma reactor as detailed by Nayak et al. (2018) and in **Chapter 2.3.3.1** was used **(Figure 11)**. The discharge was operated at atmospheric pressure in argon (Ar) with 20% admixture of O_2 (Ultra-Pure-Carrier Grade 99.9993%) at a constant total gas flow rate of 5 slm. The plasma power was kept constant at 10.3 ± 1.1 W in Ar/O_2. The Ar/O_2 plasma dominantly produced O_3 as the long-lived species. The O_3 densities in Ar/O_2 plasma was $(1.4 \pm 0.2) \times 10^{22}$ m^{-3}, as measured by UV absorption spectroscopy at 253.4 nm(Nayak, Sousa, et al., 2017). The effluent of the 2D-DBD confined within a polycarbonate tube was sent through a 100 mL protein solution (5% w/v protein in DDW) in a bubbler (PYREX® 500 mL Gas Washing Bottle with Coarse Fritted Cylinder) for treatment time of 5, 15, 30, and 45 min, in triplicate. The gas residence time in the effluent of the plasma till it reached the protein solution was ~12 s.

3.3.3.2 Nanosecond-pulsed (ns-pulsed) plasma treatment

The schematic for the ns-pulsed discharge reactor is shown in **Figure 15a**. The setup consisted of a hollow stainless-steel tube (mention diameter) as the high voltage electrode, which and was placed 7.5 mm above a 100 mL protein solution (5% w/v protein in DDW). The solution was grounded to a resistor of 77 Ω to avoid shorting of the high voltage power supply. A ns-pulse generator (NPG-18/3500N) and surrounding atmospheric air were used to generate a discharge between the powered electrode and the surface of the protein solution by applying voltage pulses at a repetition rate of 1 kHz and an amplitude of ~10 kV. The applied voltage and current in the circuit were recorded using a high-voltage probe (Tektronix P6015A) and a Rogowski coil (Pearson 2877) (**Figure 15a)**. The phase shift between the voltage and current probes was corrected using the relation between the

capacitive current and voltage as measured for voltage pulses that did not lead to plasma formation. The energy in the discharge was determined as the product of the voltage and current waveforms. Protein samples were treated with a fixed pulse energy of ~1 mJ, for 5, 15, and 30 min, in triplicate, to alter the total energy deposition into the protein solution. The power and the energy deposited on the protein solution as a function of time is shown in **Figure 15b**.

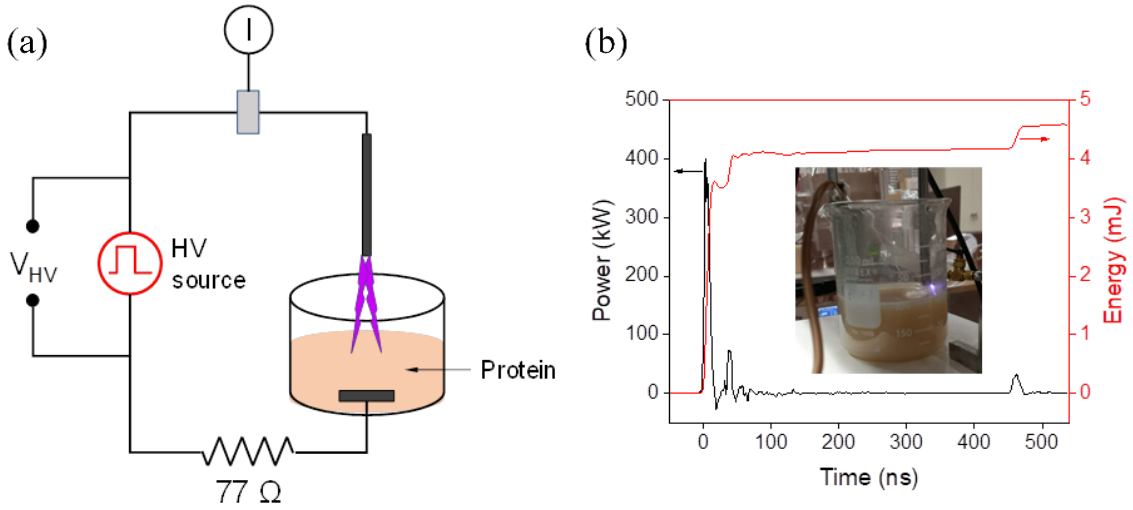

Figure 15. (a) Schematic of nanosecond-pulsed plasma (V_{HV} – high voltage probe, I – current probe), and (b) power and energy of the ns-pulsed plasma as a function of time. The picture of the discharge is also shown as an inset.

3.3.4 Handling of plasma-treated protein solutions

PPI solutions (5% w/v protein in DDW) were prepared, in triplicate, at pH 2 for all plasma treatments, to evaluate the impact of different plasma sources on structure and functionality of PPI. Immediately after treatment, protein solutions were adjusted to pH 7, dialyzed (3.5 kDa membrane), lyophilized, and stored at 4°C. Protein content (~90%) of lyophilized samples was determined following the Dumas method, and ash content (2.5-4.2%) was determined by the AOAC dry ashing method (AOAC 942.05).

3.3.5 Color measurement

The color of cPPI (reference), control PPI, and plasma treated samples was assessed, in triplicate, using a Chroma Meter CR-221 (Minolta Camera Co., Osaka, Japan), as described in **Section 2.3.5**. To assess the effect of plasma treatment on color, total color difference (ΔE) between treated and control PPI was calculated.

3.3.6 Protein profiling by gel electrophoresis

Protein profiling of cPPI, control PPI and all plasma treated samples was performed using sodium dodecyl sulfate polyacrylamide gel electrophoresis (SDS-PAGE), as described by Boyle et al. (2018). Briefly, samples (5 µL; containing ~ 50 µg protein) and Precision Plus™ MW standard (10 µL) were loaded onto a Criterion™ TGX™ 4-20% precast Tris-HCl gradient gel. The gel was electrophoresed, stained/destained, and imaged as outlined in **Section 2.3.6**.

3.3.7 Molecular weight distribution by size-exclusion – high-performance liquid chromatography (SE-HPLC)

cPPI, control PPI, and plasma treated PPIs were subjected to size-exclusion HPLC (SE-HPLC) using a Shimadzu HPLC system (Shimadzu Scientific Instruments, Colombia, MD, USA) and a Superdex 200 Increase 10/300 GL Prepacked Tricorn™ Column as described in **Section 2.3.7**. The analysis was performed at room temperature following the method of Bruckner-Guhmann et al. (2018), with modifications. Samples (1% protein, w/v), in triplicate, were prepared in three different sample buffers, pH 7 phosphate buffer (0.05 M sodium phosphate with 0.1 M sodium chloride), SDS phosphate buffer (0.05 M sodium

phosphate with 0.1 M sodium chloride and 0.1% sodium dodecyl sulfate), and SDS/BME buffer (0.05 M sodium phosphate with 0.1 M sodium chloride, 0.1% sodium dodecyl sulfate and 2.5% beta-Mercaptoethanol) to investigate the molecular weight distribution, degree of polymerization, and association of proteins through covalent and non-covalent interactions. Samples in different buffers were solubilized at room temperature for 2 hours, then passed through a 0.45 μm filter, automatically injected (100 μL) and separated isocratically using pH 7 phosphate buffer mobile phase at a flow rate of 0.5 mL per minute for a total run time of 80 minutes. Detection and analysis were performed at 280 nm as described in **Section 2.3.7**.

3.3.8 Differential scanning calorimetry (DSC)

Protein denaturation temperature and enthalpy of the different samples were determined using a DSC instrument (DSC 1 STARe System, Mettler Toledo, Columbus, OH, USA), as described in **Section 2.3.8**. Thermograms were manually integrated to obtain the peak denaturation temperature and enthalpy of denaturation for each protein using Mettler Toledo's STARe Software version 11.00.

3.3.9 Attenuated total reflectance Fourier-transform infrared spectroscopy (ATR-FTIR)

ATR-FTIR spectra of cPPI, control PPI, and plasma treated PPIs were recorded using Fourier-transform infrared spectrometer (Thermofisher Nicolett iS50 FTIR), following the method described in **Section 2.3.9**. ATR spectra were converted to transmission spectra using OMNIC® software. Second derivative of Amide I band

(1600cm^{-1} -1700 cm^{-1}) were obtained by PeakFit v. 4.12 to identify alpha-helix, beta-sheet, beta-turn, and random coil distribution.

3.3.10 Measurement of protein surface properties

Surface hydrophobicity of the different samples was determined fluorometrically using an 8-anilino-1-napthalenesulfonic acid ammonium salt (ANS) probe, based on the method outlined by Boyle et al. (2018), with modifications in fluorescence gain (40) and the use of black 96-well plate. Zeta potential was measured using a dynamic light scattering instrument (Malvern Nano Z-S Zetasizer) as outlined in **Section 2.3.10**. Zeta potential was determined by Malvern's Zetasizer software (version 7.13) using the Smoluchowski model.

3.3.11 Protein solubility

Protein solubility at pH 7 and at 5% protein concentration (w/v in DDW) was determined, in triplicate, as described in **Section 2.3.11**. Samples were assessed at room temperature and post thermal treatment (80°C for 30 min). Solubility was expressed as the percentage of soluble protein (present in the supernatant post centrifugation) compared to the total protein content determined following the Dumas method.

3.3.12 Gel strength

Strength of heat-induced gels was determined based on the as described in **Section 2.3.12** at 15% and 20% protein (w/v, in DDW), in triplicate, at pH 7. Gel strength was measured by a TA-TX Plus Texture Analyzer (Stable Micro Systems LTD, Surrey, UK) using a 100 mm diameter probe, 5 mm/s test speed, and a target distance of

0.5 mm from the plate. The maximum force measured in Newton was the rupture force of the gel.

3.3.13 Emulsification capacity

Emulsification capacity (EC) was determined, in triplicate, at 1% and 2% protein concentration (w/v in DDW), as described in **Section 2.3.13.** Emulsification capacity was expressed as g of oil emulsified by one g of protein.

3.3.14 Amino acid and non-protein molecules analysis

To characterize the potential influence of plasma processing on individual amino acids, control PPI and selected plasma treated PPI samples were analyzed for amino acid compositional changes. Sample selection for this analysis was based on the uniqueness in protein structure and functionality as a result of APPJ, 2D-DBD, and ns-pulsed treatment. Control PPI and plasma treated samples, in triplicate, were hydrolyzed by hydrochloric acid(Mao, 2019). Briefly, 50 mg of sample was mixed with 7 mL of 6N hydrochloric acid and hydrolyzed at 165 °C for 15 min using a Discover SP-D microwave digester (CEM Corporation, Matthews, NC). After the hydrolysis, 50 μL of hydrolyte was dried by nitrogen and then reconstituted in 500 μL of 50% aqueous ACN. Intact protein samples, in triplicates, were extracted for their small-molecule content, and both the hydrolytes and the PPI extracts were derivatized with dansyl chloride. The derivatized samples were analyzed by ultra-performance liquid chromatography (Acuity HPLC, Waters, Milford, MA, USA) coupled with mass spectrometry (Synapt G2-Si, Waters, Milford, MA, USA) and a BEH C18 UPLC column, following the method described by Wang et al. (2018) and Ma et al.

(2019). Characteristics of amino acid composition and non-protein molecules were captured by MarkerLynx software (Waters, Milford, MA, USA) and incorporated into a multivariate data matrix after centroiding, deisotoping, filtering, peak recognition, and integration, as described by Mao et al. (2021), with modifications. The contribution of samples to the principal components was described in a scores scatter plot of a multivariate model. The IPL-responsive metabolites were identified by analyzing the ions contributing to the principal components in a loadings scatter plot. To quantify amino acids, the ratio between the peak area of each amino acid to that of the internal standard was fitted with a standard curve using QuanLynx software (Waters, Milford, MA, USA).

3.3.15 Statistical analysis

Analysis of variance (ANOVA) was performed using SigmaPlot software version 14.0 for windows (Systat Software, San Jose, CA). Tukey-Kramer multiple means comparison test was used to determine significant differences ($P \leq 0.05$) between the means ($n = 3$) of at least three different samples. ANOVA tables can be found in **Appendix F (Tables 67-155).** A student's unpaired t-test was used to test for significant differences ($P \leq 0.05$) between the means ($n = 3$) of two different samples.

3.4 Results and Discussion

3.4.1 Effect of different plasma treatments on PPI color

While minimal changes were noted in lightness (L*), a significant decrease in yellow color (b*) of PPI was observed after all three CAP treatments **(Appendix K: Table 160)**. A similar decrease in b* of PPI upon treatment with OH radicals and O_3 was

discussed in **Section 2.4.2**. APPJ and ns-pulsed were able to generate both O_3 and OH while DBD was only able to generate O_3. Therefore, the decrease in b*of PPI after DBD treatment was only attributed to the O_3, whereas the decrease in b* of PPI after APPJ and ns-pulsed treatments was possibly attributed OH and O_3, as well as other short-lived species. With the greatest number of species at high intensity, ns-pulsed treatment had the greatest effect on color, more so at longer treatment time. A decrease in yellowness is an overall positive effect on the appearance of PPI.

3.4.2 Effect of different plasma treatments on the protein profile and molecular weight distribution

Under non-reducing conditions, intense smearing and dark bands at the top of the SDS-gel indicated the presence of highly polymerized proteins in cPPI, analyzed as a reference protein **(Figure 16, lane 2, 15, 28).** Under reducing conditions, the smearing was less apparent, yet distinct high intensity bands remained in the upper region of the gel, indicating that some polymers in cPPI were formed by covalent linkages other than disulfide bonds **(Figure 16, lane 8, 21, 33)**. This high level of polymerization in cPPI may be detrimental to its functional properties.

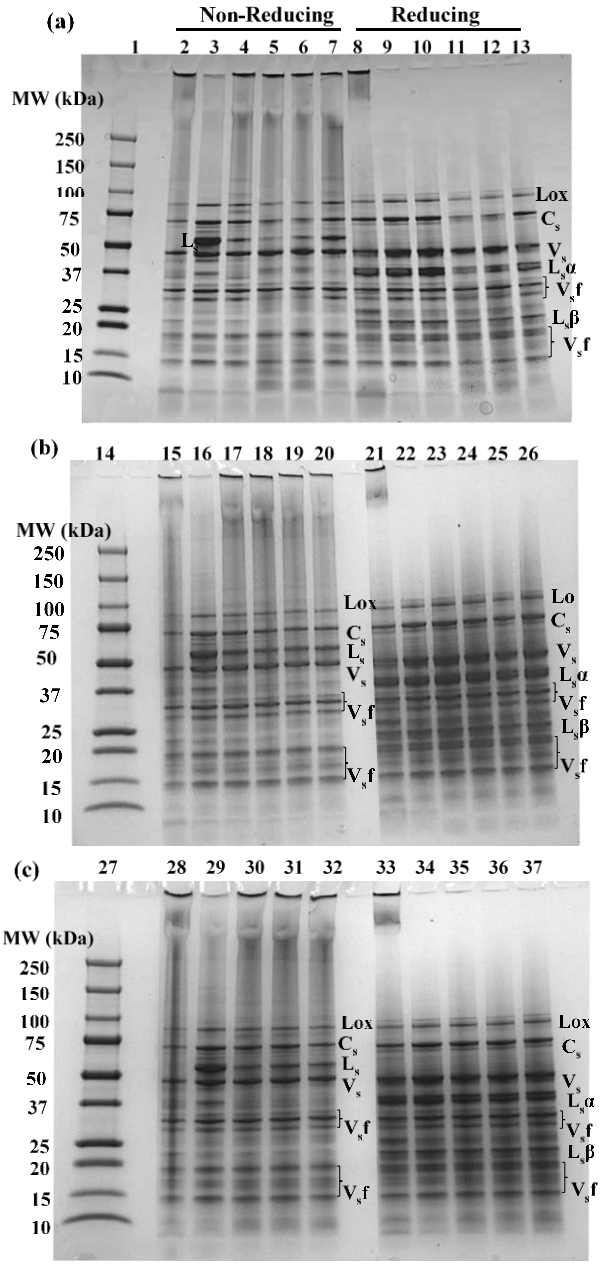

Figure 16. Figure SDS-PAGE gel visualization of the protein profiles of (a) APPJ treated samples, (b) 2D-DBD treated samples, and (c) ns-pulsed treated samples under non-reducing (Lanes 4-7, 17-20, & 30-32) and reducing (Lanes 10-13, 23-26, & 35-37) conditions. Lanes 1, 14, 27: Molecular weight (MW) marker; Lanes 2, 8, 15, 21, 28, & 33: cPPI; Lanes 3, 9, 16, 22, 29, & 34: control PPI; Lanes 4 & 10, Lanes 5 & 11, Lanes 6 & 12, Lanes 7 & 13: APPJ-5, -15, -30, and -45min, respectively; Lanes 17 & 23, Lanes 18 & 24, Lanes 19 & 25, and Lanes 20 & 26: 2D-DBD-5, -15, -30, and -45min, respectively; Lanes 30 & 35, Lanes 31 & 36, Lanes 32 & 37: ns-pulsed-5, -15, and -30, respectively. Lox: lipoxygenase; C_s: subunits of convicilin; V_s: subunits of vicilin; $L_s\alpha$: acidic peptides cleaved from legumin subunits; $L_s\beta$: basic peptide cleavage from legumin subunit; V_sf: fractions of vicilin subunits result from post-translational cleavages.

All plasma treatments (APPJ, 2D-DBD, and ns-pulsed) resulted in protein polymerization compared to the control PPI, as indicated by smearing in the upper molecular weight region of the SDS-gel under non-reducing conditions, coupled with lower intensities of the legumin, vicilin, and convicilin bands **(Figure 16 a, b, & c)**. Under reducing conditions, the smearing was no longer visible, and the intensities of the legumin, vicilin, and convicilin bands were comparable to those in the control PPI. This observation indicated that the polymerization induced by all plasma treatments occurred mostly through disulfide linkages. Protein polymerization was most intense in the ns-pulsed treated samples, followed by APPJ and 2D-DBD samples. The oxidation by O_3, and by OH radicals and other short-lived species, which were present at the highest intensity in ns-pulsed plasma, contributed to the observed polymerization. Protein polymerization through disulfide linkages has been observed previously as a result of remote DBD with air (Mahdavian Mehr & Koocheki, 2020; Meinlschmidt et al., 2016; Nyaisaba et al., 2019). The formation of high molecular weight (HMW) proteins may enhance functional properties of pea protein, namely it gelation and emulsification potential.

Interestingly, formation of low molecular weight (LMW) peptides (<15kDa) was observed in APPJ-15 and 30 min samples (**Figure 16a**, lanes 5, 6, 11, & 12), as well as ns-pulsed 5-30 min samples (**Figure 16c**, lanes 30-32 & 35-37), indicating bond cleavage that was not apparent in 2D-DBD samples (**Figure 16b**). Similarly, peptide bond cleavage was not observed in previous reports on remote DBD treatment of proteins. In addition, no bond cleavage was observed after OH radical treatment of pea protein **(Section 2.4.3)**. Therefore, the newly observed formation of LMW peptides were most likely due to the presence of electrons or other radicals in APPJ and ns-pulsed plasma. The formation of LMW proteins

after APPJ and ns-pulsed treatments could potentially affect the functionality of pea protein.

The molecular weight distribution of soluble aggregates, functional proteins (legumin, vicilin, and convicilin), and LMW proteins/peptides were further characterized using SE-HPLC (**Table 7 and Appendix L: Figure 23)**. When samples were dissolved in phosphate buffer without SDS or a reducing agent, neither non-covalent interactions nor disulfide linkages among the protein subunits were disrupted during the analysis. The molecular weight of soluble aggregates was approximately 1,200 kDa, whereas those of hexameric legumin, trimeric convicilin, and trimeric vicilin were within the expected ranges (Barac et al., 2010; Gatehouse et al., 1982; Tzitzikas et al., 2006). Insoluble aggregates did not pass through the 0.45 μm filter and consequently were not observed. The abundance of functional proteins and soluble aggregates was low in cPPI, indicating that most functional proteins formed insoluble aggregates.

Table 7. Molecular weight and relative abundance of soluble aggregates, legumin, convicilin, and vicilin present in commercial pea protein reference, control pea protein isolate (PPI), and APPJ, 2D-DBD, ns-pulsed treated PPI samples, as analyzed by size-exclusion high-performance liquid chromatography (SE-HPLC).

Samples	Relative Abundance (%) of Protein Fractions[1]											
	Phosphate Buffer[2]				Phosphate Buffer (0.1% SDS)[3]				Phosphate Buffer (0.1% SDS+ 2.5% BME)[4]			
	Soluble aggregates (~1200 kDa)	Legumin (~450 kDa)	Conviclin (~250 kDa)	Vicilin (~160 kDa)	Soluble aggregates	Legumin	Conviclin	Vicilin	Soluble aggregates	Legumin	Conviclin	Vicilin
cPPI	$13.1^{6cD\delta}$	*[5]	*	$3.42^{bcB\beta}$	$45.5^{aA\alpha}$	*	*	$7.30^{aA\alpha}$	$37.3^{aA\alpha}$	*	*	$4.92^{aA\alpha}$
PPI	$4.86^{dE\varepsilon}$	$28.2^{aA\alpha}$	$7.04^{aA\alpha}$	$9.82^{aA\alpha}$	$27.2^{cC\Upsilon}$	$9.43^{aA\alpha}$	$11.36^{aA\alpha}$	$4.04^{bB\beta}$	$30.0^{cB\Upsilon}$	$6.58^{aA\alpha}$	$8.72^{aA\alpha}$	$2.77^{bB\beta}$
APPJ-5min	26.1^{ab}	4.53^{b}	5.00^{b}	2.83^{c}	24.5^{cd}	4.01^{b}	4.33^{b}	2.14^{c}	27.9^{d}	3.08^{b}	2.55^{b}	1.45^{c}
APPJ-15min	25.5^{b}	2.29^{c}	4.38^{c}	3.79^{b}	$24.^{6cd}$	4.31^{b}	3.82^{b}	2.18^{c}	25.2^{e}	2.26^{c}	2.37^{c}	1.02^{e}
APPJ-30min	25.3^{b}	2.41^{c}	4.08^{c}	3.50^{bc}	22.8^{d}	4.38^{b}	3.62^{b}	1.08^{e}	24.4^{e}	2.11^{d}	2.22^{d}	0.97^{e}
APPJ-45min	26.9^{a}	3.42^{bc}	4.31^{c}	3.11^{bc}	30.2^{b}	4.87^{b}	2.56^{c}	1.74^{d}	32.6^{b}	2.08^{d}	1.67^{e}	1.23^{d}
2D-DBD- 5min	22.6^{C}	5.14^{B}	5.19^{B}	2.57^{C}	23.8^{D}	4.29^{B}	4.37^{B}	2.22^{C}	22.8^{C}	3.15^{B}	2.75^{BC}	1.56^{C}
2D-DBD- 15min	29.4^{B}	4.19^{D}	4.32^{C}	2.00^{CD}	21.2^{D}	4.35^{B}	4.49^{B}	2.12^{C}	18.4^{D}	2.86^{C}	2.58^{CD}	1.31^{D}
2D-DBD- 30min	34.7^{A}	3.91^{E}	4.15^{C}	1.57^{D}	32.8^{B}	3.52^{B}	3.72^{B}	1.65^{D}	29.5^{B}	2.53^{D}	2.52^{D}	1.17^{DE}
2D-DBD- 45min	24.9^{C}	4.50^{C}	4.90^{B}	1.66^{D}	24.0^{D}	4.17^{B}	4.53^{B}	1.68^{D}	18.2^{D}	2.70^{CD}	2.83^{B}	1.08^{E}
ns-pulsed-5min	36.7^{α}	5.08^{β}	5.88^{β}	3.01^{β}	32.1^{β}	5.02^{β}	5.75^{β}	2.81^{Υ}	32.5^{β}	3.75^{Υ}	3.61^{β}	1.66^{Υ}
ns-pulsed-15min	32.7^{β}	5.42^{β}	5.95^{β}	2.95^{β}	$29.0^{\beta\Upsilon}$	5.33^{β}	5.80^{β}	2.69^{Υ}	29.6^{Υ}	4.21^{β}	3.51^{β}	$2.16^{\beta\Upsilon}$
ns-pulsed-30min	27.4^{Υ}	3.69^{β}	3.69^{Υ}	3.01^{β}	21.6^{δ}	3.56^{β}	3.74^{Υ}	2.90^{Υ}	25.5^{δ}	2.62^{δ}	2.05^{Υ}	1.59^{Υ}

[1]Relative abundance (%) is the area of a specific peak divided by the total peak area for that sample; [2]Samples were dissolved in pH 7 phosphate buffer and analyzed by high-performance size exclusion chromatography (SE-HPLC); [3]Samples were dissolved in pH 7 phosphate buffer with the presence of 0.1% SDS and analyzed by high-performance size exclusion chromatography (SE-HPLC); [4]Samples were dissolved in pH 7 phosphate buffer with the presence of 0.1% SDS and 2.5% BME, and analyzed by high-performance size exclusion chromatography (SE-HPLC); [5]An asterisk (*) represents no peak was apparent in this molecular weight range; 6 Means (n = 3) in each column with lowercase letters indicate significant differences of APPJ samples in comparison to nPPI and cPPI, upper letters indicate significant differences of 2D-DBD samples in comparison to nPPI and cPPI, and Greek alphabet indicate significant differences of ns-pulsed samples in comparison to nPPI and cPPI, according to the Tukey-Kramer multiple means comparison test ($P < 0.05$).

Compared to the control PPI, all plasma treated PPIs contained a significantly higher abundance of soluble aggregates. Treatment with APPJ for 15 and 30 min resulted in a significantly lower relative abundance of soluble aggregates than 45 min treatment. This observation could be in part attributed to bond cleavage after 15 and 30 of APPJ treatment, as shown by SDS-PAGE **(Figure 16a, lanes 5, 6, 11 & 12)**. The relative abundance of soluble aggregates in 2D-DBD treated PPI was significantly higher after 15 and 30 min of treatment compared to 5 and 45 min. The decrease in soluble aggregates after 45 min 2D-DBD treatment was possibly due to formation of insoluble aggregates. Similarly, the abundance of soluble aggregates decreased significantly in ns-pulsed samples with longer treatment time, indicating as well the formation of insoluble aggregates. Ji et al. (2018) and Ji et al. (2019) reported an increase in water holding capacity and solubility of peanut protein after short-time DBD (air) treatment, and a decrease in these functional properties after long-time DBD (air) treatment. Our results indicated that the reported decrease in functionality could have been due to the formation of insoluble aggregates.

When SDS was present in the sample buffer, insoluble aggregates formed by non-covalent interactions were solubilized and resulted in a significantly (P<0.05) higher content of soluble aggregates in cPPI and control PPI (**Table 7 and Appendix L: Figure 23)**. The slight decrease in the relative abundance of soluble aggregates in most plasma treated PPIs in the presence of SDS, indicated that few of the interactions within the soluble aggregates were non-covalent. Simultaneously, proteins associating through non-covalent interactions, such as functional proteins, dissociated into subunits with molecular weights less than 100 kDa (**Appendix L: Figure 23)**.

When both SDS and BME were present in the sample buffer, insoluble aggregates formed through disulfide linkages and non-covalent interactions were solubilized, and protein subunits linked via disulfide linkages were cleaved into LMW monomers. Reduction of disulfide linkages contributed to the other observed changes in the relative abundance of the different protein fractions (**Table 7**). Observations were a combined effect of breakdown of insoluble aggregates into soluble aggregates, and reduction of soluble aggregates into monomers. Specifically, the significant increase in the relative abundance of soluble aggregates in 30 min ns-pulsed samples in BME compared to that in SDS, indicated that some insoluble aggregates were formed through disulfide linkages with the longer treatment. Therefore, longer treatment time with an intense plasma source such as ns-pulsed, might not be favorable for protein functionality.

3.4.3 Effect of different plasma treatments on the protein denaturation state

Two endothermic peaks corresponding to vicilin and legumin were observed in the control PPI **(Table 8)**. Convicilin was not seen as a separate endothermic peak because of its structural similarity to viclin. As expected, no endothermic peaks were observed for the cPPI reference, thereby indicating complete denaturation. cPPI might have been subjected to severe extraction and processing conditions that led to denaturation and subsequent polymerization **(Figure 16)**.

Table 8. Denaturation temperatures and enthalpy, secondary structure, surface hydrophobicity and surface charge of commercial pea protein reference, control pea protein isolate (PPI), and APPJ, 2D-DBD, and ns-pulsed treated PPI.

Samples	Denaturation Temperature and Enthalpy				Surface Properties		Secondary Structure			
	Vicilin		Legumin		Surface Hydrophobicity	Surface Charge	α Helix	β Sheet	β Turn	Random Coil
	Denaturation Temperature (Td, °C)	Enthalpy of Denaturation (ΔH, J g-1)	Denaturation Temperature (Td, °C)	Enthalpy of Denaturation (ΔH, J g-1)	RFI	mV	%			
cPPI	*[1]	*	*	*	$12719^{a\alpha}$	$-27.2^{aA\alpha}$	$14.5^{cB\beta}$	$46.3^{aBC\alpha\beta}$	$24.8^{aA\alpha}$	$14.5^{aA\alpha}$
PPI	$84.48^{aA\alpha 2}$	$6.39^{aA\alpha}$	91.36^{a}	1.48^{a}	$8545^{dBC\beta}$	-37.6^{bD}	$23.3^{aA\alpha}$	$44.9^{abC\beta}$	$22.8^{aA\alpha}$	$9.02^{bBC\beta\gamma}$
APPJ-5min	81.65^{b}	1.66^{b}	90.40^{a}	0.20^{b}	9349^{bc}	-37.3^{b}	19.9^{ab}	43.7^{a}	22.1^{a}	14.3^{a}
APPJ-15min	82.56^{ab}	1.35^{bc}	*	*	10774^{abc}	-35.4^{b}	18.9^{abc}	45.5^{a}	20.6^{a}	15.0^{a}
APPJ-30min	82.00^{b}	0.97^{cd}	*	*	10146^{bc}	-35.1^{b}	17.4^{bc}	44.7^{a}	21.3^{a}	16.5^{a}
APPJ-45min	81.56^{b}	0.76^{d}	*	*	11459^{ab}	-36.5^{b}	20.6^{ab}	42.2^{b}	22.1^{a}	15.1^{a}
2D-DBD-5min	82.49^{B}	1.72^{B}	*	*	8526^{BC}	-36.2^{CD}	14.8^{B}	49.7^{A}	26.1^{A}	9.40^{BC}
2D-DBD-15min	82.01^{BC}	1.34^{BC}	*	*	9203^{BC}	-34.9^{BC}	17.3^{B}	48.3^{AB}	25.8^{A}	8.65^{BC}
2D-DBD-30min	80.92^{D}	1.15^{C}	*	*	10415^{B}	-34.5^{BC}	17.0^{B}	49.9^{A}	25.6^{A}	7.56^{C}
2D-DBD-45min	81.72^{C}	1.25^{C}	*	*	8500^{C}	-33.5^{B}	17.0^{B}	46.0^{BC}	26.3^{A}	10.7^{B}
ns-pulsed-5min	81.56^{β}	1.77^{δ}	*	*	12088^{α}	-34.4^{β}	16.6^{β}	47.4^{α}	28.3^{α}	7.68^{γ}
ns-pulsed-15min	81.74^{β}	1.49^{Υ}	*	*	12354^{α}	-34.4^{β}	15.9^{β}	48.3^{α}	24.4^{α}	9.57^{β}
ns-pulsed-30min	82.05^{β}	0.48^{β}	*	*	9580^{β}	-36.1^{β}	16.3^{β}	48.6^{α}	24.6^{α}	10.6^{β}

[1]An asterisk (*) represents no peak of denaturation observed; [2]Means (n = 3) in each column with lowercase letters indicate significant differences of APPJ samples in comparison to nPPI and cPPI, upper letters indicate significant differences of 2D-DBD samples in comparison to nPPI and cPPI, and Greek alphabet indicate significant differences of ns-pulsed samples in comparison to nPPI and cPPI, according to the Tukey-Kramer multiple means comparison test ($P < 0.05$).

Several studies have reported protein denaturation/unfolding after remote DBD and APPJ treatment (Ekezie et al., 2019; Meinlschmidt et al., 2016; Sharifian et al., 2019). However, there are no reports that differentiated the effects of various plasma sources on protein denaturation. In this study, all plasma treated PPI had a significantly lower denaturation temperature and enthalpy compared to the control PPI **(Table 8)**. The extent of protein denaturation, as indicated by the enthalpy, was greater with longer plasma treatment time, regardless of the plasma sources. Among all plasma treated samples, the 30 min ns-pulsed treated PPI had the lowest enthalpy for vicilin. The presence of intense long-lived and shorted lived reactive species in ns-pulsed plasma contributed to this observation. Protein unfolding can facilitate polymerization, as more hydrophobic groups and sulfhydryl groups are exposed. The higher extent of denaturation in the 30 min ns-pulsed treated PPI resulted in the higher level of observed polymerization in this sample. Both OH and O_3 species resulted in similar denaturation pattern **(Section 2.4.4)**. APPJ treatment, which produced OH and O_3 species, reduced the enthalpy to a greater extent than DBD treatment did, which only generated long-lived O_3.

3.4.4 Effect of different plasma treatments on the protein surface properties

Significant increase in surface hydrophobicity was observed after APPJ treatment, and with longer exposure time (**Table 8**). The greater extent of protein denaturation with the increase in APPJ treatment time (5-45 min) contributed to the observed increase in surface hydrophobicity. While 2D-DBD treatment for 5 min did not result in a significant increase in surface hydrophobicity, increasing treatment time from 5 to 15 and 30 min did. Increases in surface hydrophobicity affect protein interactions and consequently their functional properties.

The surface hydrophobicity of the 45 min 2D-DBD sample was significantly lower than the other 2D-DBD samples. The observed decrease in the relative abundance of soluble aggregates after 45 min of 2D-DBD treatment compared to shorter treatment times **(Table 7)**, coupled with the increased degree of denaturation (**Table 8**), and the reduced surface hydrophobicity, confirm that the formation of insoluble aggregates was in part attributed to hydrophobic interactions. Similarly, the surface hydrophobicity of the 30 min ns-pulsed treated sample was significantly lower than that of the 5 and 15 min ns-pulsed treated samples, thus explaining the observed decrease in the relative abundance of soluble aggregates and the formation of polymers through hydrophobic interactions.

Surface charge can also directly affect protein functionality. Protein denaturation and polymerization also affect the surface charge, owing to changes in the conformation and relative exposure of different groups. The reference cPPI had the least net surface charge (**Table 8**), mostly attributed to the high content of insoluble aggregates. No significant differences in surface charge were observed after APPJ treatment, compared to the control PPI. The net surface charge after 15-45 min of 2D-DBD treatment, and after ns-pulsed treatment (all times) was significantly lower than that of the control. This observed decrease in surface charge was in part attributed to the degree of denaturation and the extent of polymerization. However, observed differences are considerably minor mostly due to formation of soluble aggregates that retained high net surface charge, and in part due to the production of LMW proteins.

3.4.5 Effect of plasma treatments on the protein secondary structure

The relative abundance of α helix, β sheet, β turn and random coil in PPI **(Table 8)** was similar to that reported by Svenja M Beck et al. (2017). The reference cPPI had a significantly lower relative amount of α helix and a higher relative amount of random coil compared to the control PPI, indicating protein denaturation at the secondary structure level. A significant decrease in the relative amount of α helix was observed after APPJ, 2D-DBD, and ns-pulsed treatment, also indicating protein denaturation at the secondary structure level. With the decrease in the relative amount of α helix, an increase in random coil was observed after APPJ treatment, whereas an increase in β sheet was noted after 2D-DBD and ns-pulsed treatments. Changes in random coil versus β sheet content will have different impacts on protein functionality. For example, increases in β sheet structure resulted in enhanced gelling and emulsification properties of various plant and animal proteins (Cao & Mezzenga, 2019).

3.4.6 Effect of plasma treatments on protein functionality

Protein solubility is important for high beverage applications, and it can influence gelation and emulsification properties, which are important for other food systems. The reference cPPI exhibited the lowest solubility under both non-heated and heated conditions **(Table 9)**. This observation was expected due to cPPI's degree of denaturation, high level of polymerization and content of insoluble aggregates, high surface hydrophobicity, and comparatively low surface charge.

Table 9. Solubility, gel strength and emulsification capacity of commercial pea protein reference, control pea protein isolate (PPI), and APPJ, 2D-DBD, and ns-pulsed treated PPI.

Samples	Solubility (5% protein)		Gel Strength (20% protein)	Emulsification Capacity (2% protein)	Emulsification Capacity (1% protein)
	Non-Heated	Heated (80°C for 30 min)	Strength (N)	mL oil/g protein	mL oil/g protein
cPPI	$24.7^{2dE\varepsilon}$	$45.5^{cC\beta}$	$2.73^{eD\Upsilon}$	$229.4^{cD\beta}$	*[1]
PPI	$82.4^{aA\alpha}$	$79.6^{aA\alpha}$	$4.00^{eD\Upsilon}$	$390.6^{dE\beta}$	*
APPJ-5min	64.5^{c}	77.2^{ab}	6.25^{d}	582.8^{a}	812.2^{ab}
APPJ-15min	68.4^{b}	72.3^{b}	12.3^{b}	533.2^{b}	737.8^{b}
APPJ-30min	68.1^{b}	75.2^{ab}	14.0^{a}	496.0^{b}	762.6^{b}
APPJ-45min	65.7^{bc}	76.5^{ab}	10.3^{c}	613.8^{a}	886.6^{a}
2D-DBD-5min	61.7^{C}	74.5^{AB}	13.3^{AB}	536.3^{C}	750.2^{B}
2D-DBD-15min	49.0^{D}	69.2^{B}	12.5^{B}	582.8^{AB}	762.6^{B}
2D-DBD-30min	68.3^{B}	78.1^{A}	14.7^{A}	610.7^{A}	837.0^{A}
2D-DBD-45min	52.1^{D}	71.0^{B}	10.3^{C}	564.2^{BC}	830.8^{A}
ns-pulsed-5min	72.2^{β}	76.5^{α}	10.4^{β}	585.9^{α}	818.4^{α}
ns-pulsed-15min	67.3^{Υ}	80.3^{α}	8.82^{β}	585.9^{α}	843.2^{α}
ns-pulsed-30min	61.1^{δ}	80.3^{α}	12.2^{α}	567.3^{α}	756.4^{α}

[1]An asterisk (*) represents no emulsion formed at 1% protein concentration; [2]Means (n = 3) in each column with lowercase letters indicate significant differences of APPJ samples in comparison to PPI and cPPI, upper letters indicate significant differences of 2D-DBD samples in comparison to PPI and cPPI, and Greek alphabet indicate significant differences of ns-pulsed samples in comparison to PPI and cPPI, according to the Tukey-Kramer multiple means comparison test ($P < 0.05$).

Compared to control PPI, a modest and sometimes significant decrease in solubility, under non-heated conditions, was observed after most plasma treatments. Under heated conditions, the solubility of most plasma treated samples was comparable to that of the control. Changes in solubility were minor due mostly to the formation of larger proportion of soluble aggregates relative to insoluble aggregates. Additionally, the enhancement in solubility upon heating of the plasma treated samples indicated that some of the aggregates formed during the treatment were associated by non-covalent interactions, some of which (H-bonding and electrostatic interactions) are disrupted upon heating. In contrast, the solubility of cPPI, while enhanced upon heating, remained relatively low because the insoluble aggregates present in cPPI were mostly formed through disulfide and other covalent linkages **(Figure 16)**. This observation is promising for non-thermal CAP processing compared to thermal processing employed during the production of cPPI.

The reference cPPI exhibited the lowest gel strength followed by the control PPI (**Table 9**). The poor gel strength of cPPI was attributed to its low solubility, high level of aggregation, and imbalance of surface hydrophobicity to the surface charge, whereas the undesirable gel strength of the control PPI was attributed mostly to the intrinsic protein profile that is low in legumin content, and partly to the comparatively low surface hydrophobicity to surface charge ratio. Legumin contains cysteine residues that can form inter- and intra-molecular disulfide linkages, contributing to gel strength. On the other hand, a good surface charge to hydrophobicity balance is needed to facilitate protein-protein and protein-water interactions, and thus contribute to a well-structured gel. All plasma treated PPIs exhibited a significantly higher gel strength compared to the control

PPI and to cPPI. This observation can be attributed to the formation of soluble aggregates, the increased surface hydrophobicity, and to the surface charge that remained relatively high after the different plasma treatments. Soluble aggregates **(Table 7)**, as well as the increased surface hydrophobicity (**Table 8**), facilitated the formation of 3D gel networking, while the relatively high surface charge **(Table 8)** enabled protein-water interactions. The 30 min 2D-DBD treated sample exhibited significantly higher gel strength compared to most other plasma treated samples. In addition to presence of soluble aggregates and increased surface hydrophobicity, enhanced gelation can be partially attributed to higher β sheet content in the 30 min 2D-DBD treated sample compared to the control PPI. Presence of soluble aggregates and increase in surface hydrophobicity was also observed after APPJ and ns-pulsed treatments, along with relatively higher β sheet content after ns-pulsed treatments, contributing to enhanced gelation. The observed protein cleavage induced by electrons and radicals under different conditions and intensities could have also contributed to gelation. APPJ samples treated for 15 and 30 min had a significantly higher gel strength compared to those treated for 5 and 45 min. The plasma-induced bond cleavages, seen in the 15 and 30 min APPJ samples, could have reduced the size of insoluble aggregates, contributing further to balanced interactions.

The emulsification capacity (EC) was measured at both 1% and 2% protein concentration, since neither the cPPI nor the control PPI formed an emulsion at 1% protein concentration **(Table 9)**. Although the EC values of plasma treated samples measured at 1% protein concentration were significantly higher than those measured at 2% protein concentration, a thicker (more viscous) emulsion was formed at 2% protein concentration. The thicker emulsion formed was most likely due to a higher protein content in the

continuous phase. Differences in EC values among plasma treated samples had similar trend at both protein concentrations. The higher EC values at 1% protein concentration were likely due to relatively less protein-protein interactions and more protein-oil and protein-water interactions at in the interface. While the reference cPPI and control PPI formed an emulsion at 2% protein concentration, both had the lowest EC among the samples, but for different reasons. Poor EC of cPPI could be attributed to the high content of large insoluble aggregates, poor hydrophilic/lipophilic balance, and limited amount of soluble proteins that can migrate to the interface. Conversely, the poor EC of the control PPI could be attributed to the inherent characteristics of the dominant proteins, compact and inflexible structure (not denatured), and the relatively high surface charge to hydrophobicity ratio. The EC, however, was significantly enhanced after all plasma treatments due to the observed structural changes that allowed for better protein adsorption at the interface, contributing to the formation of emulsions at both 1% and 2% protein. Denaturation, which contributed to a more flexible protein structure, coupled with enhanced surfaced hydrophobicity, allowed for easier migration to and better adsorption at the interface.

3.4.7 Effect of different plasma treatments on the amino acid profile and non-protein components of the isolates

Amino acid composition is a key factor when considering the nutritional quality of a food product. Takai et al. (2014) reported chemical modifications of free amino acids after CAP treatment. Therefore, it was essential to investigate any potential changes in the amino acid composition of PPI after CAP treatment **(Table 10)**.

Table 10. Amino acids content (mg/g protein) of control pea protein isolate (PPI), APPJ-5min, APPJ- 30min, 2D-DBD-30min, and ns-pulsed-30min treated PPI.

Amino acid types	PPI	APPJ-5min	APPJ-30min	2D-DBD-30min	ns-pulsed-30min
Alanine	21.95	21.58	21.33	22.19	21.60
Glycine	40.79	39.74	38.95	41.64	39.16
Phenylalanine	55.56	55.86	54.09	55.27	54.29
Glutamate	249.0	237.2	231.2	247.1	241.1
Serine	53.23	52.91	51.64	53.49	52.64
Valine	50.31	50.65	49.85	50.48	50.02
Threonine	32.46	32.69	31.99	33.28	32.42
Isoleucine + Leucine	58.82	59.29	58.54	59.01	58.55
Aspartic acid	121.5	120.3	117.27	124.2	122.0
Proline	42.02	42.71	42.43	43.41	41.98
Tyrosine	51.26[1a]	46.70[b]	44.83[b]	48.25[ab]	47.64[b]
Arginine	54.94	54.23	57.06	54.94	54.47
Lysine	63.33	62.81	60.06	61.38	62.72
Histidine	18.69	18.28	17.88	18.24	18.06

[1]Means (n = 3) in each row with lowercase letters indicate significant differences according to the Tukey-Kramer multiple means comparison test ($P < 0.05$). Means without letters indicate no significant differences.

A slight but significant decrease in the amount of tyrosine was observed after APPJ and ns-pulsed treatments, compared to the control PPI and the 2D-DBD sample treated for 30 min (**Table 10**). Hydroxylation and nitration of aromatic rings in tyrosine after direct APPJ (He) treatment was reported by Takai et al. (2014). Electrons, OH radicals, H_2O+, and He+ were present in the APPJ (He) treatment. Similarly, direct APPJ (Ar + O_2) and ns-pulsed (air) treatment in this study produced electrons and OH radicals, which could have been responsible for the observed reduction in tyrosine. Remote 2D-DBD treatment, on the other hand, without the presence of radicals and electrons, had negligible impact on the tyrosine content. Similar result was reported by Chen et al. (2019), where the amino

acid composition of milk proteins was not significantly impacted by the remote DBD treatment. While a decrease in tyrosine was observed after APPJ and ns-pulsed treatment, the overall amino acid composition was not majorly altered by the tested plasma treatments.

Small portion of sugar, fat, color, and flavor compounds were also present in PPI. Therefore, it was crucial to investigate plasma-induced changes in non-protein components. PCA showed that the chemical composition of PPI was significantly altered after plasma treatment (**Figure 17 & Appendix M: Figure 24)**.

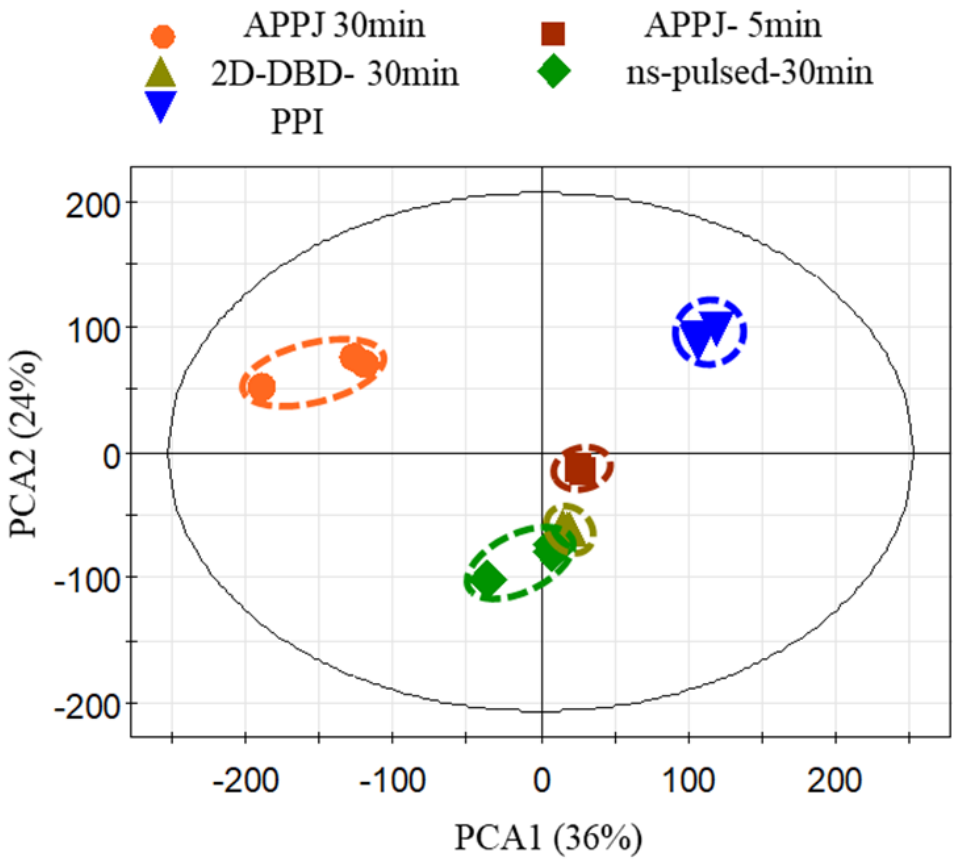

Figure 17. Score's plot of the principal components analysis (PCA) model produced from the pooled LC-MS analysis of amino acids and non-protein components. The samples in the same treatment group are circled (n=3)

Two principal components accounted for 60% of the variance in chemical composition of the control and plasma treated PPI samples. The first component (PC1) represented 36% of the variability. PC1 separated the APPJ 5min, APPJ 30min, and control PPI samples, indicating that the changes in chemical composition of PPI after APPJ treatment was time dependent. PC2, accounting for 24% of the variability, separated the APPJ, 2D-DBD, ns-pulsed treated samples, and the control, indicating that changes in chemical composition was also related to plasma sources. Structural identification and quantification of the compounds impacted by plasma treatment need further investigation to assess the safety of plasma treated samples.

3.5 Conclusions

This work demonstrated the impact of different plasma sources (APPJ, 2D-DBD, and ns-pulsed) on the color, structure, functionality, and amino acid composition of PPI. Results can be used to optimize CAP treatment for targeted protein functionality enhancement. APPJ, 2D-DBD, and ns-pulsed, resulted in protein structural changes that contributed to enhanced gelation and emulsification properties of PPI, while imparting minimal effect on its amino acid composition. Treatment with 2D-DBD ($Ar + O_2$) for 30 min is a comparatively appreciable functionalization approach due its modest and desirable structural changes, insignificant effect on amino acid composition, and significant enhancement in gelation and emulsification properties. Further optimization of ns-pulsed and APPJ treatments, in terms of intensity, gas used, and treatment time, is warranted. Finally, further characterization of newly formed compounds after plasma treatment is needed to evaluate the safety of using CAP in protein modification.

Chapter 4: Conclusions, Implications, and Recommendations

The impact of different plasma-produced reactive species (N_xO_y/O_3, O_3, H_2O_2, and OH), and different plasma sources (APPJ, 2D-DBD, and ns-pulsed) on pea protein structural characteristics, and the consequent changes in functional properties, were evaluated in this study. Additionally, color changes, amino acids composition, and non-protein components were also monitored before and after plasma treatments.

Treatment with O_3 and OH radical significantly improved the gel strength and emulsification capacity of PPI, due to unfolding the protein and consequent increase surface hydrophobicity, as well as the formation of soluble aggregates. Results confirmed that plasma sources that could effectively generate O_3 and OH radicals (oxidizing species) are preferable for pea protein functionalization. H_2O_2, on the other hand, enhanced PPI color by increasing whiteness. Reactive nitrogen species (RNS), however, require further investigations to fully elucidate their impact on the structure and functionality of PPI. Results from this work can be used to explain previously reported observations related to the impact of different CAP systems on the functional properties of proteins. These results can also be used to optimize CAP treatment, in terms of plasma species production, to induce specific structural changes and a directed enhancement in functionality.

DBD coupled with air, containing a mixture of long-lived RNS and ROS, is commonly used in protein modification studies. However, our results suggested that both the long-lived O_3 and the short-lived OH radical were important for protein functionalization. Therefore, three plasma sources that can generate long-lived and/or short-lived species were investigated. Results showed that APPJ, 2D-DBD, and ns-pulsed treatment were successful in inducing specific structural changes that lead to enhancement

in the functionality of PPI, while maintaining the amino acid composition. Specifically, 30 min 2D-DBD (Ar + O2) treatment induced sufficient functionality enhancement, while imparting moderate modification to the protein structure. APPJ and ns-pulsed treatment with the presence of short-lived species, on the other hand, resulted peptide bonds cleavage and generated low molecular weight peptides/proteins, which could be further investigated to facilitate protein hydrolysis.

Overall, this study successfully demonstrated the impact of different plasma reactive species and plasma sources on the structure and functionality of PPI. Improvement in gelation could be leveraged for applications such as meat analogues. Therefore, the texturization potential of plasma-treated pea protein isolates needs to be further characterized and explored. Additionally, characterizing the physical properties of emulsion systems using confocal laser scanning microscopy could further explain the interactions between plasma-treated protein and oil droplets, and the potential of such treatment on enhancing the physical stability of such systems. Further investigation on the role of other long-lived and short-lived species, and other gas types and treatment time on protein modification is needed to further optimize APPJ and ns-pulsed treatments. Finally, further identification of the newly formed non-protein compounds upon plasma treatment is needed to assess the safety of the plasma-treated PPI.

Reference

Adachi, M., Kanamori, J., Masuda, T., Yagasaki, K., Kitamura, K., Mikami, B., & Utsumi, S. (2003, Jun 10). Crystal structure of soybean 11S globulin: Glycinin A3B4 homohexamer. *Proceedings of the National Academy of Sciences of the United States of America, 100*(12), 7395-7400. https://doi.org/10.1073/pnas.0832158100

Adachi, M., Takenaka, Y., Gidamis, A. B., Mikami, B., & Utsumi, S. (2001, 2001/01/12/). Crystal Structure of Soybean Proglycinin A1aB1b Homotrimer. *Journal of Molecular Biology, 305*(2), 291-305. https://doi.org/https://doi.org/10.1006/jmbi.2000.4310

Altschul, A. M., & Wilcke, H. L. (2013). *New Protein Foods: Seed Storage Proteins* (Vol. 5). Academic press.

Altschul, A. M., Yatsu, L. Y., Ory, R., & Engleman, E. (1966). Seed proteins. *Annual Review of Plant Physiology, 17*(1), 113-136.

Anderson, G. H., & Moore, S. E. (2004). Dietary Proteins in the Regulation of Food Intake and Body Weight in Humans. *The Journal of Nutrition, 134*(4), 974S-979S. https://doi.org/10.1093/jn/134.4.974s

Anderson, J. W., Johnstone, B. M., & Cook-Newell, M. E. (1995, 1995/08/03). Meta-Analysis of the Effects of Soy Protein Intake on Serum Lipids. *New England Journal of Medicine, 333*(5), 276-282. https://doi.org/10.1056/NEJM199508033330502

Arntfield, S. D., & Maskus, H. D. (2011). 9 - Peas and other legume proteins. In G. O. Phillips & P. A. Williams (Eds.), *Handbook of Food Proteins* (pp. 233-266). Woodhead Publishing. https://doi.org/https://doi.org/10.1533/9780857093639.233

Arteaga, V. G., Guardia, M. A., Muranyi, I., Eisner, P., & Schweiggert-Weisz, U. (2020). Effect of enzymatic hydrolysis on molecular weight distribution, techno-functional properties and sensory perception of pea protein isolates. *Innovative Food Science & Emerging Technologies, 65*, 102449.

Ashaolu, T. (2019). Protein hydrolysates and their impact on gut microbiota: an editorial. *CPQ Med, 5*(4), 1-5.

Ashaolu, T. J. (2020, 2020/01/23). Health Applications of Soy Protein Hydrolysates. *International Journal of Peptide Research and Therapeutics*. https://doi.org/10.1007/s10989-020-10018-6

Attri, P., Yusupov, M., Park, J. H., Lingamdinne, L. P., Koduru, J. R., Shiratani, M., Choi, E. H., & Bogaerts, A. (2016). Mechanism and comparison of needle-type

non-thermal direct and indirect atmospheric pressure plasma jets on the degradation of dyes. *Scientific reports, 6*(1), 1-14.

Babault, N., Païzis, C., Deley, G., Guérin-Deremaux, L., Saniez, M.-H., Lefranc-Millot, C., & Allaert, F. A. (2015). Pea proteins oral supplementation promotes muscle thickness gains during resistance training: a double-blind, randomized, Placebo-controlled clinical trial vs. Whey protein. *Journal of the International Society of Sports Nutrition, 12*(1), 1-9.

Badenoch-Jones, J., Spencer, D., Higgins, T. J. V., & Millerd, A. (1981). The role of glycosylation in storage-protein synthesis in developing pea seeds. *Planta, 153*(3), 201-209. https://doi.org/10.1007/bf00383888

Bahrami, N., Bayliss, D., Chope, G., Penson, S., Perehinec, T., & Fisk, I. D. (2016). Cold plasma: A new technology to modify wheat flour functionality. *Food Chemistry, 202*, 247-253.

Bajaj, P. R., Tang, J., & Sablani, S. S. (2015). Pea protein isolates: Novel wall materials for microencapsulating flaxseed oil. Food and bioprocess technology, 8(12), 2418-2428.

Barać, M., Čabrilo, S., Pešić, M., Stanojević, S., Pavlićević, M., Maćej, O., & Ristić, N. (2011). Functional properties of pea (Pisum sativum, L.) protein isolates modified with chymosin. *International Journal of Molecular Sciences, 12*(12), 8372-8387.

Barac, M., Cabrilo, S., Pesic, M., Stanojevic, S., Zilic, S., Macej, O., & Ristic, N. (2010). Profile and Functional Properties of Seed Proteins from Six Pea (Pisum sativum) Genotypes. *International Journal of Molecular Sciences, 11*(12), 4973-4990. https://doi.org/10.3390/ijms11124973

Barac, M., Cabrilo, S., Stanojevic, S., Pesic, M., Pavlicevic, M., Zlatkovic, B., & Jankovic, M. (2012). Functional properties of protein hydrolysates from pea (Pisum sativum, L) seeds. *International journal of food science & technology, 47*(7), 1457-1467.

Barać, M. B., Stanojević, S. P., Jovanović, S. T., & Pešić, M. B. (2004). Soy protein modification: A review. *Acta Periodica Technologica*(35), 3-16.

Baugreet, S., Kerry, J. P., Botineştean, C., Allen, P., & Hamill, R. M. (2016). Development of novel fortified beef patties with added functional protein ingredients for the elderly. Meat Science, 122, 40-47.

Beck, S. M., Knoerzer, K., & Arcot, J. (2017, Dec). Effect of low moisture extrusion on a pea protein isolate's expansion, solubility, molecular weight distribution and secondary structure as determined by Fourier Transform Infrared Spectroscopy

(FTIR). *Journal of Food Engineering, 214*, 166-174. https://doi.org/10.1016/j.jfoodeng.2017.06.037

Beck, S. M., Knoerzer, K., & Arcot, J. (2017). Effect of low moisture extrusion on a pea protein isolate's expansion, solubility, molecular weight distribution and secondary structure as determined by Fourier Transform Infrared Spectroscopy (FTIR). *Journal of Food Engineering, 214*, 166-174.

Bildstein, M., Lohmann, M., Hennigs, C., Krause, A., & Hilz, H. (2008). An enzyme-based extraction process for the purification and enrichment of vegetable proteins to be applied in bakery products. *European Food Research and Technology, 228*(2), 177-186.

Björck, I., & Asp, N.-G. (1983). The effects of extrusion cooking on nutritional value—a literature review. *Journal of Food Engineering, 2*(4), 281-308.

Boekema, B., Vlig, M., Guijt, D., Hijnen, K., Hofmann, S., Smits, P., Sobota, A., Van Veldhuizen, E., Bruggeman, P., & Middelkoop, E. (2015). A new flexible DBD device for treating infected wounds: in vitro and ex vivo evaluation and comparison with a RF argon plasma jet. *Journal of Physics D: Applied Physics, 49*(4), 044001.

Bora, P. S., Brekke, C. J., & Powers, J. R. (1994). Heat Induced Gelation of Pea (Pisum sativum) Mixed Globulins, Vicilin and Legumin. *Journal of food science, 59*(3), 594-596. https://doi.org/10.1111/j.1365-2621.1994.tb05570.x

Bown, D., Ellis, T. H. N., & Gatehouse, J. A. (1988). The sequence of a gene encoding convicilin from pea (Pisum sativum L.) shows that convicilin differs from vicilin by an insertion near the N-terminus. *Biochemical Journal, 251*(3), 717-726. https://doi.org/10.1042/bj2510717

Boye, J. I., & Ma, Z. (2015). Impact of Processing on Bioactive Compounds of Field Peas. In (pp. 63-70). Elsevier. https://doi.org/10.1016/b978-0-12-404699-3.00008-1

Boyle, C., Hansen, L., Hinnenkamp, C., & Ismail, B. P. (2018). Emerging camelina protein: extraction, modification, and structural/functional characterization. *Journal of the American Oil Chemists' Society, 95*(8), 1049-1062.

Braşoveanu, M., Nemţanu, M., Surdu-Bob, C., Karaca, G., & Erper, I. (2015). Effect of glow discharge plasma on germination and fungal load of some cereal seeds. *Romanian Reports in Physics, 67*(2), 617-624.

Bruckner-Guhmann, M., Heiden-Hecht, T., Sozer, N., & Drusch, S. (2018, Dec). Foaming characteristics of oat protein and modification by partial hydrolysis.

European Food Research and Technology, 244(12), 2095-2106. https://doi.org/10.1007/s00217-018-3118-0

Bruggeman, P., & Schram, D. C. (2010). On OH production in water containing atmospheric pressure plasmas. *Plasma sources science and technology, 19*(4).

Bruggeman, P. J., Iza, F., & Brandenburg, R. (2017). Foundations of atmospheric pressure non-equilibrium plasmas. *Plasma sources science and technology, 26*(12), 123002.

Bruggeman, P. J., Kushner, M. J., Locke, B. R., Gardeniers, J. G., Graham, W., Graves, D. B., Hofman-Caris, R., Maric, D., Reid, J. P., & Ceriani, E. (2016). Plasma–liquid interactions: a review and roadmap. *Plasma sources science and technology, 25*(5), 053002.

Bußler, S., Steins, V., Ehlbeck, J., & Schlüter, O. (2015). Impact of thermal treatment versus cold atmospheric plasma processing on the techno-functional protein properties from Pisum sativum 'Salamanca'. *Journal of Food Engineering, 167*, 166-174.

Cao, Y., & Mezzenga, R. (2019). Food protein amyloid fibrils: Origin, structure, formation, characterization, applications and health implications. *Advances in colloid and interface science, 269*, 334-356.

Chang, J.-S., Lawless, P. A., & Yamamoto, T. (1991). Corona discharge processes. *IEEE Transactions on plasma science, 19*(6), 1152-1166.

Chao, D., & Aluko, R. E. (2018). Modification of the structural, emulsifying, and foaming properties of an isolated pea protein by thermal pretreatment. *CyTA-Journal of Food, 16*(1), 357-366.

Chao, D., Jung, S., & Aluko, R. E. (2018). Physicochemical and functional properties of high pressure-treated isolated pea protein. *Innovative Food Science & Emerging Technologies, 45*, 179-185.

Chen, D., Peng, P., Zhou, N., Cheng, Y., Min, M., Ma, Y., Mao, Q., Chen, P., Chen, C., & Ruan, R. (2019). Evaluation of Cronobacter sakazakii inactivation and physicochemical property changes of non-fat dry milk powder by cold atmospheric plasma. *Food Chemistry, 290*, 270-276.

Cheng, C., Liye, Z., & Zhan, R.-J. (2006). Surface modification of polymer fibre by the new atmospheric pressure cold plasma jet. *Surface and Coatings Technology, 200*(24), 6659-6665.

Deak, N. A., & Johnson, L. A. (2007). Effects of extraction temperature and preservation method on functionality of soy protein. *Journal of the American Oil Chemists' Society, 84*(3), 259.

Deak, N. A., Johnson, L. A., Lusas, E. W., & Rhee, K. C. (2008). 19 - Soy Protein Products, Processing, and Utilization. In L. A. Johnson, P. J. White, & R. Galloway (Eds.), *Soybeans* (pp. 661-724). AOCS Press. https://doi.org/https://doi.org/10.1016/B978-1-893997-64-6.50022-6

Delgado, C. L. (2003). Rising consumption of meat and milk in developing countries has created a new food revolution. *The Journal of Nutrition, 133*(11), 3907S-3910S.

Dickinson, C. D., Hussein, E. H. A., & Nielsen, N. C. (1989, Apr). Role of Posttranslational Cleavage in Glycinin Assembly. *Plant Cell, 1*(4), 459-469. <Go to ISI>://WOS:A1989U369300007
http://www.plantcell.org/content/plantcell/1/4/459.full.pdf

Dubois, D. K., & Hoover, W. J. (1981, 1981/03/01). Soya protein products in cereal grain foods. *Journal of the American Oil Chemists' Society, 58*(3), 343-346. https://doi.org/10.1007/BF02582375

Ekezie, F.-G. C., Cheng, J.-H., & Sun, D.-W. (2019). Effects of atmospheric pressure plasma jet on the conformation and physicochemical properties of myofibrillar proteins from king prawn (Litopenaeus vannamei). *Food Chemistry, 276*, 147-156.

Elzebroek, A. T. G. (2008). *Guide to cultivated plants*. CABI.

Endres, J. G. (2001). *Soy protein products: characteristics, nutritional aspects, and utilization*. The American Oil Chemists Society.

Farr, J. P., Smith, W. L., & Steichen, D. S. (2000). Bleaching agents. *Kirk-Othmer Encyclopedia of Chemical Technology*.

Feeney, R. E. (1977). Chemical modification of food proteins. In. ACS Publications.

Feyzi, S., Milani, E., & Golimovahhed, Q. A. (2018, 2018/01/01/). Grass Pea (Lathyrus sativus L.) Protein Isolate: The Effect of Extraction Optimization and Drying Methods on the Structure and Functional Properties. *Food Hydrocolloids, 74*, 187-196. https://doi.org/https://doi.org/10.1016/j.foodhyd.2017.07.031

Friedman, M., & Brandon, D. L. (2001). Nutritional and Health Benefits of Soy Proteins†. *Journal of Agricultural and Food Chemistry, 49*(3), 1069-1086. https://doi.org/10.1021/jf0009246

Fukushima, D. (2011). 8 - Soy proteins. In G. O. Phillips & P. A. Williams (Eds.), *Handbook of Food Proteins* (pp. 210-232). Woodhead Publishing. https://doi.org/https://doi.org/10.1533/9780857093639.210

Gao, Z., Shen, P., Lan, Y., Cui, L., Ohm, J.-B., Chen, B., & Rao, J. (2020). Effect of alkaline extraction pH on structure properties, solubility, and beany flavor of yellow pea protein isolate. *Food Research International, 131*, 109045.

Gardoni, D., Vailati, A., & Canziani, R. (2012). Decay of ozone in water: a review. *Ozone: Science & Engineering, 34*(4), 233-242.

Gatehouse, J. A., Lycett, G. W., Croy, R. R. D., & Boulter, D. (1982). The post-translational proteolysis of the subunits of vicilin from pea (Pisum sativum L.). *Biochemical Journal, 207*(3), 629-632. https://doi.org/10.1042/bj2070629

Gatehouse, J. A., Lycett, G. W., Delauney, A. J., Croy, R. R. D., & Boulter, D. (1983). Sequence specificity of the post-translational proteolytic cleavage of vicilin, a seed storage protein of pea (Pisum sativum L.). *Biochemical Journal, 212*(2), 427-432. https://doi.org/10.1042/bj2120427

Ge, J., Sun, C. X., Corke, H., Gul, K., Gan, R. Y., & Fang, Y. (2020). The health benefits, functional properties, modifications, and applications of pea (Pisum sativum L.) protein: Current status, challenges, and perspectives. *Comprehensive Reviews in Food Science and Food Safety, 19*(4), 1835-1876.

González-Pérez, S., & Arellano, J. B. (2009). Vegetable protein isolates. In *Handbook of hydrocolloids* (pp. 383-419). Elsevier.

Gorbanev, Y., Privat-Maldonado, A., & Bogaerts, A. (2018). Analysis of Short-Lived Reactive Species in Plasma–Air–Water Systems: The Dos and the Do Nots. *Analytical Chemistry, 90*(22), 13151-13158. https://doi.org/10.1021/acs.analchem.8b03336

Govindaraju, K., & Srinivas, H. (2007). Controlled enzymatic hydrolysis of glycinin: Susceptibility of acidic and basic subunits to proteolytic enzymes. *LWT-Food Science and Technology, 40*(6), 1056-1065.

Grand View Research. (2020). Protein Ingredients Market: Increasing Demand For Functional Foods Expected To Boost Market Growth. https://www.grandviewresearch.com/research-insights/protein-ingredients-market-insights-size-share. Accessed Feburary 2021.

Grand View Research. (2021). Pea Protein Market Size, Share & Trends Analysis Report By Product (Hydrolysate, Isolates, Concentrates, Textured), By Application (Meat Substitutes, Dietary Supplement, Bakery Goods), By Region, And Segment Forecasts, 2021 – 2028. https://www.grandviewresearch.com/industry-

analysis/pea-protein-market? utm_source=prnewswire&utm_medium =referral&utm_campaign=cmfe_12-may-20&utm_term=pea-protein-market&utm_content=rd. Accessed Feburary 2021.

Graves, D. B. (2012). The emerging role of reactive oxygen and nitrogen species in redox biology and some implications for plasma applications to medicine and biology. *Journal of Physics D: Applied Physics, 45*(26), 263001.

Gwiazda, S., Rutkowski, A., & Kocoń, J. (1979). Some functional properties of pea and soy bean protein preparations. *Food/Nahrung, 23*(7), 681-686.

Han, J. J., Janz, J. A., & Gerlat, M. (2010). Development of gluten-free cracker snacks using pulse flours and fractions. Food Research International, 43(2), 627-633.

Hansen, L. (2020). The Optimization and Scale-Up of Pea Protein Extractions and Impact on Structural and Functional Properties. MS Thesis, University of Minnesota. 169 pp.

Harris, J., Phan, A. N., & Zhang, K. (2018). Cold plasma catalysis as a novel approach for valorisation of untreated waste glycerol. *Green Chemistry, 20*(11), 2578-2587.

Henchion, M., Hayes, M., Mullen, A. M., Fenelon, M., & Tiwari, B. (2017). Future protein supply and demand: strategies and factors influencing a sustainable equilibrium. *Foods, 6*(7), 53.

Hettiarachchy, N. S., & Ziegler, G. R. (1994). *Protein functionality in food systems*. CRC Press.

Hoffman, J. R., & Falvo, M. J. (2004). Protein - Which is Best? *Journal of sports science & medicine, 3*(3), 118-130. https://pubmed.ncbi.nlm.nih.gov/24482589

Hou, H., & Chang, K. (2004). Structural characteristics of purified β-conglycinin from soybeans stored under four conditions. *Journal of Agricultural and Food Chemistry, 52*(26), 7931-7937.

Humiski, L. M., & Aluko, R. E. (2007). Physicochemical and Bitterness Properties of Enzymatic Pea Protein Hydrolysates. *Journal of food science, 72*(8), S605-S611. https://doi.org/10.1111/j.1750-3841.2007.00475.x

Ismail, B. P., Senaratne-Lenagala, L., Stube, A., & Brackenridge, A. (2020). Protein demand: review of plant and animal proteins used in alternative protein product development and production. *Animal Frontiers, 10*(4), 53-63. https://doi.org/10.1093/af/vfaa040

Jeong, J., Babayan, S., Tu, V., Park, J., Henins, I., Hicks, R., & Selwyn, G. (1998). Etching materials with an atmospheric-pressure plasma jet. *Plasma sources science and technology*, *7*(3), 282.

Ji, H., Dong, S., Han, F., Li, Y., Chen, G., Li, L., & Chen, Y. (2018). Effects of dielectric barrier discharge (DBD) cold plasma treatment on physicochemical and functional properties of peanut protein. *Food and bioprocess technology*, *11*(2), 344-354.

Ji, H., Han, F., Peng, S., Yu, J., Li, L., Liu, Y., Chen, Y., Li, S., & Chen, Y. (2019). Behavioral solubilization of peanut protein isolate by atmospheric pressure cold plasma (ACP) treatment. *Food and bioprocess technology*, *12*(12), 2018-2027.

Jiang, Y.-H., Cheng, J.-H., & Sun, D.-W. (2020). Effects of plasma chemistry on the interfacial performance of protein and polysaccharide in emulsion. Trends in Food Science & Technology, 98, 129-139.

Johnson, E. A., & Brekke, C. (1983). Functional properties of acylated pea protein isolates. *Journal of food science*, *48*(3), 722-725.

Kaewruang, P., Benjakul, S., Prodpran, T., Encarnacion, A. B., & Nalinanon, S. (2014). Impact of divalent salts and bovine gelatin on gel properties of phosphorylated gelatin from the skin of unicorn leatherjacket. *LWT-Food Science and Technology*, *55*(2), 477-482.

Kester, J. J., & Richardson, T. (1984, 1984/11/01/). Modification of Whey Proteins to Improve Functionality. *Journal of Dairy Science*, *67*(11), 2757-2774. https://doi.org/https://doi.org/10.3168/jds.S0022-0302(84)81633-1

Kim, Park, P. S., & Rhee, K. C. (1990). Functional properties of proteolytic enzyme modified soy protein isolate. *Journal of Agricultural and Food Chemistry*, *38*(3), 651-656.

Kimura, Y., Takashima, K., Sasaki, S., & Kaneko, T. (2018). Investigation on dinitrogen pentoxide roles on air plasma effluent exposure to liquid water solution. *Journal of Physics D: Applied Physics*, *52*(6), 064003.

Kinsella, J. E. (1979). Functional properties of soy proteins. *Journal of the American Oil Chemists' Society*, *56*(3Part1), 242-258. https://doi.org/10.1007/bf02671468

Kinsella, J. E., Damodaran, S., & German, B. (1985). Physicochemical and functional properties of oilseed proteins with emphasis on soy proteins. *New protein foods (USA)*.

Klost, M., & Drusch, S. (2019). Functionalisation of pea protein by tryptic hydrolysis–Characterisation of interfacial and functional properties. *Food Hydrocolloids, 86,* 134-140.

Kondeti, V. S. K., Zheng, Y., Luan, P., Oehrlein, G. S., & Bruggeman, P. J. (2020). O·, H·, and· OH radical etching probability of polystyrene obtained for a radio frequency driven atmospheric pressure plasma jet. *Journal of Vacuum Science & Technology A: Vacuum, Surfaces, and Films, 38*(3), 033012.

Koopman, R., Crombach, N., Gijsen, A. P., Walrand, S., Fauquant, J., Kies, A. K., Lemosquet, S., Saris, W. H., Boirie, Y., & van Loon, L. J. (2009). Ingestion of a protein hydrolysate is accompanied by an accelerated in vivo digestion and absorption rate when compared with its intact protein. *The American journal of clinical nutrition, 90*(1), 106-115.

Kutzli, I., Griener, D., Gibis, M., Schmid, C., Dawid, C., Baier, S. K., Hofmann, T., & Weiss, J. (2020, 2020/04/01/). Influence of Maillard reaction conditions on the formation and solubility of pea protein isolate-maltodextrin conjugates in electrospun fibers. *Food Hydrocolloids, 101*, 105535. https://doi.org/https://doi.org/10.1016/j.foodhyd.2019.105535

Labeling, F. A., & Act, C. P. (2004). Public Law 108–282. *Title II, 75*.

Ladjal-Ettoumi, Y., Boudries, H., Chibane, M., & Romero, A. (2016). Pea, chickpea and lentil protein isolates: Physicochemical characterization and emulsifying properties. *Food Biophysics, 11*(1), 43-51.

Lee, J. (2011). Soy protein hydrolysate; solubility, thermal stability, bioactivity, and sensory acceptability in a tea beverage.

Liao, X., Liu, D., Xiang, Q., Ahn, J., Chen, S., Ye, X., & Ding, T. (2017). Inactivation mechanisms of non-thermal plasma on microbes: A review. Food Control, 75, 83-91.

Lin, D., Zhang, Q., Xiao, L., Huang, Y., Yang, Z., Wu, Z., Tu, Z., Qin, W., Chen, H., & Wu, D. (2020). Effects of ultrasound on functional properties, structure and glycation properties of proteins: a review. *Critical Reviews in Food Science and Nutrition*, 1-11.

Lindsay, A., Byrns, B., King, W., Andhvarapou, A., Fields, J., Knappe, D., Fonteno, W., & Shannon, S. (2014). Fertilization of radishes, tomatoes, and marigolds using a large-volume atmospheric glow discharge. *Plasma Chemistry and Plasma Processing, 34*(6), 1271-1290.

Liu, J., Ru, Q., & Ding, Y. (2012). Glycation a promising method for food protein modification: Physicochemical properties and structure, a review. *Food Research International, 49*(1), 170-183. https://doi.org/10.1016/j.foodres.2012.07.034

Liu, K. (2008). 14 - Food Use of Whole Soybeans. In L. A. Johnson, P. J. White, & R. Galloway (Eds.), *Soybeans* (pp. 441-481). AOCS Press. https://doi.org/https://doi.org/10.1016/B978-1-893997-64-6.50017-2

Liu, Y., Wang, D., Wang, J., Yang, Y., Zhang, L., Li, J., & Wang, S. (2020). Functional properties and structural characteristics of phosphorylated pea protein isolate. *International journal of food science & technology, 55*(5), 2002-2010.

Lu, P., Cullen, P., & Ostrikov, K. (2016). Atmospheric Pressure Nonthermal Plasma Sources. In *Cold plasma in food and agriculture* (pp. 83-116). Elsevier.

Lu, Z. X., He, J. F., Zhang, Y. C., & Bing, D. J. (2019). Composition, physicochemical properties of pea protein and its application in functional foods. *Critical Reviews in Food Science and Nutrition*, 1-13. https://doi.org/10.1080/10408398.2019.1651248

Lukes, P., Dolezalova, E., Sisrova, I., & Clupek, M. (2014). Aqueous-phase chemistry and bactericidal effects from an air discharge plasma in contact with water: evidence for the formation of peroxynitrite through a pseudo-second-order post-discharge reaction of H2O2 and HNO2. *Plasma sources science and technology, 23*(1), 015019.

Ma, C. Y. (2015). Soybean | Soy Concentrates and Isolates. In *Reference Module in Food Science*. Elsevier. https://doi.org/https://doi.org/10.1016/B978-0-08-100596-5.00170-0

Ma, X., Sun, P., He, P., Han, P., Wang, J., Qiao, S., & Li, D. (2010). Development of monoclonal antibodies and a competitive ELISA detection method for glycinin, an allergen in soybean. *Food Chemistry, 121*(2), 546-551.

Ma, Y., Zhou, W., Chen, P., Urriola, P. E., Shurson, G. C., Ruan, R., & Chen, C. (2019). Metabolomic evaluation of scenedesmus sp. as a feed ingredient revealed dose-dependent effects on redox balance, intermediary and microbial metabolism in a mouse model. *Nutrients, 11*(9), 1971.

Ma, Z., Boye, J. I., Swallow, K., Malcolmson, L., & Simpson, B. K. (2016). Techno-functional characterization of salad dressing emulsions supplemented with pea, lentil and chickpea flours. Journal of the Science of Food and Agriculture, 96(3), 837-847.

Mahdavian Mehr, H., & Koocheki, A. (2020, 2020/09/01/). Effect of atmospheric cold plasma on structure, interfacial and emulsifying properties of Grass pea (Lathyrus

sativus L.) protein isolate. *Food Hydrocolloids, 106*, 105899. https://doi.org/https://doi.org/10.1016/j.foodhyd.2020.105899

Maninder, K., Sandhu, K. S., & Singh, N. (2007). Comparative study of the functional, thermal and pasting properties of flours from different field pea (Pisum sativum L.) and pigeon pea (Cajanus cajan L.) cultivars. *Food Chemistry, 104*(1), 259-267.

Mao, Q. (2019). Characterizing Intense Pulsed Light-Elicited Effects on Escherichia coli and Non-Fat Dry Milk Through Metabolomic and Chemometric Analysis.

Mao, Q., Liu, J., Wiertzema, J. R., Chen, D., Chen, P., Baumler, D. J., Ruan, R., & Chen, C. (2021). Identification of Quinone Degradation as a Triggering Event for Intense Pulsed Light-Elicited Metabolic Changes in Escherichia coli by Metabolomic Fingerprinting. *Metabolites, 11*(2), 102.

Marcus, R. K., & Broekaert, J. A. (2003). *Glow discharge plasmas in analytical spectroscopy*. Wiley Online Library.

Market Research Future. (2021). Global Plant Protein Ingredients Market Research Report. 778 Retrieved from https://www.marketresearchfuture.com/reports/plant-protein-ingredients 779 market-5114. Accessed Feburary 2021

Marketsandmarkets. (2021). Plant-based Protein Market by Source, Type, Form, Application, and Region. https://www.marketsandmarkets.com/Market-Reports/plant-based-protein-market-14715651.html. Accessed March 2021.

Maruyama, N., Adachi, M., Takahashi, K., Yagasaki, K., Kohno, M., Takenaka, Y., Okuda, E., Nakagawa, S., Mikami, B., & Utsumi, S. (2001, 2001/06/01). Crystal structures of recombinant and native soybean β-conglycinin β homotrimers. *European Journal of Biochemistry, 268*(12), 3595-3604. https://doi.org/10.1046/j.1432-1327.2001.02268.x

Maruyama, N., Maruyama, Y., Tsuruki, T., Okuda, E., Yoshikawa, M., & Utsumi, S. (2003, 2003/05/30/). Creation of soybean β-conglycinin β with strong phagocytosis-stimulating activity. *Biochimica et Biophysica Acta (BBA) - Proteins and Proteomics, 1648*(1), 99-104. https://doi.org/https://doi.org/10.1016/S1570-9639(03)00113-4

Maruyama, Y., Maruyama, N., Mikami, B., & Utsumi, S. (2004). Structure of the core region of the soybean [beta]-conglycinin [alpha]' subunit. *Acta Crystallographica Section D, 60*(2), 289-297. https://doi.org/doi:10.1107/S0907444903027367

Meinlschmidt, P., Ueberham, E., Lehmann, J., Reineke, K., Schlüter, O., Schweiggert-Weisz, U., & Eisner, P. (2016). The effects of pulsed ultraviolet light, cold atmospheric pressure plasma, and gamma-irradiation on the immunoreactivity of

soy protein isolate. *Innovative Food Science & Emerging Technologies, 38*, 374-383.

Middelbos, I. S., & Fahey, G. C. (2008). 9 - Soybean Carbohydrates. In L. A. Johnson, P. J. White, & R. Galloway (Eds.), *Soybeans* (pp. 269-296). AOCS Press. https://doi.org/https://doi.org/10.1016/B978-1-893997-64-6.50012-3

Mirmoghtadaie, L., Shojaee Aliabadi, S., & Hosseini, S. M. (2016, 2016/05/15/). Recent approaches in physical modification of protein functionality. *Food Chemistry, 199*, 619-627. https://doi.org/https://doi.org/10.1016/j.foodchem.2015.12.067

Misra, N., Pankaj, S., Segat, A., & Ishikawa, K. (2016). Cold plasma interactions with enzymes in foods and model systems. *Trends in Food Science & Technology, 55*, 39-47.

Misra, N., Schlüter, O., & Cullen, P. (2016). Plasma in food and agriculture. In *Cold Plasma in Food and Agriculture* (pp. 1-16). Elsevier.

Mo, X., Zhong, Z., Wang, D., & Sun, X. (2006). Soybean Glycinin Subunits: Characterization of Physicochemical and Adhesion Properties. *Journal of Agricultural and Food Chemistry, 54*(20), 7589-7593. https://doi.org/10.1021/jf060780g

Moldgy, A., Nayak, G., Aboubakr, H. A., Goyal, S. M., & Bruggeman, P. J. (2020). Inactivation of virus and bacteria using cold atmospheric pressure air plasmas and the role of reactive nitrogen species. *Journal of Physics D: Applied Physics, 53*(43), 434004.

Morr, C. (1990). Current status of soy protein functionality in food systems. *Journal of the American Oil Chemists' Society, 67*(5), 265.

Muhammad, A. I., Xiang, Q., Liao, X., Liu, D., & Ding, T. (2018). Understanding the impact of nonthermal plasma on food constituents and microstructure—a review. *Food and bioprocess technology, 11*(3), 463-486.

Murphy, C., Oikawa, S., & Phillips, S. (2016). Dietary protein to maintain muscle mass in aging: a case for per-meal protein recommendations. *J Frailty Aging, 5*(1), 49-58.

Murphy, P. A. (2008). 8 - Soybean Proteins. In L. A. Johnson, P. J. White, & R. Galloway (Eds.), *Soybeans* (pp. 229-267). AOCS Press. https://doi.org/https://doi.org/10.1016/B978-1-893997-64-6.50011-1

Nayak, G., Aboubakr, H. A., Goyal, S. M., & Bruggeman, P. J. (2018). Reactive species responsible for the inactivation of feline calicivirus by a two-dimensional array of

integrated coaxial microhollow dielectric barrier discharges in air. *Plasma Processes and Polymers, 15*(1), 1700119.

Nayak, G., Du, Y., Brandenburg, R., & Bruggeman, P. J. (2017). Effect of air flow on the micro-discharge dynamics in an array of integrated coaxial microhollow dielectric barrier discharges. *Plasma sources science and technology, 26*(3), 035001.

Nayak, G., Sousa, J. S., & Bruggeman, P. J. (2017). Singlet delta oxygen production in a 2D micro-discharge array in air: effect of gas residence time and discharge power. *Journal of Physics D: Applied Physics, 50*(10), 105205.

Nosworthy, M. G., & House, J. D. (2017). Factors influencing the quality of dietary proteins: Implications for pulses. *Cereal Chemistry, 94*(1), 49-57.

Nyaisaba, B. M., Miao, W., Hatab, S., Siloam, A., Chen, M., & Deng, S. (2019). Effects of cold atmospheric plasma on squid proteases and gel properties of protein concentrate from squid (Argentinus ilex) mantle. *Food Chemistry, 291,* 68-76.

O'Kane, F. E., Happe, R. P., Vereijken, J. M., Gruppen, H., & van Boekel, M. A. (2004). Heat-induced gelation of pea legumin: Comparison with soybean glycinin. *Journal of Agricultural and Food Chemistry, 52*(16), 5071-5078.

O'Kane, F. E., Vereijken, J. M., Gruppen, H., & Van Boekel, M. A. J. S. (2005). Gelation Behavior of Protein Isolates Extracted from 5 Cultivars ofPisum sativumL. *Journal of food science, 70*(2), C132-C137. https://doi.org/10.1111/j.1365-2621.2005.tb07073.x

Ogawa, T., Bando, N., Tsuji, H., Okajima, H., Nishikawa, K., & Sasaoka, K. (1991). Investigation of the IgE-Binding Proteins in Soybeans by Immunoblotting with the Sera of the Soybean-Sensitive Patients with Atopic Dermatitis. *37*(6), 555-565. https://doi.org/10.3177/jnsv.37.555

Ohishi, A., Watanabe, K., Urushibata, M., Utsuno, K., Ikuta, K., Sugimoto, K., & Harada, H. (1994). Detection of soybean antigenicity and reduction by twin-screw extrusion. *Journal of the American Oil Chemists' Society, 71*(12), 1391-1396.

Okazaki, S., Kogoma, M., Uehara, M., & Kimura, Y. (1993). Appearance of stable glow discharge in air, argon, oxygen and nitrogen at atmospheric pressure using a 50 Hz source. *Journal of Physics D: Applied Physics*, *26*(5), 889.

Osborne, T. B. (1924). *The vegetable proteins*. Longmans, Green and Company.

Osen, R., Toelstede, S., Wild, F., Eisner, P., & Schweiggert-Weisz, U. (2014). High moisture extrusion cooking of pea protein isolates: Raw material characteristics, extruder responses, and texture properties. *Journal of Food Engineering, 127*, 67-74.

Pankaj, S., Misra, N., & Cullen, P. (2013). Kinetics of tomato peroxidase inactivation by atmospheric pressure cold plasma based on dielectric barrier discharge. *Innovative Food Science & Emerging Technologies, 19*, 153-157.

Pietrysiak, E., Smith, D. M., Smith, B. M., & Ganjyal, G. M. (2018). Enhanced functionality of pea-rice protein isolate blends through direct steam injection processing. *Food Chemistry, 243*, 338-344.

Pignatello, J. J., Oliveros, E., & MacKay, A. (2006). Advanced oxidation processes for organic contaminant destruction based on the Fenton reaction and related chemistry. *Critical reviews in environmental science and technology, 36*(1), 1-84.

Popkin, B. M., Adair, L. S., & Ng, S. W. (2012). Global nutrition transition and the pandemic of obesity in developing countries. *Nutrition reviews, 70*(1), 3-21.

Prak, K., Nakatani, K., Katsube-Tanaka, T., Adachi, M., Maruyama, N., & Utsumi, S. (2005, May 4). Structure-function relationships of soybean proglycinins at subunit levels. *Journal of Agricultural and Food Chemistry, 53*(9), 3650-3657. https://doi.org/10.1021/jf047811x

Prakash, R., Hossain, A. M., Pal, U., Kumar, N., Khairnar, K., & Mohan, M. K. (2017). Dielectric Barrier Discharge based Mercury-free plasma UV-lamp for efficient water disinfection. *Scientific reports, 7*(1), 1-8.

Reichert, R. D. (1982). Air Classification of Peas (Pisum sativum) Varying Widely in Protein Content. *Journal of food science, 47*(4), 1263-1267. https://doi.org/10.1111/j.1365-2621.1982.tb07662.x

Renkema, J., Knabben, J., & Van Vliet, T. (2001). Gel formation by β-conglycinin and glycinin and their mixtures. *Food Hydrocolloids, 15*(4-6), 407-414.

Riaz, M. N. (2011). 15 - Texturized vegetable proteins. In G. O. Phillips & P. A. Williams (Eds.), *Handbook of Food Proteins* (pp. 395-418). Woodhead Publishing. https://doi.org/https://doi.org/10.1533/9780857093639.395

Rickert, D., Johnson, L., & Murphy, P. (2004). Functional Properties of Improved Glycinin and β-nglycinin Fractions. *Journal of food science, 69*(4), FCT303-FCT311.

Rutherfurd, S. M., Fanning, A. C., Miller, B. J., & Moughan, P. J. (2015). Protein Digestibility-Corrected Amino Acid Scores and Digestible Indispensable Amino Acid Scores Differentially Describe Protein Quality in Growing Male Rats. *The Journal of Nutrition, 145*(2), 372-379. https://doi.org/10.3945/jn.114.195438

Samanta, K., Jassal, M., & Agrawal, A. K. (2006). Atmospheric pressure glow discharge plasma and its applications in textile.

Samukawa, S., Hori, M., Rauf, S., Tachibana, K., Bruggeman, P., Kroesen, G., Whitehead, J. C., Murphy, A. B., Gutsol, A. F., Starikovskaia, S., Kortshagen, U., Boeuf, J.-P., Sommerer, T. J., Kushner, M. J., Czarnetzki, U., & Mason, N. (2012). The 2012 Plasma Roadmap. *Journal of Physics D: Applied Physics, 45*(25), 253001. https://doi.org/10.1088/0022-3727/45/25/253001

Sarangapani, C., Misra, N., Milosavljevic, V., Bourke, P., O'Regan, F., & Cullen, P. (2016). Pesticide degradation in water using atmospheric air cold plasma. *Journal of Water Process Engineering, 9*, 225-232.

Schwenke, K. D. (1997). Enzyme and chemical modification. *Food proteins and their applications, Damodaran S., Paraf A.(Hrsg.), Marcel Dekker, New York*, 393-423.

Segat, A., Misra, N., Cullen, P., & Innocente, N. (2015). Atmospheric pressure cold plasma (ACP) treatment of whey protein isolate model solution. *Innovative Food Science & Emerging Technologies, 29*, 247-254.

Segat, A., Misra, N., Fabbro, A., Buchini, F., Lippe, G., Cullen, P. J., & Innocente, N. (2014). Effects of ozone processing on chemical, structural and functional properties of whey protein isolate. *Food Research International, 66*, 365-372.

Shand, P. J., Ya, H., Pietrasik, Z., & Wanasundara, P. K. J. P. D. (2007, 2007/01/01/). Physicochemical and textural properties of heat-induced pea protein isolate gels. *Food Chemistry, 102*(4), 1119-1130. https://doi.org/https://doi.org/10.1016/j.foodchem.2006.06.060

Sharifian, A., Soltanizadeh, N., & Abbaszadeh, R. (2019). Effects of dielectric barrier discharge plasma on the physicochemical and functional properties of myofibrillar proteins. *Innovative Food Science & Emerging Technologies, 54*, 1-8.

Singh, A., Meena, M., Kumar, D., Dubey, A. K., & Hassan, M. I. (2015). Structural and functional analysis of various globulin proteins from soy seed. *Critical Reviews in Food Science and Nutrition, 55*(11), 1491-1502.

Singh, P., Kumar, R., Sabapathy, S., & Bawa, A. (2008). Functional and edible uses of soy protein products. *Comprehensive Reviews in Food Science and Food Safety, 7*(1), 14-28.

Sirtori, C. R., Triolo, M., Bosisio, R., Bondioli, A., Calabresi, L., De Vergori, V., Gomaraschi, M., Mombelli, G., Pazzucconi, F., & Zacherl, C. (2012). Hypocholesterolaemic effects of lupin protein and pea protein/fibre combinations

in moderately hypercholesterolaemic individuals. *British Journal of Nutrition, 107*(8), 1176-1183.

Smith, D. M. (2017). Protein separation and characterization procedures. In *Food analysis* (pp. 431-453). Springer.

Söderberg, J. (2013). Functional properties of legume proteins compared to egg proteins and their potential as egg replacers in vegan food.

Son, D.-Y., Lee, B.-R., Shon, D.-W., Lee, K.-S., Ahn, K.-M., Nam, S.-Y., & Lee, S.-I. (2000). Allergenicity change of soybean proteins by thermal treatment. *Korean Journal of Food Science and Technology, 32*(4), 959-963.

Stone, A. K., Karalash, A., Tyler, R. T., Warkentin, T. D., & Nickerson, M. T. (2015, 2015/10/01/). Functional attributes of pea protein isolates prepared using different extraction methods and cultivars. *Food Research International, 76*, 31-38. https://doi.org/https://doi.org/10.1016/j.foodres.2014.11.017

Subedi, D. P., Joshi, U. M., & San Wong, C. (2017). Dielectric barrier discharge (DBD) plasmas and their applications. In *Plasma Science and Technology for Emerging Economies* (pp. 693-737). Springer.

Surowsky, B., Bußler, S., & Schlüter, O. (2016). Cold plasma interactions with food constituents in liquid and solid food matrices. In *Cold plasma in food and agriculture* (pp. 179-203). Elsevier.

Świątecka, D., Markiewicz, L. H., & Wroblewska, B. (2012). Pea protein hydrolysate as a factor modulating the adhesion of bacteria to enterocytes, epithelial proliferation and cytokine secretion–an in vitro study. *Centr Eur J Immunol, 37*(3), 227-231.

Takai, E., Kitamura, T., Kuwabara, J., Ikawa, S., Yoshizawa, S., Shiraki, K., Kawasaki, H., Arakawa, R., & Kitano, K. (2014). Chemical modification of amino acids by atmospheric-pressure cold plasma in aqueous solution. *Journal of Physics D: Applied Physics, 47*(28), 285403.

Tamm, F., Herbst, S., Brodkorb, A., & Drusch, S. (2016, 2016/07/01/). Functional properties of pea protein hydrolysates in emulsions and spray-dried microcapsules. *Food Hydrocolloids, 58*, 204-214. https://doi.org/https://doi.org/10.1016/j.foodhyd.2016.02.032

Tandang-Silvas, M. R. G., Fukuda, T., Fukuda, C., Prak, K., Cabanos, C., Kimura, A., Itoh, T., Mikami, B., Utsumi, S., & Maruyama, N. (2010, Jul). Conservation and divergence on plant seed 11S globulins based on crystal structures. *Biochimica Et Biophysica Acta-Proteins and Proteomics, 1804*(7), 1432-1442. https://doi.org/10.1016/j.bbapap.2010.02.016

Tanger, C., Engel, J., & Kulozik, U. (2020, 2020/04/19/). Influence of extraction conditions on the conformational alteration of pea protein extracted from pea flour. *Food Hydrocolloids*, 105949. https://doi.org/https://doi.org/10.1016/j.foodhyd.2020.105949

Thanh, V. H., & Shibasaki, K. (1978, 1978/05/01). Major proteins of soybean seeds. Subunit structure of .beta.-conglycinin. *Journal of Agricultural and Food Chemistry*, *26*(3), 692-695. https://doi.org/10.1021/jf60217a026

Thrane, M., Paulsen, P., Orcutt, M., & Krieger, T. (2017). Soy protein: Impacts, production, and applications. In *Sustainable protein sources* (pp. 23-45). Elsevier.

Tolouie, H., Mohammadifar, M. A., Ghomi, H., & Hashemi, M. (2018). Cold atmospheric plasma manipulation of proteins in food systems. *Critical Reviews in Food Science and Nutrition*, *58*(15), 2583-2597. https://www.tandfonline.com/doi/pdf/10.1080/10408398.2017.1335689?needAccess=true

Tong, L.-T., Xiao, T., Wang, L., Lu, C., Liu, L., Zhou, X., Wang, A., Qin, W., & Wang, F. Pea Protein Reduce Serum Cholesterol Levels in Hypercholesterolemia Hamsters by Modulating Compositions of Gut Microbiota and Metabolites.

Tosh, S. M., & Yada, S. (2010, 2010/03/01/). Dietary fibres in pulse seeds and fractions: Characterization, functional attributes, and applications. *Food Research International*, *43*(2), 450-460. https://doi.org/https://doi.org/10.1016/j.foodres.2009.09.005

Tsumura, K., Saito, T., Tsuge, K., Ashida, H., Kugimiya, W., & Inouye, K. (2005). Functional properties of soy protein hydrolysates obtained by selective proteolysis. *LWT-Food Science and Technology*, *38*(3), 255-261.

Tulbek, M. C., Lam, R. S. H., Wang, Y., Asavajaru, P., & Lam, A. (2017). Chapter 9 - Pea: A Sustainable Vegetable Protein Crop. In S. R. Nadathur, J. P. D. Wanasundara, & L. Scanlin (Eds.), *Sustainable Protein Sources* (pp. 145-164). Academic Press. https://doi.org/https://doi.org/10.1016/B978-0-12-802778-3.00009-3

Tyler, R., RT, T., CG, Y., & FW, S. (1981). Air Classification of legumes. I: Seperation efficiency, yield, and composition of the strach and protein fractions.

Tzitzikas, E. N., Vincken, J.-P., De Groot, J., Gruppen, H., & Visser, R. G. F. (2006). Genetic Variation in Pea Seed Globulin Composition. *Journal of Agricultural and Food Chemistry*, *54*(2), 425-433. https://doi.org/10.1021/jf0519008

Utsumi, S., Matsumura, Y., & Mori, T. (1997). Structure-function relationships of soy proteins. *Food Science and Technology-New York-Marcel Dekker-*, 257-292.

Van Vliet, S., Burd, N. A., & Van Loon, L. J. (2015). The Skeletal Muscle Anabolic Response to Plant- versus Animal-Based Protein Consumption. *The Journal of Nutrition, 145*(9), 1981-1991. https://doi.org/10.3945/jn.114.204305

Vu Huu, T., & Kazuo, S. (1977, 1977/02/22/). Beta-conglycinin from soybean proteins. Isolation and immunological and physicochemical properties of the monomeric forms. *Biochimica et Biophysica Acta (BBA) - Protein Structure, 490*(2), 370-384. https://doi.org/https://doi.org/10.1016/0005-2795(77)90012-5

Walter, J., Greenberg, Y., Sriramarao, P., & Ismail, B. P. (2016, 2016/12/15/). Limited hydrolysis combined with controlled Maillard-induced glycation does not reduce immunoreactivity of soy protein for all sera tested. *Food Chemistry, 213*, 742-752. https://doi.org/https://doi.org/10.1016/j.foodchem.2016.07.012

Wang, F., Zhang, Y., Xu, L., & Ma, H. (2020, 2020/06/01/). An efficient ultrasound-assisted extraction method of pea protein and its effect on protein functional properties and biological activities. *LWT, 127*, 109348. https://doi.org/https://doi.org/10.1016/j.lwt.2020.109348

Wang, L., Yao, D., Urriola, P. E., Hanson, A. R., Saqui-Salces, M., Kerr, B. J., Shurson, G. C., & Chen, C. (2018). Identification of activation of tryptophan–NAD+ pathway as a prominent metabolic response to thermally oxidized oil through metabolomics-guided biochemical analysis. *The Journal of nutritional biochemistry, 57*, 255-267.

Wang, Q., & Ismail, B. (2012). Effect of Maillard-induced glycosylation on the nutritional quality, solubility, thermal stability and molecular configuration of whey proteinv. *International Dairy Journal, 25*(2), 112-122.

Were, L., Hettiarachchy, N., & Kalapathy, U. (1997). Modified soy proteins with improved foaming and water hydration properties. *Journal of food science, 62*(4), 821-824.

WHO. (1991). *Protein Quality Evaluation: Report of the Joint FAO/WHO Expert Consultation, Bethesda, Md., USA 4-8 December 1989* (Vol. 51). Food & Agriculture Org.

Winter, J., Brandenburg, R., & Weltmann, K. (2015). Atmospheric pressure plasma jets: an overview of devices and new directions. *Plasma sources science and technology, 24*(6), 064001.

Wong, W. W., Smith, E., Stuff, J. E., Hachey, D. L., Heird, W. C., & Pownell, H. J. (1998). Cholesterol-lowering effect of soy protein in normocholesterolemic and hypercholesterolemic men. *The American journal of clinical nutrition, 68*(6), 1385S-1389S.

Yada, R. Y. (2017). *Proteins in food processing*. Woodhead Publishing.

Yamauchi, F., Sato, M., Sato, W., Kamata, Y., & Shibasaki, K. (1981, 1981/12/01). Isolation and Identification of a New Type of β-Conglycinin in Soybean Globulins. *Agricultural and Biological Chemistry, 45*(12), 2863-2868. https://doi.org/10.1080/00021369.1981.10864970

Yang, Y., Churchward-Venne, T. A., Burd, N. A., Breen, L., Tarnopolsky, M. A., & Phillips, S. M. (2012). Myofibrillar protein synthesis following ingestion of soy protein isolate at rest and after resistance exercise in elderly men. *Nutrition & metabolism, 9*(1), 1-9.

Zakaria, F., & RF, M. (1978). Improvement of the emulsification properties of soy protein by limited pepsin hydrolysis. *Sci. Technol. Alment,* PP. 42-44.

Appendix A: Calibration curve for Determining the Molecular weight of Protein on SE-HPLC

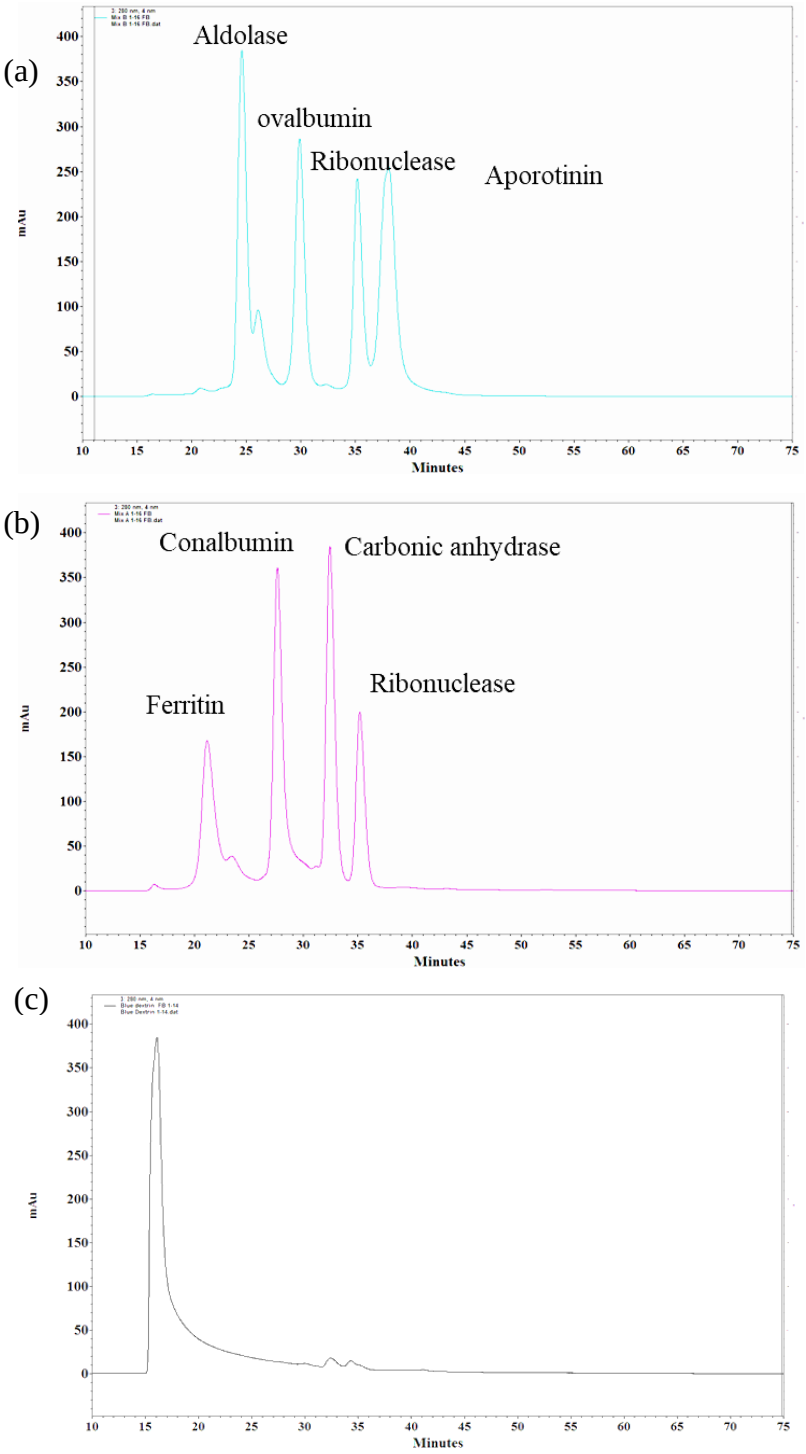

Figure 18. Chromatographic separation for the (a) low molecular weight and (b)high molecular weight standard proteins (c) blue dextrin on Superdex 200 Increase 10/300 GL

column. Standard proteins, ferritin (440 kDa), aldolase (158 kDa), conalbumin (75 kDa), ovalbumin (43 kDa), carbonic anhydrase (29 kDa), ribonuclease (13.7 kDa), and aprotinin (6.5 kDa), were used to calibrate the column.

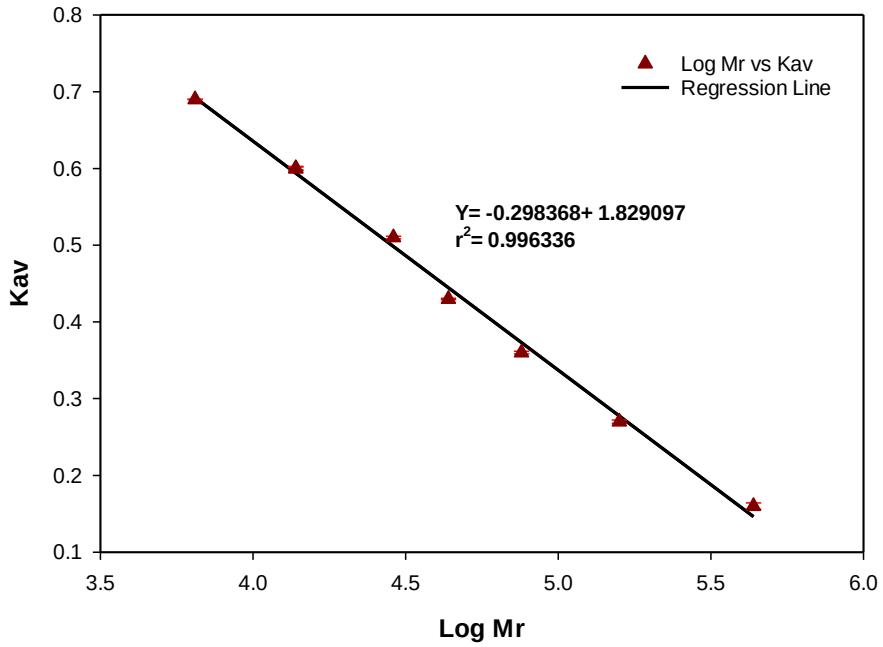

Figure 19. Calibration curve for the standard proteins on Superdex 200 Increase 10/300 GL column.

Sample Calculation for Protein Size:

$$Kav = \frac{Ve-Vo}{Vc-Vo} \quad (1)$$

$$Vo = 8.03mL \quad (2)$$

$$Vc = 24mL \quad (3)$$

$$\text{Kav} = -0.298368\text{LogMr} + 1.829097 \quad (4)$$

Thus,

$$\text{Molecular weight (Da)} = 10^{\frac{\frac{Ve-8.03}{24-8.03}-1.829097)}{0.298368}}$$

The elution volume of legumin is 9.946 mL, so the molecular weight of legumin is 534.9 kDa.

Appendix B: Sample Spectrum for Determining Protein Secondary Structure

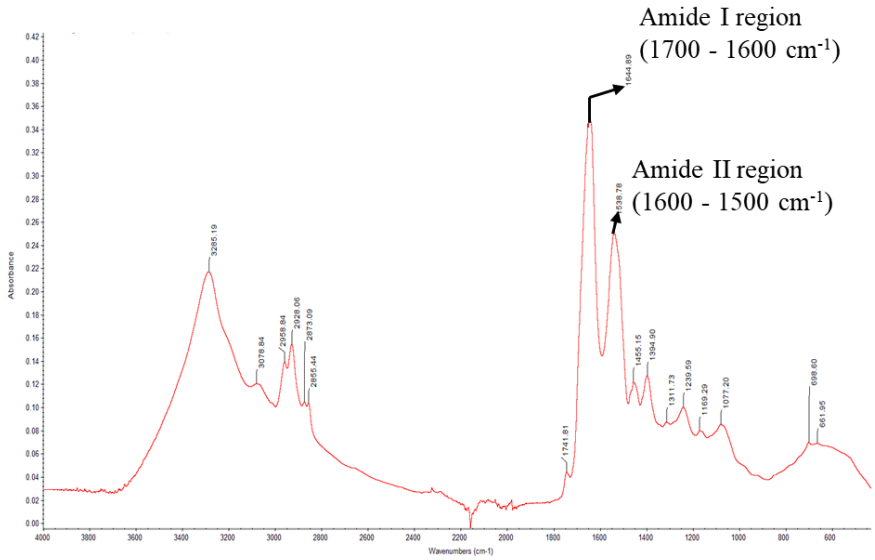

Figure 20. Original FTIR-ATR Spectrum of PPI

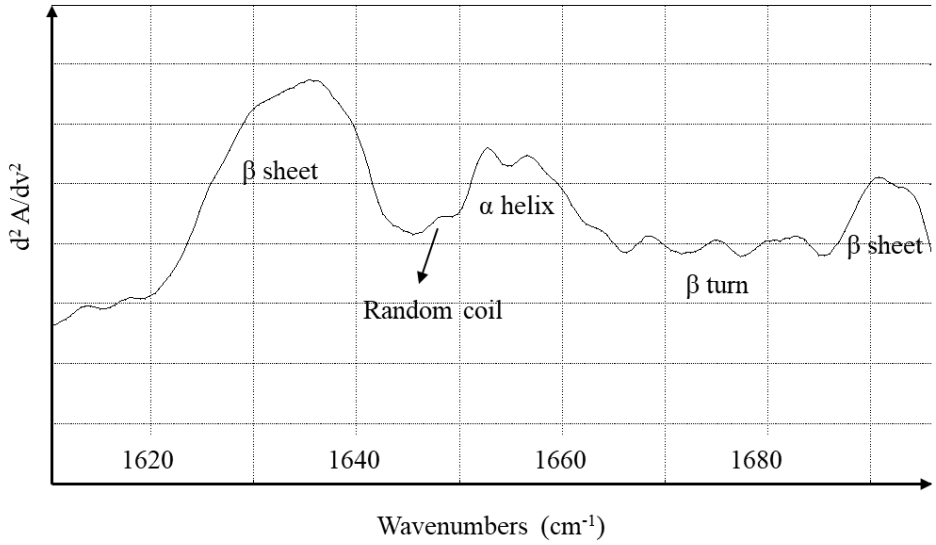

Figure 21. Second-derivative Spectrum of PPI

The original FTIR-ATR spectrum of PPI was shown in **Figure 20**. Second derivative of Amide I band (1600cm^{-1} -1700 cm^{-1}) **(Figure 21)** were obtained by PeakFit v. 4.12 to identify alpha-helix, beta-sheet, beta-turn, and random coil, according to the range of 1648-1660, 1612-1641 and 1684-1694, 1662-1684, and 1640-1650, respectively.

Appendix C: Sample Calculation for Determining Surface Hydrophobicity Index

Net Relative Fluorescence Intensity (RFI) at a single protein concentration:

$\text{Net RFI} = \text{RFI}_{final} - \text{RFI}_{initial}$

$\text{RFI}_{initial} = \text{Sample}_{initial} - \text{Blank}_{initial}$

$\text{RFI}_{final} = \text{Sample}_{final} - \text{Blank}_{final}$

Where:

$\text{Sample}_{initial}$ = fluorescence emission of protein sample before ANS probe is added

$\text{Blank}_{intiail}$ = fluorescence emission of buffer blank before ANS probe is added

Sample_{final} = fluorescence emission of protein sample after ANS probe is added and 15-minute incubation at room temperature

Blankfinal = fluorescence emission of buffer blank after ANS probe is added and 15-minute incubation at room temperature

Example calculation for PPI at 0.05% protein:

$\text{RFI}_{initial} = 16 - 15.8 = 0.2$

$\text{RFI}_{final} = 464 - 20.5 = 443.5$

$\text{Net RFI} = 443.5 - 0.2 = 443.3$

Surface Hydrophobicity Index:

Net RFI values for all concentrations of protein solution (0.05%, 0.025%, 0.02%, 0.015%, 0.01%, and 0.005% protein) are plotted against protein concentration, as seen in **Figure 22**.

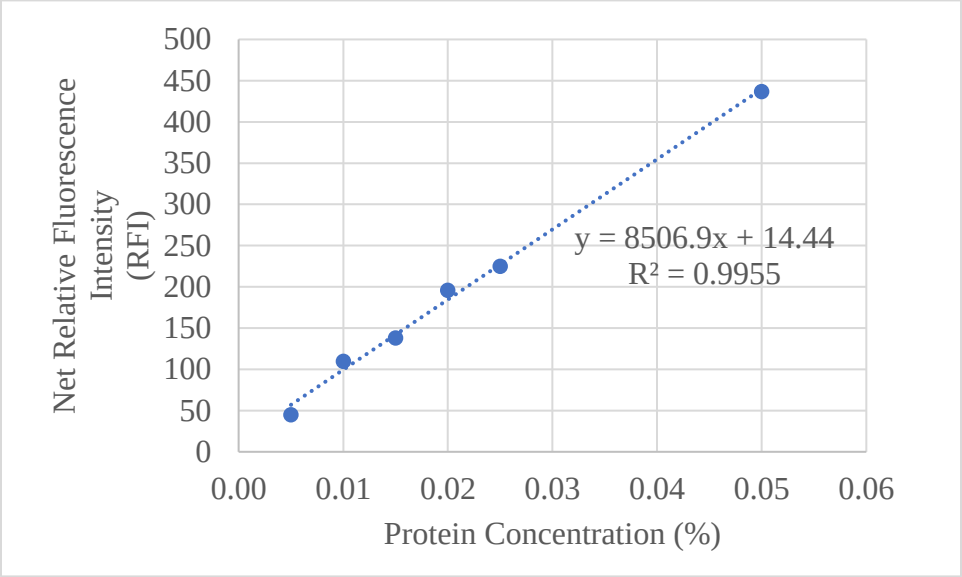

Figure 22. Net Relative Fluorescence Intensity (RFI) plotted against protein concentration (%) for PPI to determine surface hydrophobicity index.

The slope of the trendline in **Figure 22** is the surface hydrophobicity index 8506.9, r^2=0.9955.

The final value for surface hydrophobicity index is the average of three replicates.

Appendix D: Sample Calculation for Determining Protein Solubility

Protein Solubility of Pea Protein Isolate:

$$\%\ protein\ solubility = \frac{\%\ supernatant\ protein}{\%\ initial\ protein} \times 100\%$$

$$\%\ protein\ solubility = \frac{4.77}{5.43} \times 100\% = 87.84\%$$

% initial protein and % supernatant protein were determined by Dumas method, before and after centrifugation (15,682 x g for 10 minutes).

Appendix E: Sample Calculation for Determining Protein Emulsification Capacity

Emulsification Capacity of Pea Protein Isolate:

$$EC = \frac{volume\ of\ oil\ titrated\ (mL) \times\ density\ of\ oil\ (\frac{g}{mL})}{mass\ of\ protein\ (g)}$$

$$EC = \frac{38\ mL \times\ 0.93\ (\frac{g}{mL})}{0.1\ g} = 353.4\ \frac{g\ oil}{g\ protein}$$

Where:

0.93 g/mL = density of corn oil

0.1 g = grams of protein in 5 mL of a 2% protein solution

Appendix F: ANOVA Tables

Table 11. Analysis of variance on the effect of plasma reactive species on the area percentage of soluble aggregates present in samples analyzed by SE-HPLC.

Sample Analysis	Source of Variation	DF	SS	MS	F	P
cPPI, PPI Control- pH7, PPI Control- pH2, mPPI- N_xO_y /O_3 pH2, mPPI- O_3 pH2, mPPI- H_2O_2 pH2, mPPI- OH pH2	Between Groups	6	3000.86	500.143	33.511	<0.001
	Residual	14	208.944	14.925		
	Total	20	3209.8			

Table 12. Analysis of variance on the effect of plasma reactive species on the area percentage of legumin present in samples analyzed by SE-HPLC.

Sample Analysis	Source of Variation	DF	SS	MS	F	P
cPPI*, PPI Control- pH7, PPI Control- pH2, mPPI- N_xO_y /O_3 pH2, mPPI- O_3 pH2, mPPI- H_2O_2 pH2 mPPI- OH Radicals pH2	Between Groups	5	671.477	134.295	93.518	<0.001
	Residual	12	17.232	1.436		
	Total	17	688.71			

* No legumin peak was apparent in the chromatogram of cPPI.

Table 13. Analysis of variance on the effect of plasma reactive species on the area percentage of vicilin present in samples analyzed by SE-HPLC.

Sample Analysis	Source of Variation	DF	SS	MS	F	P
cPPI, PPI Control- pH7, PPI Control- pH2, mPPI- N_xO_y /O_3 pH2, mPPI- O_3 pH2, mPPI- H_2O_2 pH2 mPPI- OH Radicals pH2	Between Groups	6	108.046	18.008	46.165	<0.001
	Residual	14	5.461	0.39		
	Total	20	113.507			

Table 14. Analysis of variance on the effect of plasma reactive species on the area percentage of convicilin present in samples analyzed by SE-HPLC.

Sample Analysis	Source of Variation	DF	SS	MS	F	P
cPPI*, PPI Control- pH7, PPI Control- pH2, mPPI- N_xO_y /O_3 pH2, mPPI- O_3 pH2, mPPI- H_2O_2 pH2 mPPI- OH Radicals pH2	Between Groups	5	129.88	25.976	59.045	<0.001
	Residual	12	5.279	0.44		
	Total	17	135.159			

* No convicilin peak was apparent in the chromatogram of cPPI.

Table 15. Analysis of variance on the effect of plasma reactive species on the thermal denaturation temperature of the vicilin peak on DSC.

Sample Analysis	Source of Variation	DF	SS	MS	F	P
cPPI*, PPI Control- pH7, PPI Control- pH2, mPPI- N_xO_y /O_3 pH2, mPPI- O_3 pH2, mPPI- H_2O_2 pH2 mPPI- OH Radicals pH2	Between Groups	5	26.035	5.207	19.495	<0.001
	Residual	11	2.938	0.267		
	Total	16	28.974			

*cPPI was completely denatured before analysis. No peak of denaturation observed.

Table 16. Analysis of variance on the effect of plasma reactive species on the enthalpy of denaturation of the vicilin peak on DSC.

Sample Analysis	Source of Variation	DF	SS	MS	F	P
cPPI*, PPI Control- pH7, PPI Control- pH2, mPPI- N_xO_y /O_3 pH2, mPPI- O_3 pH2, mPPI- H_2O_2 pH2 mPPI- OH Radicals pH2	Between Groups	5	41.692	8.338	354.046	<0.001
	Residual	11	0.259	0.0236		
	Total	16	41.951			

*cPPI was completely denatured before analysis. No peak of denaturation observed.

Table 17. Analysis of variance on the effect of plasma reactive species on the relative percentage of α helix on IR spectra.

Sample Analysis	Source of Variation	DF	SS	MS	F	P
cPPI, PPI Control- pH7, PPI Control- pH2, mPPI- N_xO_y /O_3 pH2, mPPI- O_3 pH2, mPPI- H_2O_2 pH2 mPPI- OH Radicals pH2	Between Groups	6	102.534	17.089	3.617	0.022
	Residual	14	66.151	4.725		
	Total	20	168.686			

Table 18. Analysis of variance on the effect of plasma reactive species on the relative percentage of β sheet on IR spectra.

Sample Analysis	Source of Variation	DF	SS	MS	F	P
cPPI, PPI Control- pH7, PPI Control- pH2, mPPI- N_xO_y /O_3 pH2, mPPI- O_3 pH2, mPPI- H_2O_2 pH2 mPPI- OH Radicals pH2	Between Groups	6	257.915	42.986	17.882	<0.001
	Residual	14	33.653	2.404		
	Total	20	291.569			

Table 19. Analysis of variance on the effect of plasma reactive species on the relative percentage of random coil on IR spectra.

Sample Analysis	Source of Variation	DF	SS	MS	F	P
cPPI, PPI Control- pH7, PPI Control- pH2, mPPI- N_xO_y /O_3 pH2, mPPI- O_3 pH2, mPPI- H_2O_2 pH2 mPPI- OH Radicals pH2	Between Groups	6	171.811	28.635	9.147	<0.001
	Residual	14	43.829	3.131		
	Total	20	215.64			

Table 20. Analysis of variance on the effect of plasma reactive species on the relative percentage of β turn on IR spectra.

Sample Analysis	Source of Variation	DF	SS	MS	F	P
cPPI, PPI Control- pH7, PPI Control- pH2, mPPI- N_xO_y /O_3 pH2, mPPI- O_3 pH2, mPPI- H_2O_2 pH2 mPPI- OH Radicals pH2	Between Groups	6	171.811	28.635	9.147	<0.001
	Residual	14	43.829	3.131		
	Total	20	215.64			

Table 21. Analysis of variance on the effect of plasma reactive species on surface hydrophobicity of PPI.

Sample Analysis	Source of Variation	DF	SS	MS	F	P
cPPI, PPI Control- pH7, PPI Control- pH2, mPPI- N_xO_y /O_3 pH2, mPPI- O_3 pH2, mPPI- H_2O_2 pH2 mPPI- OH Radicals pH2	Between Groups	6	46672769.86	777879 5	15.057	<0.001
	Residual	14	7232939.633	516639		
	Total	20	53905709.49			

Table 22. Analysis of variance on the effect of plasma reactive species on surface charge of PPI.

Sample Analysis	Source of Variation	DF	SS	MS	F	P
cPPI, PPI Control- pH7, PPI Control- pH2, mPPI- N_xO_y /O_3 pH2, mPPI- O_3 pH2, mPPI- H_2O_2 pH2 mPPI- OH Radicals pH2	Between Groups	6	330.97	55.162	23.247	<0.001
	Residual	14	33.22	2.373		
	Total	20	364.19			

Table 23. Analysis of variance on the effect of plasma reactive species on solubility of non-heated PPI at pH 7.

Sample Analysis	Source of Variation	DF	SS	MS	F	P
cPPI, PPI Control- pH7, PPI Control- pH2, mPPI- N_xO_y /O_3 pH2, mPPI- O_3 pH2, mPPI- H_2O_2 pH2 mPPI- OH Radicals pH2	Between Groups	6	7750.81	1291.8	89.2	<0.001
	Residual	14	202.75	14.482		
	Total	20	7953.56			

Table 24. Analysis of variance on the effect of plasma reactive species on solubility of heated (at 80°C) PPI at pH 7.

Sample Analysis	Source of Variation	DF	SS	MS	F	P
cPPI, PPI Control- pH7, PPI Control- pH2, mPPI- N_xO_y /O_3 pH2, mPPI- O_3 pH2, mPPI- H_2O_2 pH2 mPPI- OH Radicals pH2	Between Groups	6	3977.2	662.866	44.311	<0.001
	Residual	14	209.432	14.959		
	Total	20	4186.63			

Table 25. Analysis of variance on the effect of plasma reactive species on gel strength of 15% pea protein gels.

Sample Analysis	Source of Variation	DF	SS	MS	F	P
cPPI*, PPI Control- pH7*, PPI Control- pH2*, mPPI- N_xO_y /O_3 pH2, mPPI- O_3 pH2, mPPI- H_2O_2 pH2*, mPPI- OH Radicals pH2	Between Groups	2	6.731	3.365	2.542	0.159
	Residual	6	7.943	1.324		
	Total	8	14.674			

*No gels formed at 15% protein level.

Table 26. Analysis of variance on the effect of plasma reactive species on gel strength of 20% pea protein gels.

Sample Analysis	Source of Variation	DF	SS	MS	F	P
cPPI, PPI Control- pH7, PPI Control- pH2, mPPI- N_xO_y /O_3 pH2, mPPI- O_3 pH2, mPPI- H_2O_2 pH2, mPPI- OH Radicals pH2	Between Groups	6	1240.41	206.735	24.311	<0.001
	Residual	14	119.051	8.504		
	Total	20	1359.46			

Table 27. Analysis of variance on the effect of plasma reactive species on emulsification capacity of 2% pea protein solutions.

Sample Analysis	Source of Variation	DF	SS	MS	F	P
cPPI, PPI Control- pH7, PPI Control- pH2, mPPI- N_xO_y /O_3 pH2, mPPI- O_3 pH2, mPPI- H_2O_2 pH2, mPPI- OH Radicals pH2	Between Groups	6	924520	154087	192.005	<0.001
	Residual	14	11235.2	802.513		
	Total	20	935755			

Table 28. Analysis of variance on the effect of plasma reactive species on the lightness (L*) of PPI.

Sample Analysis	Source of Variation	DF	SS	MS	F	P
cPPI*, PPI Control- pH7, PPI Control- pH2, mPPI- N_xO_y /O_3 pH2, mPPI- O_3 pH2, mPPI- H_2O_2 pH2, mPPI- OH Radicals pH2	Between Groups	5	49.846	9.969	23.448	<0.001
	Residual	12	5.102	0.425		
	Total	17	54.948			

*Statistical analysis did not include cPPI because cPPI is a reference sample.

Table 29. Analysis of variance on the effect of plasma reactive species on the red and green color (a*) of PPI.

Sample Analysis	Source of Variation	DF	SS	MS	F	P
cPPI*, PPI Control- pH7, PPI Control- pH2, mPPI- N_xO_y /O_3 pH2, mPPI- O_3 pH2, mPPI- H_2O_2 pH2, mPPI- OH Radicals pH2	Between Groups	5	2.591	0.518	4.197	0.019
	Residual	12	1.482	0.123		
	Total	17	4.073			

*Statistical analysis did not include cPPI because cPPI is a reference sample.

Table 30. Analysis of variance on the effect of plasma reactive species on the yellow and blue color (b*) of PPI.

Sample Analysis	Source of Variation	DF	SS	MS	F	P
cPPI*, PPI Control- pH7, PPI Control- pH2, mPPI- N_xO_y /O_3 pH2, mPPI- O_3 pH2, mPPI- H_2O_2 pH2, mPPI- OH Radicals pH2	Between Groups	5	80.615	16.123	18.814	<0.001
	Residual	12	10.283	0.857		
	Total	17	90.898			

*Statistical analysis did not include cPPI because cPPI is a reference sample.

Table 31. Analysis of variance on the total color differences of mPPIs compared to pH 7 PPI control.

Sample Analysis	Source of Variation	DF	SS	MS	F	P
cPPI*, PPI Control- pH7*, PPI Control- pH2, mPPI- N_xO_y /O_3 pH2, mPPI- O_3 pH2, mPPI- H_2O_2 pH2, mPPI- OH Radicals pH2	Between Groups	4	29.377	7.344	6.847	0.006
	Residual	10	10.726	1.073		
	Total	14	40.103			

*Statistical analysis did not include cPPI and PPI Control- pH7 as a reference sample and control, respectively.

Table 32. Analysis of variance on the effect of plasma reactive species on the area percentage of soluble aggregates present in pH 7 non-dialyzed samples analyzed by SE-HPLC.

Sample Analysis	Source of Variation	DF	SS	MS	F	P
cPPI, PPI Control- pH7, mPPI- N_xO_y /O_3 pH7, mPPI- O_3 pH7, mPPI- H_2O_2 pH7, mPPI- OH Radicals pH7	Between Groups	5	124.391	24.878	216.667	<0.001
	Residual	12	1.378	0.115		
	Total	17	125.769			

Table 33. Analysis of variance on the effect of plasma reactive species on the area percentage of legumin present in pH 7 non-dialyzed samples analyzed by SE-HPLC.

Sample Analysis	Source of Variation	DF	SS	MS	F	P
cPPI*, PPI Control- pH7, mPPI- N_xO_y /O_3 pH7, mPPI- O_3 pH7, mPPI- H_2O_2 pH7, mPPI- OH Radicals pH7	Between Groups	4	76.798	19.2	5.282	0.015
	Residual	10	36.35	3.635		
	Total	14	113.149			

* No legumin peak was apparent in the chromatogram of cPPI.

Table 34. Analysis of variance on the effect of plasma reactive species on the area percentage of vicilin in pH 7 non-dialyzed samples analyzed by SE-HPLC.

Sample Analysis	Source of Variation	DF	SS	MS	F	P
cPPI, PPI Control- pH7, mPPI- N_xO_y /O_3 pH7, mPPI- O_3 pH7, mPPI- H_2O_2 pH7, mPPI- OH Radicals pH7	Between Groups	5	64.375	12.875	128.144	<0.001
	Residual	12	1.206	0.1		
	Total	17	65.58			

Table 35. Analysis of variance on the effect of plasma reactive species on the area percentage of convicilin present in pH 7 non-dialyzed samples analyzed by SE-HPLC.

Sample Analysis	Source of Variation	DF	SS	MS	F	P
cPPI*, PPI Control- pH7, mPPI- N_xO_y /O_3 pH7, mPPI- O_3 pH7, mPPI- H_2O_2 pH7, mPPI- OH Radicals pH7	Between Groups	4	25.778	6.444	46.869	<0.001
	Residual	10	1.375	0.138		
	Total	14	27.153			

* No convicilin peak was apparent in the chromatogram of cPPI.

Table 36. Analysis of variance on the effect of plasma reactive species on the area percentage of soluble aggregates present in pH 2 non-dialyzed samples analyzed by SE-HPLC.

Sample Analysis	Source of Variation	DF	SS	MS	F	P
cPPI, PPI Control- pH2, mPPI- N_xO_y /O_3 pH2, mPPI- O_3 pH2, mPPI- H_2O_2 pH2, mPPI- OH Radicals pH2	Between Groups	5	1869.29	373.857	1121.78	<0.001
	Residual	12	3.999	0.333		
	Total	17	1873.28			

Table 37. Analysis of variance on the effect of plasma reactive species on the area percentage of legumin present in pH 2 non-dialyzed samples analyzed by SE-HPLC.

Sample Analysis	Source of Variation	DF	SS	MS	F	P
cPPI, PPI Control- pH2, mPPI- N_xO_y /O_3 pH2, mPPI- O_3 pH2, mPPI- H_2O_2 pH2, mPPI- OH Radicals pH2	Between Groups	4	17.446	4.362	138.286	<0.001
	Residual	10	0.315	0.0315		
	Total	14	17.762			

* No legumin peak was apparent in the chromatogram of cPPI.

Table 38. Analysis of variance on the effect of plasma reactive species on the area percentage of vicilin in pH 2 non-dialyzed samples analyzed by SE-HPLC.

Sample Analysis	Source of Variation	DF	SS	MS	F	P
cPPI, PPI Control- pH2, mPPI- N_xO_y /O_3 pH2, mPPI- O_3 pH2, mPPI- H_2O_2 pH2, mPPI- OH Radicals pH2	Between Groups	5	21.8	4.36	193.257	<0.001
	Residual	12	0.271	0.0226		
	Total	17	22.071			

Table 39. Analysis of variance on the effect of plasma reactive species on the area percentage of convicilin present in pH 2 non-dialyzed samples analyzed by SE-HPLC

Sample Analysis	Source of Variation	DF	SS	MS	F	P
cPPI, PPI Control- pH2, mPPI- N_xO_y /O_3 pH2, mPPI- O_3 pH2, mPPI- H_2O_2 pH2, mPPI- OH Radicals pH2	Between Groups	4	16.321	4.08	441.27	<0.001
	Residual	10	0.0925	0.00925		
	Total	14	16.414			

* No convicilin peak was apparent in the chromatogram of cPPI.

Table 40. Analysis of variance on the effect of plasma reactive on the thermal denaturation temperature of the vicilin peak present in pH 7 non-dialyzed samples analyzed by DSC

Sample Analysis	Source of Variation	DF	SS	MS	F	P
cPPI*, PPI Control- pH7, mPPI- N_xO_y /O_3 pH7, mPPI- O_3 pH7, mPPI- H_2O_2 pH7, mPPI- OH Radicals pH7	Between Groups	4	8.486	2.121	32.764	<0.001
	Residual	5	0.324	0.0648		
	Total	9	8.81			

*cPPI was completely denatured before analysis. No peak of denaturation observed.

Table 41. Analysis of variance on the effect of plasma reactive species on the enthalpy of denaturation of the vicilin peak present in pH 7 non-dialyzed samples analyzed by DSC.

Sample Analysis	Source of Variation	DF	SS	MS	F	P
cPPI*, PPI Control- pH7, mPPI- N_xO_y /O_3 pH7, mPPI- O_3 pH7, mPPI- H_2O_2 pH7, mPPI- OH Radicals pH7	Between Groups	4	3.883	0.971	79.966	<0.001
	Residual	5	0.0607	0.0121		
	Total	9	3.944			

*cPPI was completely denatured before analysis. No peak of denaturation observed.

Table 42. Analysis of variance on the effect of plasma reactive species on the thermal denaturation temperature of the legumin peak present in pH 7 non-dialyzed samples analyzed by DSC.

Sample Analysis	Source of Variation	DF	SS	MS	F	P
cPPI*, PPI Control- pH7, mPPI- N_xO_y /O_3 pH7, mPPI- O_3 pH7, mPPI- H_2O_2 pH7, mPPI- OH Radicals pH7	Between Groups	4	4.939	1.235	5.395	0.046
	Residual	5	1.144	0.229		
	Total	9	6.083			

*cPPI was completely denatured before analysis. No peak of denaturation observed.

Table 43. Analysis of variance on the effect of plasma reactive species on the enthalpy of denaturation of the legumin peak present in pH 7 non-dialyzed samples analyzed by DSC.

Sample Analysis	Source of Variation	DF	SS	MS	F	P
cPPI*, PPI Control- pH7, mPPI- N_xO_y /O_3 pH7, mPPI- O_3 pH7, mPPI- H_2O_2 pH7, mPPI- OH Radicals pH7	Between Groups	4	0.811	0.203	137.969	<0.001
	Residual	5	0.00735	0.00147		
	Total	9	0.819			

*cPPI was completely denatured before analysis. No peak of denaturation observed.

Table 44. Analysis of variance on the effect of plasma reactive species on the thermal denaturation temperature of the vicilin peak present in pH 2 non-dialyzed samples analyzed by DSC.

Sample Analysis	Source of Variation	DF	SS	MS	F	P
cPPI*, PPI Control- pH2, mPPI- N_xO_y /O_3 pH2, mPPI- O_3 pH2, mPPI- H_2O_2 pH2, mPPI- OH Radicals pH2	Between Groups	4	31.745	7.936	45.459	<0.001
	Residual	5	0.873	0.175		
	Total	9	32.618			

*cPPI was completely denatured before analysis. No peak of denaturation observed.

Table 45. Analysis of variance on the effect of plasma reactive species on the enthalpy of denaturation of the vicilin peak present in pH 2 non-dialyzed samples analyzed by DSC.

Sample Analysis	Source of Variation	DF	SS	MS	F	P
cPPI*, PPI Control- pH2, mPPI- N_xO_y /O_3 pH2, mPPI- O_3 pH2, mPPI- H_2O_2 pH2, mPPI- OH Radicals pH2	Between Groups	4	4.431	1.108	97.096	<0.001
	Residual	5	0.0571	0.0114		
	Total	9	4.488			

*cPPI was completely denatured before analysis. No peak of denaturation observed.

Table 46. Analysis of variance on the effect of plasma reactive species on the relative percentage of α helix present in pH 7 non-dialyzed samples analyzed by FTIR.

Sample Analysis	Source of Variation	DF	SS	MS	F	P
cPPI, PPI Control- pH7, mPPI- N_xO_y /O_3 pH7, mPPI- O_3 pH7, mPPI- H_2O_2 pH7, mPPI- OH Radicals pH7	Between Groups	5	104.264	20.853	11.054	0.005
	Residual	6	11.319	1.887		
	Total	11	115.584			

Table 47. Analysis of variance on the effect of plasma reactive species on the relative percentage of α helix present in pH 2 non-dialyzed samples analyzed by FTIR.

Sample Analysis	Source of Variation	DF	SS	MS	F	P
cPPI, PPI Control- pH2, mPPI- N_xO_y /O_3 pH2, mPPI- O_3 pH2, mPPI- H_2O_2 pH2, mPPI- OH Radicals pH2	Between Groups	5	74.673	14.935	10.215	0.007
	Residual	6	8.773	1.462		
	Total	11	83.445			

Table 48. Analysis of variance on the effect of plasma reactive species on the relative percentage of β sheet present in pH 7 non-dialyzed samples analyzed by FTIR.

Sample Analysis	Source of Variation	DF	SS	MS	F	P
cPPI, PPI Control- pH7, mPPI- N_xO_y /O_3 pH7, mPPI- O_3 pH7, mPPI- H_2O_2 pH7, mPPI- OH Radicals pH7	Between Groups	5	13.808	2.762	0.858	0.557
	Residual	6	19.322	3.22		
	Total	11	33.13			

Table 49. Analysis of variance on the effect of plasma reactive species on the relative percentage of β sheet present in pH 2 non-dialyzed samples analyzed by FTIR.

Sample Analysis	Source of Variation	DF	SS	MS	F	P
cPPI, PPI Control- pH2, mPPI- N_xO_y /O_3 pH2, mPPI- O_3 pH2, mPPI- H_2O_2 pH2, mPPI- OH Radicals pH2	Between Groups	5	29.49	5.898	8.181	0.012
	Residual	6	4.325	0.721		
	Total	11	33.816			

Table 50. Analysis of variance on the effect of plasma reactive species the relative percentage of β turn present in pH 7 non-dialyzed samples analyzed by FTIR.

Sample Analysis	Source of Variation	DF	SS	MS	F	P
cPPI, PPI Control- pH7, mPPI- N_xO_y /O_3 pH7, mPPI- O_3 pH7, mPPI- H_2O_2 pH7, mPPI- OH Radicals pH7	Between Groups	5	18.301	3.66	1.741	0.259
	Residual	6	12.614	2.102		
	Total	11	30.915			

Table 51. Analysis of variance on the effect of plasma reactive species on the relative percentage of β turn present in pH 2 non-dialyzed samples analyzed by FTIR.

Sample Analysis	Source of Variation	DF	SS	MS	F	P
cPPI, PPI Control- pH2, mPPI- N_xO_y /O_3 pH2, mPPI- O_3 pH2, mPPI- H_2O_2 pH2, mPPI- OH Radicals pH2	Between Groups	5	28.558	5.712	1.346	0.36
	Residual	6	25.452	4.242		
	Total	11	54.01			

Table 52. Analysis of variance on the effect of plasma reactive species on the relative percentage of random coil present in pH 7 non-dialyzed samples analyzed by FTIR.

Sample Analysis	Source of Variation	DF	SS	MS	F	P
cPPI, PPI Control- pH7, mPPI- N_xO_y /O_3 pH7, mPPI- O_3 pH7, mPPI- H_2O_2 pH7, mPPI- OH Radicals pH7	Between Groups	5	44.451	8.89	43.318	<0.001
	Residual	6	1.231	0.205		
	Total	11	45.682			

Table 53. Analysis of variance on the effect of plasma reactive species on the relative percentage of random coil present in pH 2 non-dialyzed samples analyzed by FTIR.

Sample Analysis	Source of Variation	DF	SS	MS	F	P
cPPI, PPI Control- pH2, mPPI- N_xO_y /O_3 pH2, mPPI- O_3 pH2, mPPI- H_2O_2 pH2, mPPI- OH Radicals pH2	Between Groups	5	31.094	6.219	6.516	0.021
	Residual	6	5.726	0.954		
	Total	11	36.82			

Table 54. Analysis of variance on the effect of plasma reactive species on surface hydrophobicity of pea protein modified at pH 7.

Sample Analysis	Source of Variation	DF	SS	MS	F	P
cPPI, PPI Control- pH7, mPPI- N_xO_y /O_3 pH7, mPPI- O_3 pH7, mPPI- H_2O_2 pH7, mPPI- OH Radicals pH7	Between Groups	5	51158510.68	10231702.14	24.22	<0.001
	Residual	12	5069412.467	422451.039		
	Total	17	56227923.14			

Table 55. Analysis of variance on the effect of plasma reactive species on surface hydrophobicity of pea protein modified at pH 2 without dialysis.

Sample Analysis	Source of Variation	DF	SS	MS	F	P
cPPI, PPI Control- pH2, mPPI- N_xO_y /O_3 pH2, mPPI- O_3 pH2, mPPI- H_2O_2 pH2, mPPI- OH Radicals pH2	Between Groups	5	45735832.99	9147166.598	16.1	<0.001
	Residual	12	6817634.813	568136.234		
	Total	17	52553467.81			

Table 56. Analysis of variance on the effect of plasma reactive species on surface charge of pH 7 pea protein modified at pH 7.

Sample Analysis	Source of Variation	DF	SS	MS	F	P
cPPI, PPI Control- pH7, mPPI- N_xO_y /O_3 pH7, mPPI- O_3 pH7, mPPI- H_2O_2 pH7, mPPI- OH Radicals pH7	Between Groups	5	276.423	55.285	48.307	<0.001
	Residual	12	13.733	1.144		
	Total	17	290.156			

Table 57. Analysis of variance on the effect of plasma reactive species on surface charge of pea protein modified at pH 2 without dialysis.

Sample Analysis	Source of Variation	DF	SS	MS	F	P
cPPI, PPI Control- pH2, mPPI- N_xO_y /O_3 pH2, mPPI- O_3 pH2, mPPI- H_2O_2 pH2, mPPI- OH Radicals pH2	Between Groups	5	13.547	2.709	8.616	0.001
	Residual	12	3.773	0.314		
	Total	17	17.32			

Table 58. Analysis of variance on the effect of plasma reactive species on the solubility at pH 7 of not-heated pea protein modified at pH 7.

Sample Analysis	Source of Variation	DF	SS	MS	F	P
cPPI, PPI Control- pH7, mPPI- N_xO_y /O_3 pH7, mPPI- O_3 pH7, mPPI- H_2O_2 pH7, mPPI- OH Radicals pH7	Between Groups	5	8275.96	1655.19	341.722	<0.001
	Residual	12	58.124	4.844		
	Total	17	8334.09			

Table 59. Analysis of variance on the effect of plasma reactive species on the solubility at pH 7 of heated (at 80°C) pea protein modified at pH 7.

Sample Analysis	Source of Variation	DF	SS	MS	F	P
cPPI, PPI Control- pH7, mPPI- N_xO_y /O_3 pH7, mPPI- O_3 pH7, mPPI- H_2O_2 pH7, mPPI- OH Radicals pH7	Between Groups	5	3270.24	654.048	59.111	<0.001
	Residual	12	132.777	11.065		
	Total	17	3403.02			

Table 60. Analysis of variance on the effect of plasma reactive species on the solubility at pH 7 of not-heated pea protein modified at pH 2 without dialysis.

Sample Analysis	Source of Variation	DF	SS	MS	F	P
cPPI, PPI Control- pH2, mPPI- N_xO_y /O_3 pH2, mPPI- O_3 pH2, mPPI- H_2O_2 pH2, mPPI- OH Radicals pH2	Between Groups	5	5756.07	1151.21	250.704	<0.001
	Residual	12	55.103	4.592		
	Total	17	5811.17			

Table 61. Analysis of variance on the effect of plasma reactive species on the solubility at pH 7 of heated (80°C) pea protein modified at pH 2 without dialysis.

Sample Analysis	Source of Variation	DF	SS	MS	F	P
cPPI, PPI Control- pH2, mPPI- N_xO_y /O_3 pH2, mPPI- O_3 pH2, mPPI- H_2O_2 pH2, mPPI- OH Radicals pH2	Between Groups	5	1931.71	386.341	28.559	<0.001
	Residual	12	162.332	13.528		
	Total	17	2094.04			

Table 62. Analysis of variance on the effect of plasma reactive species on the gel strength of 15% pea protein gels formed by pea protein modified at pH 2 without dialysis.

Sample Analysis	Source of Variation	DF	SS	MS	F	P
cPPI*, PPI Control- pH2*, mPPI- N_xO_y /O_3 pH2, mPPI- O_3 pH2, mPPI- H_2O_2 pH2, mPPI- OH Radicals pH2	Between Groups	3	11.96	3.987	9.52	0.005
	Residual	8	3.35	0.419		
	Total	11	15.31			

*No gels formed at 15% protein level.

Table 63. Analysis of variance on the effect of plasma reactive species on the gel strength of 20% pea protein gels formed by pea protein modified at pH 7.

Sample Analysis	Source of Variation	DF	SS	MS	F	P
cPPI, PPI Control- pH7, mPPI- N_xO_y /O_3 pH7,	Between Groups	5	169.868	33.974	12.554	<0.001
mPPI- O_3 pH7, mPPI- H_2O_2 pH7, mPPI- OH Radicals pH7	Residual	12	32.473	2.706		
	Total	17	202.342			

Table 64. Analysis of variance on the effect of plasma reactive species on the gel strength of 20% pea protein gels formed by pea protein modified at pH 2 without dialysis.

Sample Analysis	Source of Variation	DF	SS	MS	F	P
cPPI, PPI Control- pH2, mPPI- N_xO_y /O_3 pH2,	Between Groups	5	410.139	82.028	30.046	<0.001
mPPI- O_3 pH2, mPPI- H_2O_2 pH2, mPPI- OH Radicals pH2	Residual	12	32.761	2.73		
	Total	17	442.9			

Table 65. Analysis of variance on the effect of plasma reactive species on the emulsification capacity of 2% pea protein modified at pH 7.

Sample Analysis	Source of Variation	DF	SS	MS	F	P
cPPI, PPI Control- pH7, mPPI- N_xO_y /O_3	Between Groups	5	55166.2	11033.2	74.071	<0.001
pH7, mPPI- O_3 pH7, mPPI- H_2O_2 pH7, mPPI- OH Radicals pH7	Residual	12	1787.46	148.955		
	Total	17	56953.7			

Table 66. Analysis of variance on the effect of plasma reactive species on emulsification capacity of 2% pea protein modified at pH 2 without dialysis.

Sample Analysis	Source of Variation	DF	SS	MS	F	P
cPPI, PPI Control- pH2, mPPI- N_xO_y /O_3 pH2,	Between Groups	5	390517	78103.4	113.669	<0.001
mPPI- O_3 pH2, mPPI- H_2O_2 pH2, mPPI- OH Radicals pH2	Residual	12	8245.38	687.115		
	Total	17	398762			

Table 67. Analysis of variance on the effect of treatment time of APPJ on the area percentage of soluble aggregates present in samples analyzed by SE-HPLC.

Sample Analysis	Source of Variation	DF	SS	MS	F	P
cPPI, PPI, APPJ-5min, APPJ- 15min, APPJ-30min, APPJ-45min	Between Groups	5	1259.465	251.893	2003.66	<0.001
	Residual	12	1.509	0.126		
	Total	17	1260.973			

Table 68. Analysis of variance on the effect of treatment time of 2D-DBD on the area percentage of soluble aggregates present in samples analyzed by SE-HPLC.

Sample Analysis	Source of Variation	DF	SS	MS	F	P
cPPI, PPI, 2D-DBD-5min, 2D-DBD-15min, 2D-DBD-30min, 2D-DBD-45min	Between Groups	5	1792.91	358.582	258.746	<0.001
	Residual	12	16.63	1.386		
	Total	17	1809.54			

Table 69. Analysis of variance on the effect of treatment time of ns-pulsed on the area percentage of soluble aggregates present in samples analyzed by SE-HPLC.

Sample Analysis	Source of Variation	DF	SS	MS	F	P
cPPI, PPI, ns-pulsed-5min, ns-pulsed-15min, ns-pulsed-30min, ns-pulsed-45min	Between Groups	4	2191.958	547.99	17053.6	<0.001
	Residual	10	0.321	0.0321		
	Total	14	2192.28			

Table 70. Analysis of variance on the effect of treatment time of APPJ on the area percentage of legumin present in samples analyzed by SE-HPLC.

Sample Analysis	Source of Variation	DF	SS	MS	F	P
cPPI*, PPI, APPJ-5min, APPJ- 15min, APPJ-30min, APPJ-45min	Between Groups	4	1518.662	379.666	966.464	<0.001
	Residual	10	3.928	0.393		
	Total	14	1522.591			

* No legumin peak was apparent in the chromatogram of cPPI.

Table 71. Analysis of variance on the effect of treatment time of 2D-DBD on the area percentage of legumin present in samples analyzed by SE-HPLC.

Sample Analysis	Source of Variation	DF	SS	MS	F	P
cPPI*, PPI, 2D-DBD-5min, 2D-DBD- 15min, 2D-DBD-30min, 2D-DBD- 45min	Between Groups	4	4.972	1.243	122.836	<0.001
	Residual	10	0.101	0.0101		
	Total	14	5.074			

* No legumin peak was apparent in the chromatogram of cPPI.

Table 72. Analysis of variance on the effect of treatment time of ns-pulsed on the area percentage of legumin present in samples analyzed by SE-HPLC.

Sample Analysis	Source of Variation	DF	SS	MS	F	P
cPPI*, PPI, ns-pulsed-5min, ns-pulsed- 15min, ns-pulsed-30min, ns-pulsed-45min	Between Groups	3	1248.384	416.128	850.485	<0.001
	Residual	8	3.914	0.489		
	Total	11	1252.298			

* No legumin peak was apparent in the chromatogram of cPPI.

Table 73. Analysis of variance on the effect of treatment time of APPJ on the area percentage of convicilin present in samples analyzed by SE-HPLC.

Sample Analysis	Source of Variation	DF	SS	MS	F	P
cPPI*, PPI, APPJ-5min, APPJ- 15min, APPJ-30min, APPJ-45min	Between Groups	4	17.596	4.399	290.942	<0.001
	Residual	10	0.151	0.0151		
	Total	14	17.747			

* No convicilin peak was apparent in the chromatogram of cPPI.

Table 74. Analysis of variance on the effect of treatment time of 2D-DBD on the area percentage of convicilin present in samples analyzed by SE-HPLC.

Sample Analysis	Source of Variation	DF	SS	MS	F	P
cPPI*, PPI, 2D-DBD-5min, 2D-DBD- 15min, 2D-DBD-30min, 2D-DBD- 45min	Between Groups	4	16.018	4.004	180.379	<0.001
	Residual	10	0.222	0.0222		
	Total	14	16.24			

* No convicilin peak was apparent in the chromatogram of cPPI.

Table 75. Analysis of variance on the effect of treatment time of ns-pulsed on the area percentage of convicilin present in samples analyzed by SE-HPLC.

Sample Analysis	Source of Variation	DF	SS	MS	F	P
cPPI*, PPI, ns-pulsed-5min, ns-pulsed- 15min, ns-pulsed-30min, ns-pulsed- 45min	Between Groups	3	17.781	5.927	351.933	<0.001
	Residual	8	0.135	0.0168		
	Total	11	17.916			

* No convicilin peak was apparent in the chromatogram of cPPI.

Table 76. Analysis of variance on the effect of treatment time of APPJ on the area percentage of vicilin present in samples analyzed by SE-HPLC.

Sample Analysis	Source of Variation	DF	SS	MS	F	P
cPPI, PPI, APPJ-5min, APPJ- 15min, APPJ-30min, APPJ-45min	Between Groups	5	107.044	21.409	292.158	<0.001
	Residual	12	0.879	0.0733		
	Total	17	107.923			

Table 77. Analysis of variance on the effect of treatment time of 2D-DBD on the area percentage of vicilin present in samples analyzed by SE-HPLC.

Sample Analysis	Source of Variation	DF	SS	MS	F	P
cPPI, PPI, 2D-DBD-5min, 2D-DBD- 15min, 2D-DBD-30min, 2D-DBD- 45min	Between Groups	5	150.677	30.135	408.74	<0.001
	Residual	12	0.885	0.0737		
	Total	17	151.562			

Table 78. Analysis of variance on the effect of treatment time of ns-pulsed on the area percentage of vicilin present in samples analyzed by SE-HPLC.

Sample Analysis	Source of Variation	DF	SS	MS	F	P
cPPI, PPI, ns-pulsed-5min, ns-pulsed- 15min, ns-pulsed-30min, ns-pulsed- 45min	Between Groups	4	108.954	27.238	317.07	<0.001
	Residual	10	0.859	0.0859		
	Total	14	109.813			

Table 79. Analysis of variance on the effect of treatment time of APPJ on the area percentage of soluble aggregates present in samples dissolved in 0.1% SDS phosphate buffer and analyzed by SE-HPLC.

Sample Analysis	Source of Variation	DF	SS	MS	F	P
cPPI, PPI, APPJ- 5min, APPJ- 15min, APPJ- 30min, APPJ- 45min	Between Groups	5	1068.893	213.779	201.441	<0.001
	Residual	12	12.735	1.061		
	Total	17	1081.628			

Table 80. Analysis of variance on the effect of treatment time of 2D-DBD on the area percentage of soluble aggregates present in samples dissolved in 0.1% SDS phosphate buffer and analyzed by SE-HPLC.

Sample Analysis	Source of Variation	DF	SS	MS	F	P
cPPI, PPI, 2D-DBD- 5min, 2D-DBD- 15min, 2D-DBD-30min, 2D-DBD-45min	Between Groups	5	1210.458	242.092	231.336	<0.001
	Residual	12	12.558	1.046		
	Total	17	1223.016			

Table 81. Analysis of variance on the effect of treatment time of ns-pulsed on the area percentage of soluble aggregates present in samples dissolved in 0.1% SDS phosphate buffer and analyzed by SE-HPLC.

Sample Analysis	Source of Variation	DF	SS	MS	F	P
cPPI, PPI, ns-pulsed- 5min, ns-pulsed- 15min, ns-pulsed-30min, ns-pulsed- 45min	Between Groups	4	959.433	239.858	177.983	<0.001
	Residual	10	13.476	1.348		
	Total	14	972.91			

Table 82. Analysis of variance on the effect of treatment time of APPJ on the area percentage of legumin present in samples dissolved in 0.1% SDS phosphate buffer and analyzed by SE-HPLC.

Sample Analysis	Source of Variation	DF	SS	MS	F	P
cPPI*, PPI, APPJ- 5min, APPJ- 15min, APPJ- 30min, APPJ- 45min	Between Groups	4	62.09	15.523	14.76	<0.001
	Residual	10	10.517	1.052		
	Total	14	72.607			

Table 83. Analysis of variance on the effect of treatment time of 2D-DBD on the area percentage of legumin present in samples dissolved in 0.1% SDS phosphate buffer and analyzed by SE-HPLC.

Sample Analysis	Source of Variation	DF	SS	MS	F	P
cPPI*, PPI, 2D-DBD- 5min, 2D-DBD- 15min, 2D-DBD-30min, 2D-DBD- 45min	Between Groups	4	70.051	17.513	16.657	<0.001
	Residual	10	10.514	1.051		
	Total	14	80.565			

* No legumin peak was apparent in the chromatogram of cPPI.

Table 84. Analysis of variance on the effect of treatment time of ns-pulsed on the area percentage of legumin present in samples dissolved in 0.1% SDS phosphate buffer and analyzed by SE-HPLC.

Sample Analysis	Source of Variation	DF	SS	MS	F	P
cPPI*, PPI, ns-pulsed- 5min, ns-pulsed- 15min, ns-pulsed-30min, ns-pulsed- 45min	Between Groups	3	57.119	19.04	14.48	0.001
	Residual	8	10.519	1.315		
	Total	11	67.638			

* No legumin peak was apparent in the chromatogram of cPPI.

Table 85. Analysis of variance on the effect of treatment time of APPJ on the area percentage of convicilin present in samples dissolved in 0.1% SDS phosphate buffer and analyzed by SE-HPLC.

Sample Analysis	Source of Variation	DF	SS	MS	F	P
cPPI*, PPI, APPJ- 5min, APPJ- 15min, APPJ-30min, APPJ- 45min	Between Groups	4	150.316	37.579	380.072	<0.001
	Residual	10	0.989	0.0989		
	Total	14	151.305			

* No convicilin peak was apparent in the chromatogram of cPPI.

Table 86. Analysis of variance on the effect of treatment time of 2D-DBD on the area percentage of convicilin present in samples dissolved in 0.1% SDS phosphate buffer and analyzed by SE-HPLC.

Sample Analysis	Source of Variation	DF	SS	MS	F	P
cPPI*, PPI, 2D-DBD- 5min, 2D-DBD- 15min, 2D-DBD-30min, 2D-DBD- 45min	Between Groups	4	121.726	30.432	309.096	<0.001
	Residual	10	0.985	0.0985		
	Total	14	122.711			

* No convicilin peak was apparent in the chromatogram of cPPI.

Table 87. Analysis of variance on the effect of treatment time of ns-pulsed on the area percentage of convicilin present in samples dissolved in 0.1% SDS phosphate buffer and analyzed by SE-HPLC.

Sample Analysis	Source of Variation	DF	SS	MS	F	P
cPPI*, PPI, ns-pulsed- 5min, ns-pulsed- 15min, ns-pulsed-30min, ns-pulsed- 45min	Between Groups	3	96.611	32.204	260.547	<0.001
	Residual	8	0.989	0.124		
	Total	11	97.599			

* No convicilin peak was apparent in the chromatogram of cPPI.

Table 88. Analysis of variance on the effect of treatment time of APPJ on the area percentage of vicilin present in samples dissolved in 0.1% SDS phosphate buffer and analyzed by SE-HPLC.

Sample Analysis	Source of Variation	DF	SS	MS	F	P
cPPI, PPI, APPJ- 5min, APPJ- 15min, APPJ-30min, APPJ- 45min	Between Groups	5	78.582	15.716	756.203	<0.001
	Residual	12	0.249	0.0208		
	Total	17	78.831			

Table 89. Analysis of variance on the effect of treatment time of 2D-DBD on the area percentage of vicilin present in samples dissolved in 0.1% SDS phosphate buffer and analyzed by SE-HPLC.

Sample Analysis	Source of Variation	DF	SS	MS	F	P
cPPI, PPI, 2D-DBD- 5min, 2D-DBD- 15min, 2D-DBD-30min, 2D-DBD- 45min	Between Groups	5	73.014	14.603	702.621	<0.001
	Residual	12	0.249	0.0208		
	Total	17	73.263			

Table 90. Analysis of variance on the effect of treatment time of ns-pulsed on the area percentage of vicilin present in samples dissolved in 0.1% SDS phosphate buffer and analyzed by SE-HPLC.

Sample Analysis	Source of Variation	DF	SS	MS	F	P
cPPI, PPI, ns-pulsed- 5min, ns-pulsed- 15min, ns-pulsed-30min, ns-pulsed-45min	Between Groups	4	45.642	11.41	446.418	<0.001
	Residual	10	0.256	0.0256		
	Total	14	45.897			

Table 91. Analysis of variance on the effect of treatment time of APPJ on the area percentage of soluble aggregates present in samples dissolved in 0.1% SDS + 2.5% BME phosphate buffer and analyzed by SE-HPLC.

Sample Analysis	Source of Variation	DF	SS	MS	F	P
cPPI, PPI, APPJ- 5min, APPJ- 15min, APPJ- 30min, APPJ- 45min	Between Groups	5	355.481	71.096	476.693	<0.001
	Residual	12	1.79	0.149		
	Total	17	357.27			

Table 92. Analysis of variance on the effect of treatment time of 2D-DBD on the area percentage of soluble aggregates present in samples dissolved in 0.1% SDS + 2.5% BME phosphate buffer and analyzed by SE-HPLC.

Sample Analysis	Source of Variation	DF	SS	MS	F	P
cPPI, PPI, 2D-DBD- 5min, 2D-DBD- 15min, 2D-DBD-30min, 2D-DBD- 45min	Between Groups	5	857.654	171.531	766.618	<0.001
	Residual	12	2.685	0.224		
	Total	17	860.339			

Table 93. Analysis of variance on the effect of treatment time of ns-pulsed on the area percentage of soluble aggregates present in samples dissolved in 0.1% SDS + 2.5% BME phosphate buffer and analyzed by SE-HPLC.

Sample Analysis	Source of Variation	DF	SS	MS	F	P
cPPI, PPI, ns-pulsed- 5min, ns-pulsed- 15min, ns-pulsed- 30min, ns-pulsed- 45min	Between Groups	4	226.868	56.717	333.512	<0.001
	Residual	10	1.701	0.17		
	Total	14	228.569			

Table 94. Analysis of variance on the effect of treatment time of APPJ on the area percentage of legumin present in samples dissolved in 0.1% SDS + 2.5% BME phosphate buffer and analyzed by SE-HPLC.

Sample Analysis	Source of Variation	DF	SS	MS	F	P
cPPI*, PPI, APPJ- 5min, APPJ- 15min, APPJ- 30min, APPJ- 45min	Between Groups	4	44.182	11.045	17625.7	<0.001
	Residual	10	0.00627	0.00063		
	Total	14	44.188			

* No legumin peak was apparent in the chromatogram of cPPI.

Table 95. Analysis of variance on the effect of treatment time of 2D-DBD on the area percentage of legumin present in samples dissolved in 0.1% SDS + 2.5% BME phosphate buffer and analyzed by SE-HPLC.

Sample Analysis	Source of Variation	DF	SS	MS	F	P
cPPI*, PPI, 2D-DBD- 5min, 2D-DBD- 15min, 2D-DBD-30min, 2D-DBD- 45min	Between Groups	4	34.682	8.671	1329.84	<0.001
	Residual	10	0.0652	0.00652		
	Total	14	34.748			

* No legumin peak was apparent in the chromatogram of cPPI.

Table 96. Analysis of variance on the effect of treatment time of ns-pulsed on the area percentage of legumin present in samples dissolved in 0.1% SDS + 2.5% BME phosphate buffer and analyzed by SE-HPLC.

Sample Analysis	Source of Variation	DF	SS	MS	F	P
cPPI*, PPI, ns-pulsed- 5min, ns-pulsed- 15min, ns-pulsed-30min, ns-pulsed- 45min	Between Groups	3	24.982	8.327	758.762	<0.001
	Residual	8	0.0878	0.011		
	Total	11	25.07			

* No legumin peak was apparent in the chromatogram of cPPI.

Table 97. Analysis of variance on the effect of treatment time of APPJ on the area percentage of convicilin present in samples dissolved in 0.1% SDS + 2.5% BME phosphate buffer and analyzed by SE-HPLC.

Sample Analysis	Source of Variation	DF	SS	MS	F	P
cPPI*, PPI, APPJ- 5min, APPJ- 15min, APPJ-30min, APPJ- 45min	Between Groups	4	103.323	25.831	31501	<0.001
	Residual	10	0.0082	0.00082		
	Total	14	103.332			

* No convicilin peak was apparent in the chromatogram of cPPI.

Table 98. Analysis of variance on the effect of treatment time of 2D-DBD on the area percentage of convicilin present in samples dissolved in 0.1% SDS + 2.5% BME phosphate buffer and analyzed by SE-HPLC.

Sample Analysis	Source of Variation	DF	SS	MS	F	P
cPPI*, PPI, 2D-DBD- 5min, 2D-DBD- 15min, 2D-DBD-30min, 2D-DBD- 45min	Between Groups	4	88.051	22.013	3144.7	<0.001
	Residual	10	0.07	0.007		
	Total	14	88.121			

* No convicilin peak was apparent in the chromatogram of cPPI.

Table 99. Analysis of variance on the effect of treatment time of ns-pulsed on the area percentage of convicilin present in samples dissolved in 0.1% SDS + 2.5% BME phosphate buffer and analyzed by SE-HPLC.

Sample Analysis	Source of Variation	DF	SS	MS	F	P
cPPI*, PPI, ns-pulsed-5min, ns-pulsed- 15min, ns-pulsed-30min, ns-pulsed- 45min	Between Groups	3	76.709	25.57	3835.46	<0.001
	Residual	8	0.0533	0.00667		
	Total	11	76.762			

Table 100. Analysis of variance on the effect of treatment time of APPJ on the area percentage of vicilin present in samples dissolved in 0.1% SDS + 2.5% BME phosphate buffer and analyzed by SE-HPLC.

Sample Analysis	Source of Variation	DF	SS	MS	F	P
cPPI, PPI, APPJ- 5min, APPJ- 15min, APPJ-30min, APPJ- 45min	Between Groups	5	36.027	7.205	2447.09	<0.001
	Residual	12	0.0353	0.00294		
	Total	17	36.062			

Table 101. Analysis of variance on the effect of treatment time of 2D-DBD on the area percentage of vicilin present in samples dissolved in 0.1% SDS + 2.5% BME phosphate buffer and analyzed by SE-HPLC.

Sample Analysis	Source of Variation	DF	SS	MS	F	P
cPPI, PPI, 2D-DBD- 5min, 2D-DBD- 15min, 2D-DBD-30min, 2D-DBD-45min	Between Groups	5	33.576	6.715	1237.19	<0.001
	Residual	12	0.0651	0.00543		
	Total	17	33.641			

Table 102. Analysis of variance on the effect of treatment time of ns-pulsed on the area percentage of vicilin present in samples dissolved in 0.1% SDS + 2.5% BME phosphate buffer and analyzed by SE-HPLC.

Sample Analysis	Source of Variation	DF	SS	MS	F	P
cPPI, PPI, ns-pulsed-5min, ns-pulsed-15min, ns-pulsed-30min, ns-pulsed-45min	Between Groups	4	22.497	5.624	78.181	<0.001
	Residual	10	0.719	0.0719		
	Total	14	23.217			

Table 103. Analysis of variance on the effect of treatment time of APPJ on thermal denaturation temperature for the vicilin peak on DSC.

Sample Analysis	Source of Variation	DF	SS	MS	F	P
cPPI*, PPI, APPJ- 5min, APPJ- 15min, APPJ-30min, APPJ- 45min	Between Groups	4	12.874	3.218	7.838	0.005
	Residual	9	3.696	0.411		
	Total	13	16.569			

*cPPI was completely denatured before analysis. No peak of denaturation observed.

Table 104. Analysis of variance on the effect of treatment time of 2D-DBD on thermal denaturation temperature for the vicilin peak on DSC.

Sample Analysis	Source of Variation	DF	SS	MS	F	P
cPPI*, PPI, 2D-DBD-5min, 2D-DBD- 15min, 2D-DBD-30min, 2D-DBD- 45min	Between Groups	4	16.37	4.093	89.97	<0.001
	Residual	9	0.409	0.0455		
	Total	13	16.78			

*cPPI was completely denatured before analysis. No peak of denaturation observed.

Table 105. Analysis of variance on the effect of treatment time of ns-pulsed on thermal denaturation temperature for the vicilin peak on DSC.

Sample Analysis	Source of Variation	DF	SS	MS	F	P
cPPI*, PPI, ns-pulsed-5min, ns-pulsed- 15min, ns-pulsed-30min	Between Groups	3	12.253	4.084	56.333	<0.001
	Residual	7	0.508	0.0725		
	Total	10	12.761			

*cPPI was completely denatured before analysis. No peak of denaturation observed.

Table 106. Analysis of variance on the effect of treatment time of APPJ on enthalpy of denaturation for the vicilin peak on DSC.

Sample Analysis	Source of Variation	DF	SS	MS	F	P
cPPI*, PPI, APPJ- 5min, APPJ- 15min, APPJ-30min, APPJ- 45min	Between Groups	4	47.867	11.967	358.763	<0.001
	Residual	9	0.3	0.0334		
	Total	13	48.167			

*cPPI was completely denatured before analysis. No peak of denaturation observed.

Table 107. Analysis of variance on the effect of treatment time of 2D-DBD on enthalpy of denaturation for the vicilin peak on DSC.

Sample Analysis	Source of Variation	DF	SS	MS	F	P
cPPI*, PPI, 2D-DBD- 5min, 2D-DBD- 15min, 2D-DBD-30min, 2D-DBD- 45min	Between Groups	4	43.819	10.955	488.082	<0.001
	Residual	9	0.202	0.0224		
	Total	13	44.021			

*cPPI was completely denatured before analysis. No peak of denaturation observed.

Table 108. Analysis of variance on the effect of treatment time of ns-pulsed on enthalpy of denaturation for the vicilin peak on DSC.

Sample Analysis	Source of Variation	DF	SS	MS	F	P
cPPI*, PPI, ns-pulsed-5min, ns-pulsed- 15min, ns-pulsed-30min	Between Groups	3	46.003	15.334	2193.6	<0.001
	Residual	7	0.0489	0.00699		
	Total	10	46.052			

*cPPI was completely denatured before analysis. No peak of denaturation observed.

Table 109. Analysis of variance on the effect of treatment time of APPJ on surface hydrophobicity of PPI.

Sample Analysis	Source of Variation	DF	SS	MS	F	P
cPPI, PPI, APPJ-5min, APPJ- 15min, APPJ-30min, APPJ-45min	Between Groups	5	33566187.11	6713237	12.564	<0.001
	Residual	12	6411681.333	534307		
	Total	17	39977868.44			

Table 110. Analysis of variance on the effect of treatment time of 2D-DBD on surface hydrophobicity of PPI.

Sample Analysis	Source of Variation	DF	SS	MS	F	P
cPPI, PPI, 2D-DBD-5min, 2D-DBD-15min, 2D-DBD-30min, 2D-DBD-45min	Between Groups	5	42023497.61	8404700	17.658	<0.001
	Residual	12	5711700	475975		
	Total	17	47735197.61			

Table 111. Analysis of variance on the effect of treatment time of ns-pulsed on surface hydrophobicity of PPI.

Sample Analysis	Source of Variation	DF	SS	MS	F	P
cPPI, PPI, ns-pulsed-5min, ns-pulsed- 15min, ns-pulsed-30min	Between Groups	4	41991875.6	1E+07	17.118	<0.001
	Residual	10	6132653.333	613265		
	Total	14	48124528.93			

Table 112. Analysis of variance on the effect of treatment time of APPJ on surface charge of PPI.

Sample Analysis	Source of Variation	DF	SS	MS	F	P
cPPI, PPI, APPJ- 5min, APPJ- 15min, APPJ-30min, APPJ- 45min	Between Groups	5	224.084	44.817	26.659	<0.001
	Residual	12	20.173	1.681		
	Total	17	244.258			

Table 113. Analysis of variance on the effect of treatment time of 2D-DBD on surface charge of PPI.

Sample Analysis	Source of Variation	DF	SS	MS	F	P
cPPI, PPI, 2D-DBD- 5min, 2D-DBD- 15min, 2D-DBD-30min, 2D-DBD- 45min	Between Groups	5	195.54	39.108	44.952	<0.001
	Residual	12	10.44	0.87		
	Total	17	205.98			

Table 114. Analysis of variance on the effect of treatment time of ns-pulsed on surface charge of PPI.

Sample Analysis	Source of Variation	DF	SS	MS	F	P
cPPI, PPI, ns-pulsed-5min, ns-pulsed- 15min, ns-pulsed-30min	Between Groups	4	193.617	48.404	29.732	<0.001
	Residual	10	16.28	1.628		
	Total	14	209.897			

Table 115. Analysis of variance on the effect of treatment time of APPJ on the relative abundance of β sheet in PPI on IR spectra.

Sample Analysis	Source of Variation	DF	SS	MS	F	P
cPPI, PPI, APPJ- 5min, APPJ- 15min, APPJ-30min, APPJ- 45min	Between Groups	5	30.891	6.178	5.263	0.009
	Residual	12	14.087	1.174		
	Total	17	44.978			

Table 116. Analysis of variance on the effect of treatment time of 2D-DBD on the relative abundance of β sheet in PPI on IR spectra.

Sample Analysis	Source of Variation	DF	SS	MS	F	P
cPPI, PPI, 2D-DBD-5min, 2D-DBD- 15min, 2D-DBD-30min, 2D-DBD- 45min	Between Groups	5	64.74	12.948	16.741	<0.001
	Residual	12	9.281	0.773		
	Total	17	74.021			

Table 117. Analysis of variance on the effect of treatment time of ns-pulsed on the relative abundance of β sheet in PPI on IR spectra.

Sample Analysis	Source of Variation	DF	SS	MS	F	P
cPPI, PPI, ns-pulsed- 5min, ns-pulsed- 15min, ns-pulsed-30min	Between Groups	4	27.534	6.883	8.285	0.003
	Residual	10	8.309	0.831		
	Total	14	35.842			

Table 118. Analysis of variance on the effect of treatment time of APPJ on the relative abundance of random coil in PPI on IR spectra.

Sample Analysis	Source of Variation	DF	SS	MS	F	P
cPPI, PPI, APPJ- 5min, APPJ- 15min, APPJ-30min, APPJ- 45min	Between Groups	5	101.415	20.283	26.127	<0.001
	Residual	12	9.316	0.776		
	Total	17	110.73			

Table 119. Analysis of variance on the effect of treatment time of 2D-DBD on the relative abundance of random coil in PPI on IR spectra.

Sample Analysis	Source of Variation	DF	SS	MS	F	P
cPPI, PPI, 2D-DBD- 5min, 2D-DBD- 15min, 2D-DBD- 30min, 2D-DBD- 45min	Between Groups	5	89.001	17.8	19.419	<0.001
	Residual	12	10.999	0.917		
	Total	17	100.001			

Table 120. Analysis of variance on the effect of treatment time of ns-pulsed on the relative abundance of random coil in PPI on IR spectra.

Sample Analysis	Source of Variation	DF	SS	MS	F	P
cPPI, PPI, ns-pulsed- 5min, ns-pulsed- 15min, ns-pulsed- 30min	Between Groups	4	79.671	19.918	43.839	<0.001
	Residual	10	4.543	0.454		
	Total	14	84.214			

Table 121. Analysis of variance on the effect of treatment time of APPJ on the relative abundance of α helix in PPI on IR spectra.

Sample Analysis	Source of Variation	DF	SS	MS	F	P
cPPI, PPI, APPJ- 5min, APPJ- 15min, APPJ-30min, APPJ- 45min	Between Groups	5	134.027	26.805	9.792	<0.001
	Residual	12	32.849	2.737		
	Total	17	166.877			

Table 122. Analysis of variance on the effect of treatment time of 2D-DBD on the relative abundance of α helix in PPI on IR spectra.

Sample Analysis	Source of Variation	DF	SS	MS	F	P
cPPI, PPI, 2D-DBD- 5min, 2D-DBD- 15min, 2D-DBD-30min, 2D-DBD- 45min	Between Groups	5	150.609	30.122	9.927	<0.001
	Residual	12	36.412	3.034		
	Total	17	187.021			

Table 123. Analysis of variance on the effect of treatment time of ns-pulsed on the relative abundance of α helix in PPI on IR spectra.

Sample Analysis	Source of Variation	DF	SS	MS	F	P
cPPI, PPI, ns-pulsed- 5min, ns-pulsed- 15min, ns-pulsed-30min	Between Groups	4	142.088	35.522	11.908	<0.001
	Residual	10	29.829	2.983		
	Total	14	171.917			

Table 124. Analysis of variance on the effect of treatment time of APPJ on the relative abundance of β turn in PPI on IR spectra.

Sample Analysis	Source of Variation	DF	SS	MS	F	P
cPPI, PPI, APPJ- 5min, APPJ- 15min, APPJ-30min, APPJ- 45min	Between Groups	5	31.483	6.297	2.775	0.068
	Residual	12	27.229	2.269		
	Total	17	58.711			

Table 125. Analysis of variance on the effect of treatment time of 2D-DBD on the relative abundance of β turn in PPI on IR spectra.

Sample Analysis	Source of Variation	DF	SS	MS	F	P
cPPI, PPI, 2D-DBD-5min, 2D-DBD-15min, 2D-DBD-30min, 2D-DBD-45min	Between Groups	5	24.983	4.997	1.62	0.229
	Residual	12	37.022	3.085		
	Total	17	62.005			

Table 126. Analysis of variance on the effect of treatment time of ns-pulsed on the relative abundance of β turn in PPI on IR spectra.

Sample Analysis	Source of Variation	DF	SS	MS	F	P
cPPI, PPI, ns-pulsed- 5min, ns-pulsed- 15min, ns-pulsed-30min	Between Groups	4	49.147	12.287	2.536	0.106
	Residual	10	48.444	4.844		
	Total	14	97.591			

Table 127. Analysis of variance on the effect of treatment time of APPJ on solubility at pH 7 of not-heated pea protein isolates.

Sample Analysis	Source of Variation	DF	SS	MS	F	P
cPPI, PPI, APPJ- 5min, APPJ- 15min, APPJ-30min, APPJ- 45min	Between Groups	5	5707.227	1141.445	663.453	<0.001
	Residual	12	20.646	1.72		
	Total	17	5727.872			

Table 128. Analysis of variance on the effect of treatment time of 2D-DBD on solubility at pH 7 of not-heated pea protein isolates.

Sample Analysis	Source of Variation	DF	SS	MS	F	P
cPPI, PPI, 2D-DBD-5min, 2D-DBD-15min, 2D-DBD-30min, 2D-DBD-45min	Between Groups	5	5758.94	1151.788	538.775	<0.001
	Residual	12	25.653	2.138		
	Total	17	5784.593			

Table 129. Analysis of variance on the effect of treatment time of ns-pulsed on solubility at pH 7 of not-heated pea protein isolates.

Sample Analysis	Source of Variation	DF	SS	MS	F	P
cPPI, PPI, ns-pulsed- 5min, ns-pulsed- 15min, ns-pulsed-30min	Between Groups	4	5808.336	1452.084	524.445	<0.001
	Residual	10	27.688	2.769		
	Total	14	5836.024			

Table 130. Analysis of variance on the effect of treatment time of APPJ on solubility at pH 7 of heated (at 80 C°) pea protein isolates.

Sample Analysis	Source of Variation	DF	SS	MS	F	P
cPPI, PPI, APPJ-5min, APPJ- 15min, APPJ-30min, APPJ-45min	Between Groups	5	2440.869	488.174	119.434	<0.001
	Residual	12	49.049	4.087		
	Total	17	2489.918			

Table 131. Analysis of variance on the effect of treatment time of 2D-DBD on solubility at pH 7 of heated (at 80 C°) pea protein isolates.

Sample Analysis	Source of Variation	DF	SS	MS	F	P
cPPI, PPI, 2D-DBD-5min, 2D-DBD-15min, 2D-DBD-30min, 2D-DBD-45min	Between Groups	5	2340.784	468.157	97.146	<0.001
	Residual	12	57.829	4.819		
	Total	17	2398.614			

Table 132. Analysis of variance on the effect of treatment time of ns-pulsed on solubility at pH 7 of heated pea protein isolates.

Sample Analysis	Source of Variation	DF	SS	MS	F	P
cPPI, PPI, ns-pulsed- 5min, ns-pulsed- 15min, ns-pulsed-30min	Between Groups	4	2754.344	688.586	128.81	<0.001
	Residual	10	53.457	5.346		
	Total	14	2807.802			

Table 133. Analysis of variance on the effect of treatment time of APPJ on gel strength of 20% pea protein gels.

Sample Analysis	Source of Variation	DF	SS	MS	F	P
cPPI, PPI, APPJ- 5min, APPJ- 15min, APPJ-30min, APPJ- 45min	Between Groups	5	317.975	63.595	210.676	<0.001
	Residual	12	3.622	0.302		
	Total	17	321.597			

Table 134. Analysis of variance on the effect of treatment time of 2D-DBD on gel strength of 20% pea protein gels.

Sample Analysis	Source of Variation	DF	SS	MS	F	P
cPPI, PPI, 2D-DBD-5min, 2D-DBD- 15min, 2D-DBD-30min, 2D-DBD- 45min	Between Groups	5	382.761	76.552	157.057	<0.001
	Residual	12	5.849	0.487		
	Total	17	388.61			

Table 135. Analysis of variance on the effect of treatment time of ns-pulsed on gel strength of 20% pea protein gels.

Sample Analysis	Source of Variation	DF	SS	MS	F	P
cPPI, PPI, ns-pulsed-5min, ns-pulsed- 15min, ns-pulsed-30min	Between Groups	4	203.034	50.759	129.747	<0.001
	Residual	10	3.912	0.391		
	Total	14	206.946			

Table 136. Analysis of variance on the effect of treatment time of APPJ on emulsification capacity of 2% pea protein solutions.

Sample Analysis	Source of Variation	DF	SS	MS	F	P
cPPI, PPI, APPJ-5min, APPJ- 15min, APPJ-30min, APPJ-45min	Between Groups	5	306462.9	61292.58	296.651	<0.001
	Residual	12	2479.38	206.615		
	Total	17	308942.28			

Table 137. Analysis of variance on the effect of treatment time of 2D-DBD on emulsification capacity of 2% pea protein solutions.

Sample Analysis	Source of Variation	DF	SS	MS	F	P
cPPI, PPI, 2D-DBD-5min, 2D-DBD- 15min, 2D-DBD-30min, 2D-DBD- 45min	Between Groups	5	325529.14	65105.828	241.957	<0.001
	Residual	12	3228.96	269.08		
	Total	17	328758.1			

Table 138. Analysis of variance on the effect of treatment time of ns-pulsed on emulsification capacity of 2% pea protein solutions.

Sample Analysis	Source of Variation	DF	SS	MS	F	P
cPPI, PPI, ns-pulsed-5min, ns-pulsed- 15min, ns-pulsed-30min	Between Groups	4	301527.2	75381.801	384.515	<0.001
	Residual	10	1960.44	196.044		
	Total	14	303487.64			

Table 139. Analysis of variance on the effect of treatment time of APPJ on emulsification capacity of 1% pea protein solutions.

Sample Analysis	Source of Variation	DF	SS	MS	F	P
cPPI*, PPI*, APPJ- 5min, APPJ- 15min, APPJ-30min, APPJ- 45min	Between Groups	3	38747.52	12915.84	12.444	0.002
	Residual	8	8303.04	1037.88		
	Total	11	47050.56			

Table 140. Analysis of variance on the effect of treatment time of 2D-DBD on emulsification capacity of 1% pea protein solutions.

Sample Analysis	Source of Variation	DF	SS	MS	F	P
cPPI*, PPI*, 2D-DBD-5min, 2D-DBD- 15min, 2D-DBD-30min, 2D-DBD- 45min	Between Groups	3	18307.05	6102.35	10.583	0.004
	Residual	8	4612.8	576.6		
	Total	11	22919.85			

Table 141. Analysis of variance on the effect of treatment time of ns-pulsed on emulsification capacity of 1% pea protein solutions.

Sample Analysis	Source of Variation	DF	SS	MS	F	P
cPPI*, PPI*, ns-pulsed- 5min, ns-pulsed- 15min, ns-pulsed-30min	Between Groups	2	11993.28	5996.64	3.545	0.096
	Residual	6	10148.16	1691.36		
	Total	8	22141.44			

Table 142. Analysis of variance on the alanine content of plasma treated pea protein isolates.

Sample Analysis	Source of Variation	DF	SS	MS	F	P
PPI, 2D-DBD- 30min, ns-pulsed- 30min, APPJ- 5min, APPJ-30min	Between Groups	4	1.199	0.3	0.68	0.623
	Residual	9	3.969	0.441		
	Total	13	5.167			

Table 143. Analysis of variance on the glycine content of plasma treated pea protein isolates.

Sample Analysis	Source of Variation	DF	SS	MS	F	P
PPI, 2D-DBD- 30min, ns-pulsed- 30min, APPJ- 5min, APPJ-30min	Between Groups	4	14.208	3.552	1.144	0.396
	Residual	9	27.951	3.106		
	Total	13	42.159			

Table 144. Analysis of variance on the phenylalanine content of plasma treated pea protein isolates.

Sample Analysis	Source of Variation	DF	SS	MS	F	P
PPI, 2D-DBD- 30min, ns-pulsed- 30min, APPJ- 5min, APPJ-30min	Between Groups	4	6.45	1.612	0.575	0.688
	Residual	9	25.237	2.804		
	Total	13	31.687			

Table 145. Analysis of variance on the glutamate content of plasma treated pea protein isolates.

Sample Analysis	Source of Variation	DF	SS	MS	F	P
PPI, 2D-DBD- 30min, ns-pulsed- 30min, APPJ- 5min, APPJ-30min	Between Groups	4	525.952	131.488	2.226	0.147
	Residual	9	531.62	59.069		
	Total	13	1057.572			

Table 146. Analysis of variance on the serine content of plasma treated pea protein isolates.

Sample Analysis	Source of Variation	DF	SS	MS	F	P
PPI, 2D-DBD- 30min, ns-pulsed- 30min, APPJ- 5min, APPJ-30min	Between Groups	4	4.734	1.183	0.31	0.865
	Residual	9	34.412	3.824		
	Total	13	39.145			

Table 147. Analysis of variance on the valine content of plasma treated pea protein isolates.

Sample Analysis	Source of Variation	DF	SS	MS	F	P
PPI, 2D-DBD-30min, ns-pulsed-30min, APPJ- 5min, APPJ-30min	Between Groups	4	1.13	0.283	0.16	0.954
	Residual	9	15.941	1.771		
	Total	13	17.071			

Table 148. Analysis of variance on the threonine content of plasma treated pea protein isolates.

Sample Analysis	Source of Variation	DF	SS	MS	F	P
PPI, 2D-DBD-30min, ns-pulsed-30min, APPJ- 5min, APPJ-30min	Between Groups	4	2.32	0.58	0.351	0.837
	Residual	9	14.852	1.65		
	Total	13	17.172			

Table 149. Analysis of variance on the Leu/Ile content of plasma treated pea protein isolates.

Sample Analysis	Source of Variation	DF	SS	MS	F	P
PPI, 2D-DBD-30min, ns-pulsed-30min, APPJ- 5min, APPJ-30min	Between Groups	4	1.11	0.278	0.0889	0.984
	Residual	9	28.095	3.122		
	Total	13	29.205			

Table 150. Analysis of variance on the aspartic acid content of plasma treated pea protein isolates.

Sample Analysis	Source of Variation	DF	SS	MS	F	P
PPI, 2D-DBD-30min, ns-pulsed-30min, APPJ- 5min, APPJ-30min	Between Groups	4	61.935	15.484	1.269	0.351
	Residual	9	109.85	12.206		
	Total	13	171.784			

Table 151. Analysis of variance on the proline content of plasma treated pea protein isolates.

Sample Analysis	Source of Variation	DF	SS	MS	F	P
PPI, 2D-DBD-30min, ns-pulsed-30min, APPJ- 5min, APPJ-30min	Between Groups	4	4.107	1.027	0.869	0.519
	Residual	9	10.64	1.182		
	Total	13	14.747			

Table 152. Analysis of variance on the tyrosine content of plasma treated pea protein isolates.

Sample Analysis	Source of Variation	DF	SS	MS	F	P
PPI, 2D-DBD-30min, ns-pulsed-30min, APPJ- 5min, APPJ-30min	Between Groups	4	57.601	14.4	8.459	0.004
	Residual	9	15.321	1.702		
	Total	13	72.922			

Table 153. Analysis of variance on the arginine content of plasma treated pea protein isolates.

Sample Analysis	Source of Variation	DF	SS	MS	F	P
PPI, 2D-DBD-30min, ns-pulsed-30min, APPJ- 5min, APPJ-30min	Between Groups	4	11.119	2.78	1.212	0.37
	Residual	9	20.634	2.293		
	Total	13	31.753			

Table 154. Analysis of variance on the lysine content of plasma treated pea protein isolates.

Sample Analysis	Source of Variation	DF	SS	MS	F	P
PPI, 2D-DBD-30min, ns-pulsed-30min, APPJ- 5min, APPJ-30min	Between Groups	4	16.913	4.228	0.997	0.457
	Residual	9	38.158	4.24		
	Total	13	55.071			

Table 155. Analysis of variance on the histidine content of plasma treated pea protein isolates.

Sample Analysis	Source of Variation	DF	SS	MS	F	P
PPI, 2D-DBD-30min, ns-pulsed-30min, APPJ- 5min, APPJ-30min	Between Groups	4	0.972	0.243	0.67	0.629
	Residual	9	3.263	0.363		
	Total	13	4.235			

Appendix G: Color of mPPIs treated at pH 2 with dialysis

Table 156. Color (L* a* b*) of commercial pea protein reference, non-modified pea protein controls, and plasma modified pea protein isolates treated at pH 2 with dialysis.

Samples	L*	a*	b*	ΔE
PPI Control- pH7	79.45^{1bc}	-3.84^{ab}	$+28.90^{a}$	
PPI Control- pH2	80.39^{b}	-3.10^{a}	$+25.46^{b}$	3.77^{b}
mPPI- N_xO_y /O_3 pH2	78.43^{c}	-4.09^{b}	$+25.67^{b}$	3.40^{b}
mPPI- O_3 pH2	77.77^{c}	-3.52^{ab}	$+24.74^{b}$	4.53^{ab}
mPPI- H_2O_2 pH2	82.87^{a}	-4.26^{b}	$+24.07^{bc}$	5.94^{ab}
mPPI- OH pH2	78.84^{bc}	-3.67^{ab}	$+21.82^{c}$	7.15^{a}
cPPI	*84.68*	*-5.61*	*+27.77*	

[1]Means (n = 3) in each column with different lowercase letters indicate significant differences among samples, according to the Tukey-Kramer multiple means comparison test ($P < 0.05$).

Appendix H: Protein profile of mPPIs treated at pH 7& pH 2 without dialysis, analyzed by SE-HPLC

Table 157. Molecular weight and relative abundance of soluble aggregates, legumin, convicilin, and vicilin present in commercial pea protein reference, non-modified pea protein controls, and plasma modified pea protein isolates treated at pH 7 and pH 2 (without dialysis).

Protein fractions[1]	Molecular weight (kDa)	Relative Abundance (%)[2]										
		cPPI	PPI Control-pH7	mPPI-N_xO_y/O_3 pH7	mPPI-O_3 pH7	mPPI-H_2O_2 pH7	mPPI-OH pH7	PPI Control-pH2	mPPI-N_xO_y/O_3 pH2	mPPI-O_3 pH2	mPPI-H_2O_2 pH2	mPPI-OH pH2
Soluble aggregates (association of legumin, vicilin and other protein fractions)	~1200	10.27^{5Ae}	2.82^{B*4}	3.18^{C*}	3.55^{C*}	3.06^{C*}	5.48^{B*}	10.17^{e}	16.07^{d}	27.52^{c}	36.6^{a}	30.18^{b}
Legumin	~450	N/A[3]	22.01^{A*}	23.86^{A*}	26.39^{A*}	25.17^{A*}	20.69^{B*}	7.67^{a}	5.51^{c}	5.27^{d}	6.08^{b}	5.42^{e}
Convicilin	~ 250	N/A	8.52^{A*}	6.15^{B*}	6.48^{B*}	7.02^{B*}	5.22^{C*}	5.81^{a}	4.67^{b}	4.52^{b}	3.88^{c}	3.22^{d}
Vicilin	~160	2.36^{De}	11.59^{A*}	10.24^{B*}	9.52^{B*}	9.37^{B*}	7.56^{C*}	6.12^{a}	5.04^{b}	5.25^{b}	3.94^{c}	3.26^{d}

[1]Samples were dissolved in pH 7 phosphate buffer and analyzed by high-performance size exclusion chromatography (SE-HPLC);

[2]Relative abundance (%) is the area of a specific peak divided by the total peak area for that sample;

[3]N/A: not available. No peak was apparent in this molecular weight range;

[4]An asterisk (*) indicates a significant difference between a pH 7 and pH 2 plasma treated sample, according to a two-samples t-test ($P < 0.05$);

[5]Means (n=3) in each row with different uppercase letters indicate significant differences of samples under pH 7 plasma treatment, and lowercase letters indicate significant differences of samples under pH 2 plasma treatment, according to the Tukey-Kramer multiple means comparison test ($P < 0.05$).

Appendix I: Structure characterization of mPPIs treated at pH 7& pH 2 without dialysis

Table 158. Denaturation temperatures and enthalpy, secondary structure, surface hydrophobicity and surface charge of commercial pea protein references, non-modified pea protein controls, and plasma modified pea protein isolates at pH 7 and pH 2 (without dialysis).

Samples	Denaturation Temperature and Enthalpy				Surface properties		Secondary Structure			
	Vicilin		Legumin		Surface Hydrophobicity	Surface Charge	α Helix	β Sheet	β Turn	Random Coil
	Denaturation Temperature (Td, °C)	Enthalpy of Denaturation (ΔH, J g-1)	Denaturation Temperature (Td, °C)	Enthalpy of Denaturation (ΔH, J g-1)	RFI	mV	Relative Percentage			
cPPI	N/A[1]	N/A	N/A	N/A	12719^{Ab}	-27.2^{Abc}	15.0^{Bb}	45.9^{Aa}	24.2^{A}	14.9^{A}
PPI Control- pH7	84.5^{A*2}	6.39^{A3}	91.4^{A}	1.48^{A}	8545^{B}	-37.6^{B*}	24.5^{A}	44.5^{A}	21.6^{A}	9.41^{B}
mPPI- N_xO_y/O_3 pH7	82.3^{B*}	6.08^{A}	90.5^{A}	1.10^{B}	8657^{B}	-37.5^{B*}	22.2^{A}	44.5^{A}	23.0^{A}	10.3^{B}
mPPI- O_3 pH7	82.2^{B*}	6.39^{A}	91.8^{A}	0.75^{C}	7743^{B*}	-38.4^{B*}	20.2^{AB}	47.3^{A}	23.1^{A}	9.46^{B*}
mPPI- H_2O_2 pH7	82.0^{B*}	6.23^{A}	89.9^{A}	1.51^{A}	9157^{B*}	-38.0^{B*}	21.2^{A}	44.5^{A}	24.5^{A}	9.66^{B}
mPPI- OH pH7	83.0^{B*}	4.74^{B}	90.2^{A}	1.36^{A}	7831^{B*}	-36.7^{B*}	22.2^{A}	46.4^{A}	21.2^{A}	10.3^{B}
PPI Control- pH2	90.1^{b3}	2.51^{a}	N/A[1]	N/A	9201^{c}	-27.2^{bc}	23.0^{a}	43.7^{b}	20.2^{a}	13.1^{ab}
mPPI- N_xO_y/O_3 pH2	89.5^{b}	1.44^{b}	N/A	N/A	10191^{c}	-26.8^{b}	20.5^{a}	46.3^{a}	21.7^{a}	11.5^{ab}
mPPI- O_3 pH2	86.5^{c}	0.80^{c}	N/A	N/A	10735^{bc}	-28.1^{c}	21.2^{a}	48.7^{a}	20.0^{a}	10.1^{b}
mPPI- H_2O_2 pH2	92.1^{a}	1.84^{b}	N/A	N/A	13965^{a}	-25.2^{a}	20.9^{a}	46.9^{ab}	21.4^{a}	10.8^{b}
mPPI- OH pH2	89.9^{b}	0.73^{c}	N/A	N/A	10881^{bc}	-27.2^{bc}	20.8^{a}	44.9^{b}	23.3^{a}	11.0^{ab}

[1] N/A: not available. No peak of denaturation observed;

[2] An asterisk (*) indicates a significant difference between a pH 7 and pH 2 plasma treated sample, according to a two-samples t-test ($P < 0.05$);

[3] Means (n = 2 or 3) in each column with different uppercase letters indicate significant differences of samples under pH 7 plasma treatment, and lowercase letters indicate significant differences of samples under pH 2 plasma treatment, according to the Tukey-Kramer multiple means comparison test ($P < 0.05$).

Appendix J: Functional properties of mPPIs treated at pH 7& pH 2 without dialysis

Table 159. Solubility, gel strength and emulsification capacity of commercial pea protein references, non-modified pea protein controls, and non-dialyzed plasma modified pea protein isolates at pH 7 and pH 2 (without dialysis).

Samples	Solubility (5%)		Gel Strength (15% protein)	Gel Strength (20% protein)	Emulsification Capacity (2%)
	Non-Heated	Heated (80°C for 30 min)	Strength (N)	Strength (N)	mL oil/ g protein
cPPI	23.9^{Bd2}	41.9^{Bc}	N/A[1]	2.73^{Db}	229.4^{Cc}
PPI Control- pH7	82.4^{A*3}	79.6^{A*}	N/A	5.69^{BCD}	341.0^{B*}
mPPI- N_xO_y/O_3 pH7	82.0^{A*}	77.0^{A*}	N/A	9.46^{AB}	381.3^{A*}
mPPI- O_3 pH7	81.0^{A*}	74.6^{A}	N/A	11.6^{A}	384.4^{A*}
mPPI- H_2O_2 pH7	82.3^{A*}	77.6^{A*}	N/A	4.40^{CD*}	375.1^{A*}
mPPI- OH pH7	79.1^{A*}	80.0^{A*}	N/A	8.71^{ABC}	381.3^{A*}
PPI Control- pH2	48.6^{c}	50.1^{c}	N/A	6.46^{b}	610.7^{b}
mPPI- N_xO_y/O_3 pH2	43.8^{c}	48.3^{c}	2.49^{b}	13.4^{a}	601.4^{b}
mPPI- O_3 pH2	78.4^{a}	71.6^{a}	3.43^{b}	14.9^{a}	694.4^{a}
mPPI- H_2O_2 pH2	64.9^{b}	61.4^{b}	5.25^{a}	16.1^{a}	567.3^{b}
mPPI- OH pH2	66.9^{b}	64.8^{ab}	3.99^{ab}	12.1^{a}	561.1^{b}

[1] N/A: not available. No gels formed at 15% protein concentration;

[2] Means (n=3) in each column with different uppercase letters indicate significant differences of samples under pH 7 plasma treatment, and lowercase letters indicate significant differences of samples under pH 2 plasma treatment, according to the Tukey-Kramer multiple means comparison test ($P < 0.05$);

[3] An asterisk (*) indicates a significant difference between a pH 7 and pH 2 plasma treated sample, according to a two-samples t-test ($P < 0.05$).

Appendix K: Color of APPJ, 2D-DBD, and ns-pulsed treated PPI

Table 160. Color (L* a* b*) of commercial pea protein reference (cPPI), control pea protein isolate (PPI), and APPJ, 2D-DBD, and ns-pulsed treated PPI.

Samples	L*	a*	b*	ΔE
cPPI	84.68	-5.61	+27.77	
PPI	$79.4^{1abA\alpha}$	$-3.84^{aC\gamma}$	$28.9^{aA\alpha}$	
APPJ-5min	79.7^{a}	-3.28^{a}	24.8^{b}	4.14^{a}
APPJ-15min	80.7^{a}	-3.45^{a}	23.8^{b}	5.30^{a}
APPJ-30min	79.2^{a}	-2.98^{a}	23.3^{b}	5.70^{a}
APPJ-45min	79.1^{b}	-2.98^{a}	23.5^{b}	5.50^{a}
2D-DBD-5min	78.5^{B}	-3.00^{B}	25.5^{C}	3.61^{C}
2D-DBD-15min	75.9^{C}	-2.46^{A}	25.2^{C}	5.32^{A}
2D-DBD-30min	77.6^{B}	-3.54^{C}	25.1^{C}	4.28^{B}
2D-DBD-45min	77.8^{B}	-3.37^{C}	26.1^{B}	3.37^{C}
ns-pulsed-5min	79.6^{α}	-3.15^{β}	23.2^{β}	5.72^{γ}
ns-pulsed-15min	$79.3^{\alpha\beta}$	-2.88^{β}	21.9^{γ}	7.03^{β}
ns-pulsed-30min	78.5^{β}	-2.54^{α}	21.2^{δ}	7.89^{α}

[1]Means (n = 3) in each column with lowercase letters indicate significant differences of APPJ samples in comparison to PPI and cPPI, upper letters indicate significant differences of 2D-DBD samples in comparison to PPI and cPPI, and Greek alphabet indicate significant differences of ns-pulsed samples in comparison to PPI and PPI, according to the Tukey-Kramer multiple means comparison test ($P < 0.05$).

Appendix L: Percent relative abundance of different protein fractions in different plasma treated PPIs

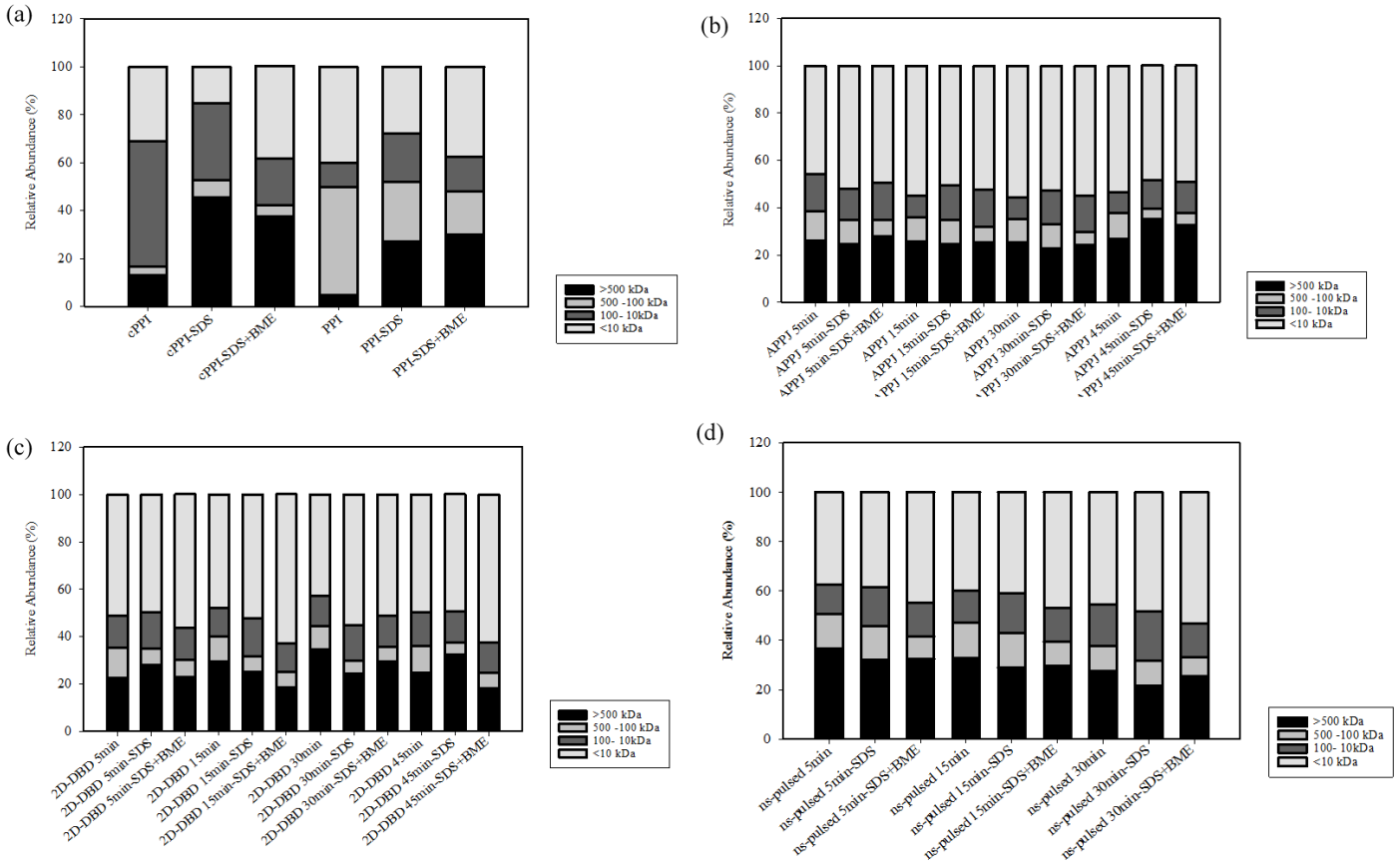

Figure 23. Percent relative abundance of different protein fractions in (a) commercial pea protein reference (cPPI), control PPI, as well as (b) APPJ, (c) 2D-DBD, and (d) ns-pulsed treated PPI dissolved in pH 7 phosphate buffer, 0.1% SDS phosphate buffer, and 0.1% SDS and 2.5% BME phosphate buffer, and analyzed by size-exclusion high-performance chromatography (SE-HPLC). Bars distribution represents means of n = 3.

Appendix M: Loadings plot of the PCA model

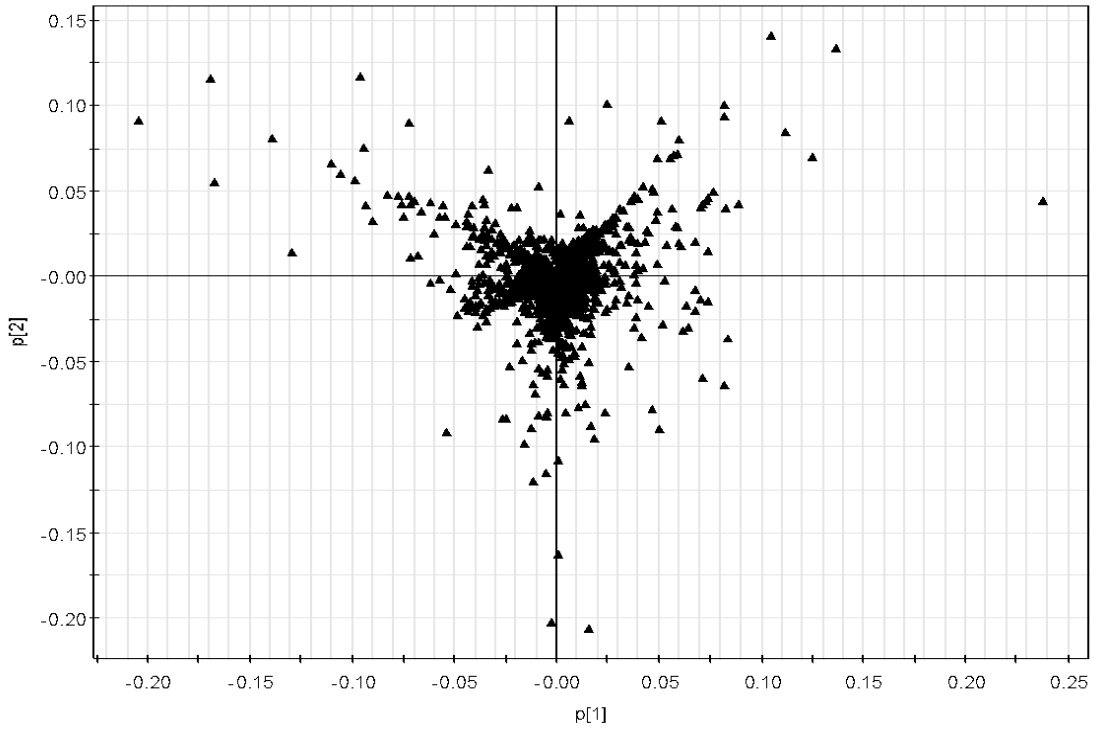

Figure 24. Loadings plot of the PCA model produced from the pooled LC-MS analysis of amino acids and non-protein components.